Mesozoic-Cenozoic Deformation History of Egypt

7

Adel R. Moustafa

Contents

Abstract

Detailed surface and subsurface structural data indicate that the Mesozoic-Cenozoic deformation history of Egypt witnessed four main phases of deformation related to the movements between the African Plate and the surrounding plates. The first phase (Tethyan rifting) started in Middle-Late Triassic almost to the end of Early Cretaceous due to the divergent movement between the Afro-Arabian Plate and Eurasian Plate and led to the formation of NE-SW to ENE-WSW oriented extensional basins in northern Egypt as well as normal faults of the same orientation in the central and southern areas. The second phase was also extensional and led to opening of NW-SE to WNW-ESE oriented rift basins during the Cretaceous-Early Tertiary time. This phase of deformation is probably related to the opening of the South Atlantic and the divergence between the Afro-Arabian and South American Plates. The third phase is compressional and resulted from the convergence between the Afro-Arabian and Eurasian Plates leading to inversion of the Tethyan extensional basins. Onshore data indicate that basin inversion was transpressive, started at Santonian time and continued to the Miocene. Offshore areas in the Herodotus Basin and eastern part of the Nile Cone indicate continued convergence and folding till present time. The fourth phase is related to divergence between the African and Arabian Plates in Late Oligocene-Miocene time forming the Gulf of Suez-Ancestral Red Sea rift. Both rifts were separated from each other by the left-lateral Dead Sea Transform at Late Miocene time leading to continued opening of the Red Sea Basin. This chapter deals with the first three phases whereas the fourth phase is dealt with in a separate chapter in this book.

7.1 Introduction

A wealth of data and new concepts has accumulated in the last three decades since the publication of Said's (1990) book on the Geology of Egypt. These data include detailed surface structural mapping of different areas of Egypt as well as subsurface geological information from industry 3D seismic and boreholes especially for the northern Western Desert and onshore/offshore Nile Delta. All of these new geological data and information have led to better understanding of the deformation history of Egypt.

The Phanerozoic structures of Egypt have gone through several stages of study. The earliest stage includes works that concentrated mainly on studying the stratigraphy of certain area(s) with little attention to the structures that appeared as single lines on the geological map(s) accompanying these studies (e.g. Ball 1900; Ball and Beadnell

A. R. Moustafa (✉)
Department of Geology, Ain Shams University, Cairo, 11566, Egypt
e-mail: armoustafa@sci.asu.edu.eg; ; armoustafa@hotmail.com

Z. Hamimi et al. (eds.), *The Geology of Egypt*, Regional Geology Reviews,
https://doi.org/10.1007/978-3-030-15265-9_7

1903; Beadnell 1909; Moon and Sadek 1921; among others). In these studies, the structures were not the main objective and represented only minor parts of the works. Among these studies, Sadek's 1926 geological map of the area between Gebel Ataqa and the North Galala Plateau is different due to the amount of structural details shown on the map. A later stage during the forties of the last century by geologists of Standard Oil Company of Egypt involved surface geological mapping of several areas in northern Egypt in search of suitable drilling sites for hydrocarbon exploration (e.g. Foley 1942; Bowles 1945; Iskandar 1946; Jones 1946; Shata and Sourial 1946; among others). These studies concentrated on the geometries and age of the mapped structures which form hydrocarbon traps. Mapping efforts increased in the fifties and early-mid 1960s, when structural symbols appeared on the maps instead of the simple lines on the maps of the earliest stage (e.g. Faris 1948; Shukri and Akmal 1953; Farag and Ismail 1955; Shukri and Ayouty 1956; Al-Far 1966; among others). A notable gap in the Egyptian surface structural studies accompanied the Israeli occupation of Sinai in 1967, lasting until the mid 1980s. During this stage, Israeli geologists carried out several detailed studies on Sinai (e.g. Garfunkel and Bartov 1977; Hildebrand et al. 1974; Bartov 1974; Bartov et al. 1980; Eyal et al. 1981; among others). A flourishing stage of detailed structural studies started in the mid 1980s and involved detailed surface structural studies of different areas of Egypt (e.g. studies of the present author and his colleagues since 1985; Abdel Khalek et al. 1993; Khalil and McClay 2002; Abd-Allah et al. 2004; Dupuis et al. 2011; Noweir and Fawwaz 2011; Sakran and Said 2018; among others). Subsurface studies on the other hand started with the exploration of hydrocarbons and the availability of new technology for better imaging of the subsurface. Reliable subsurface structural studies used 3D seismic data since the mid 1980s. Although detailed and regional subsurface structural mapping was achieved by oil companies, most of these maps are confidential and only small areas were released for publication (e.g. Deibis 1982; Karaaly et al. 1994; Nemec 1996; Matresu et al. 2016; among others).

The data and information presented in this chapter concern mainly the Mesozoic and Cenozoic rocks whereas older (Paleozoic) sequences are still less well understood due to the few Paleozoic outcrops and insufficient subsurface data. The latter is related to the low resolution of seismic reflection data at the depth of these rocks as well as insufficient (and non-released) deep borehole penetrations. A fairly good number of Paleozoic penetrations by operating oil companies in the area west and southwest of Shoushan Basin is not released yet.

The new geological data and information has been used for reaching a reasonable understanding of the Mesozoic-Cenozoic deformation history of Egypt as detailed in this chapter. The information presented in this chapter depends mainly on the author's own work as well as published works of other investigators that are cited. Published works relying on detailed structural studies and/or reliable data have been used whereas works providing concepts that are not supported by reliable data have been ignored. The stratigraphic sections of the discussed areas are shown in the Fig. 7.33.

7.2 Phases of Deformation

The Mesozoic-Cenozoic deformation of Egypt is a result of the movement of the African Plate and the surrounding (Eurasian, Arabian, and South American) Plates. Surface and subsurface geological data have helped recognition of several phases of deformation including extensional deformation leading to opening of rift basins and compressional deformation leading to closure of some of these basins. The extensional deformations were associated with volcanic events which have been dated with reasonable accuracy.

Four main deformations have been recognized in the Mesozoic-Cenozoic rock record as follows (Fig. 7.1):

1. Early Mesozoic (Tethyan) rifting phase formed rift basins/sub-basins oriented NE-SW to ENE-WSW affecting mainly the northern part of Egypt due to opening of the Neotethys and divergence between the Afro-Arabian and Eurasian Plates. Basin opening in the Jurassic most probably started also at Middle/Late Triassic based on local data. Extension continued also during the Early Cretaceous. Extensional basins related to this phase of deformation are well recognized in the northern Western Desert (Kattaniya, Mubarak, Alamein-Razzak, Matruh, and Shoushan Basins as well as small sub-basins within the area of the later Abu Gharadig Basin); northern Eastern Desert (Wadi Araba and Shabraweet area); and northern Sinai (Maghara, Yelleg and Halal Basins as well as other similar basins in the northern offshore area). Extension generally decreases to the south creating NE and ENE oriented normal faults with small slip, as in the central Western Desert (Bahariya Oases and northern Farafra) and southern Western Desert (Nubia Fault System).
2. Cretaceous rifting phase created extensional basins oriented NW-SE to WNW-ESE in different areas of Egypt such as Upper Egypt (Kom Ombo Basin), Nile Valley (Asyut and Beni Sueif Basins), as well as the northern Western Desert (e.g. Abu Gharadig Basin). This extensional phase may be attributed to the far field stress associated with the opening of the South Atlantic leading to reactivation of NW-SE and WNW-ESE oriented Precambrian faults and shear zones in the mentioned areas, among other areas in Africa. In addition to the mentioned

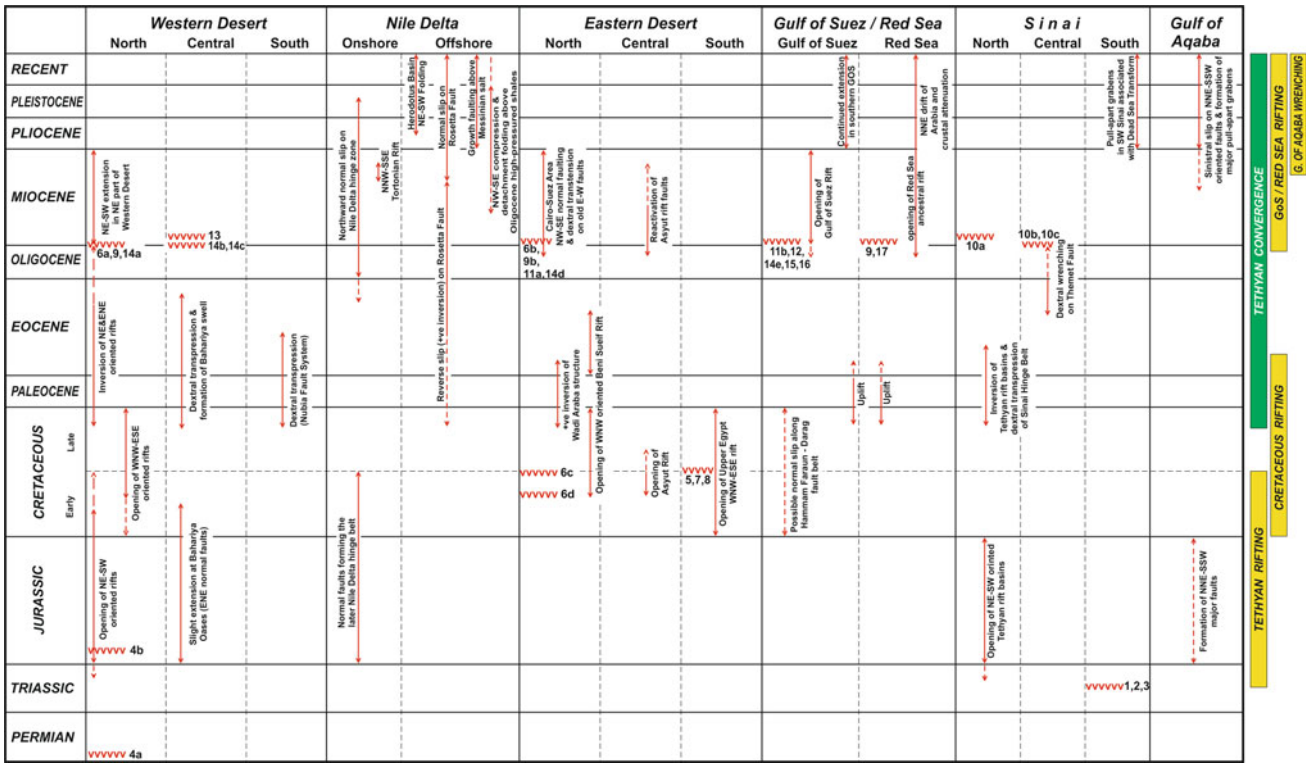

Fig. 7.1 Mesozoic-Cenozoic deformation events of Egypt and their associated volcanicity (represented by v-symbols with their cited references). Cited References are: 1: Moussa (1987); Um Bogma olivine basalt sill (233–243 Ma). 2: Roufaiel et al. (1989); Um Bogma olivine basalt sill (233–243 Ma). 3: Meneisy (1986); Um Bogma olivine basalt sill (233–243 Ma). 4: El Shazly (1977); a—Rabat-1 well olivine basalt (293 ± 12 Ma), b—Kattaniya well olivine basalt (191 ± 19 Ma). 5: Hashad and El Reedy (1979); Wadi Natash olivine basalt (104 ± 7 Ma). 6: Meneisy and Kreuzer (1974a), a—W. Samalut basalt (23 ± 2 Ma), b—Abu Zaabal basalt (23 ± 1 Ma), c—Wadi Abu Darag olivine basalt (113–115 Ma), d—Wadi Araba olivine basalt (125 ± 4 Ma). 7: Meneisy and Kreuzer (1974b); SED nepheline Syenite and alkali syenite (88–96 Ma). 8: Serencsits et al. (1979); SED nepheline Syenite and alkali syenite (88–96 Ma). 9: Meneisy and Abdel Aal (1983); a—G. Qatrani basalt (23–24 Ma), b—Qattamia basalt (22 ± 2 Ma). 10: Steinitz et al. (1978); a—G. Iktefa basalt (20 ± 1 Ma), b—Raqabet El Naam basalt (25 ± 2 Ma), c—Themed basalt (20 ± 1 Ma). 11: Meneisy (1990); a—El Gafra basalt (22 ± 2 Ma), b—G. Matulla basalt (24 ± 1 Ma). 12: Steen (1982); G. Araba, W. Tayiba, & W. Nukhul basalt (18–22 ± 1 Ma). 13: Meneisy and El Kalioubi (1975); Bahariya Oases basalt (18–20 Ma). 14: Bosworth et al. (2015b); a—G. Qattrani & West Faiyum basalt (22–24 Ma), b—Bahariya Oases basalts (23–25 Ma), c—Qaret Dab'a basalt (SW Beni Sueif) (23 Ma), d—Qattamia graben basalt (21 Ma), e—W. Tayiba, W. Nukhul, & W. Araba (S. Sinai) (22–23 Ma). 15: Bosworth and McClay (2001); S. side of G. Ataqa basalt dike (25.7 ± 1.7 Ma). 16: Ott d'Estevou et al. (1986); G. Monsill (Gharamul) basalt dike (24.7 ± 0.6 Ma). 17: Roussel et al. (1986); Sharm El Bahari basalt flow (24.9 ± 0.6 Ma)

Cretaceous basins, the northern part of the Gulf of Suez area is believed to have suffered similar extension leading to reactivation of a NW-SE oriented shear zone extending from the Darag Fault that bounds the eastern side of the North Galala Plateau at present time to the Hammam Faraun Fault on the other side of the gulf and the Rihba Shear Zone of Younes and McClay (2002).

3. Late Cretaceous to Recent Tethyan convergence of the African and Eurasian Plates affected the Egyptian territories by compressive stress since Late Cretaceous time. The direction of compression changed with time and space depending on the convergence direction of the two plates and the irregular shape of the Africa-Eurasia plate boundary. Compression started intensively during Santonian time in the ESE to SE direction (Smith 1971; Eyal and Reches 1983; Letouzey 1986) perhaps allover the Egyptian territories and continued to present time with slight clockwise rotation to the SE and SSE and local change to the SW direction at the eastern part of the Nile Cone. Focal mechanisms of the 1955 and the 2012 Nile Delta earthquakes by Costantinescu et al. (1966) and Abu El-Nader et al. (2013), respectively indicate that the present-day compressive stress affecting the northern and western outer parts of the Nile Cone is NNW to NW (N333–346°). Plate convergence led to inversion of the Jurassic extensional basins/sub-basins in northern Egypt. Detailed surface geological mapping indicates that inversion was probably transpressive with small dextral slip. Further south, convergence led to uplift of different areas above sea level with marked hiatuses in the rock

record, e.g. the southern part of the Gulf of Suez and northern part of the Red Sea region. Compressive stress also affected other areas farther south (in central and southern Egypt), such as the Bahariya-Farafra area as well as the southern Western Desert where ENE oriented faults of the Nubia Fault System were reactivated by dextral slip (Issawi 1968 and 1971; El Etr et al. 1982; Sakran and Said 2018; Hamimi et al. 2018). Continued convergence in the Neogene affected mainly the northernmost areas of Egypt such as the offshore Mediterranean areas due to subduction of the African Plate underneath the Eurasian Plate. This led to detachment folding in the central and eastern parts of the Nile Cone above Lower Oligocene ductile shales and was followed by gravity movement of the uppermost Miocene-Recent sediments above the Messinian salt, reactivation of main faults such as the Rosetta Fault by oblique extension, and NE-SW oriented folds of the Herodotus Basin.

4. NNW-SSE oriented Neogene rifting phase led to opening of the Gulf of Suez—ancestral Red Sea rift in Late Oligocene and Miocene times followed by continued opening and crustal thinning of the northern Red Sea area and separation from the Gulf of Suez rift by the Dead Sea transform fault since Late Miocene time. This rifting phase was triggered by the divergence of the Afro-Arabian Plate signaling the early phases of separation of Arabia from Africa. It also involved reactivation of a possibly Early Mesozoic NNE-SSW oriented fault belt forming the Dead Sea Transform at Late Miocene-Present time. Reactivation of nearby NW-SE oriented Cretaceous rift faults lying close to the Neogene rifts occurred in some areas such as Asyut Basin, Beni Sueif Basin, and the Abu Darag-Hammam Faraun-Rihba Shear Zone. The Gulf of Suez/Red Sea rift system and the Dead Sea transform are dealt with in a separate chapter (Moustafa and Khalil, this book).

7.2.1 Early Mesozoic Tethyan Rifting

Tethyan rifting affected the northern onshore and offshore areas of Egypt and led to opening of NE to ENE oriented basins/sub-basins in the northern areas and formation of normal faults of the same orientation in the central and southern areas of Egypt. Tethyan rifting is attributed to the divergent movement between the Afro-Arabian and Eurasian Plates. Detailed subsurface mapping of the northern Western Desert using 3D seismic and borehole data helped identification of several Tethyan extensional basins such as Kattaniya, Mubarak, Alamein-Razzak, Matruh and Shoushan Basins (Fig. 7.2). The Faghur Basin (Bosworth et al. 2015a) is considered here to be part of the Shoushan Basin. These extensional basins are oriented NE to ENE except Matruh Basin which is oriented NNE perhaps due to reactivation of old structural fabric (Moustafa et al. 2002). The NE to ENE oriented basins had half graben geometry with NNW tilt and are bounded by major normal faults on their northwestern sides. The easternmost one of these basins (Kattaniya Basin) seems to slightly extend further east into the Eastern Desert. In the Eastern Desert itself, as well as in northern Sinai, similar NE to ENE oriented extensional basins were also formed but with opposite polarity where the major basin-bounding faults lie on the southeastern sides of the basins. An accommodation zone between the northern Western Desert basins and the northern Eastern Desert—northern Sinai basins has not been mapped yet but is expected to be in vicinity of the present course of the Nile close to the longitude of Cairo. Continuation of the Tethyan basins further north in the Mediterranean offshore area is obvious in offshore northern Sinai but is difficult to map further west due to the large thickness of Neogene sediments of the Nile deep sea fan (Nile Cone) overlying such basins. The Rosetta Fault bounding the western side of the Nile Cone shows structural features at the top Mesozoic-Tortonian rocks that may indicate that it formed the boundary of one of these Tethyan extensional basins (Abd El-Fattah et al. 2018).

The stratigraphic sections in the Tethyan basins record extension during the Jurassic and Early Cretaceous times but local areas show evidence of onset of basin opening at Middle/Late Triassic time as follows:

1. The Triassic Qiseib Formation (Abdallah et al. 1963) or its synonym the Budra Formation (Weissbrod 1969) is made up of brick-red, purple to varicolored siltstone with some shale and sandstone beds of fluvial origin and is 327 m thick in Wadi Budra (Weissbrod 1969). The Budra Formation is underlain by a 20 m thick olivine basalt sill of Middle Triassic age (233–243 Ma based on K-Ar dating; Meneisy 1986; Moussa 1987; Roufaiel et al. 1989) at Wadi Sidri-Wadi Budra area (west-central Sinai). The sill is well exposed in the Um Bogma-Wadi Budra-Wadi Sidri area in the form of isolated patches that extend southward to Wadi Feiran (Moustafa 1992, 2004). These red clastics and the underlying basalt are perhaps related to the early stages of opening of the NeoTethys and its associated extensional basins in northern Egypt.
2. The lowermost unit of the syn-rift section in Matruh and Shoushan Basins is made up of red beds deposited on the top Paleozoic unconformity surface. Local deposition of these red beds changes from one area to another due to the irregular nature of the unconformity surface as well as the onlap of syn-rift deposits on the top Paleozoic unconformity. These red beds include the Ras Qattara (or

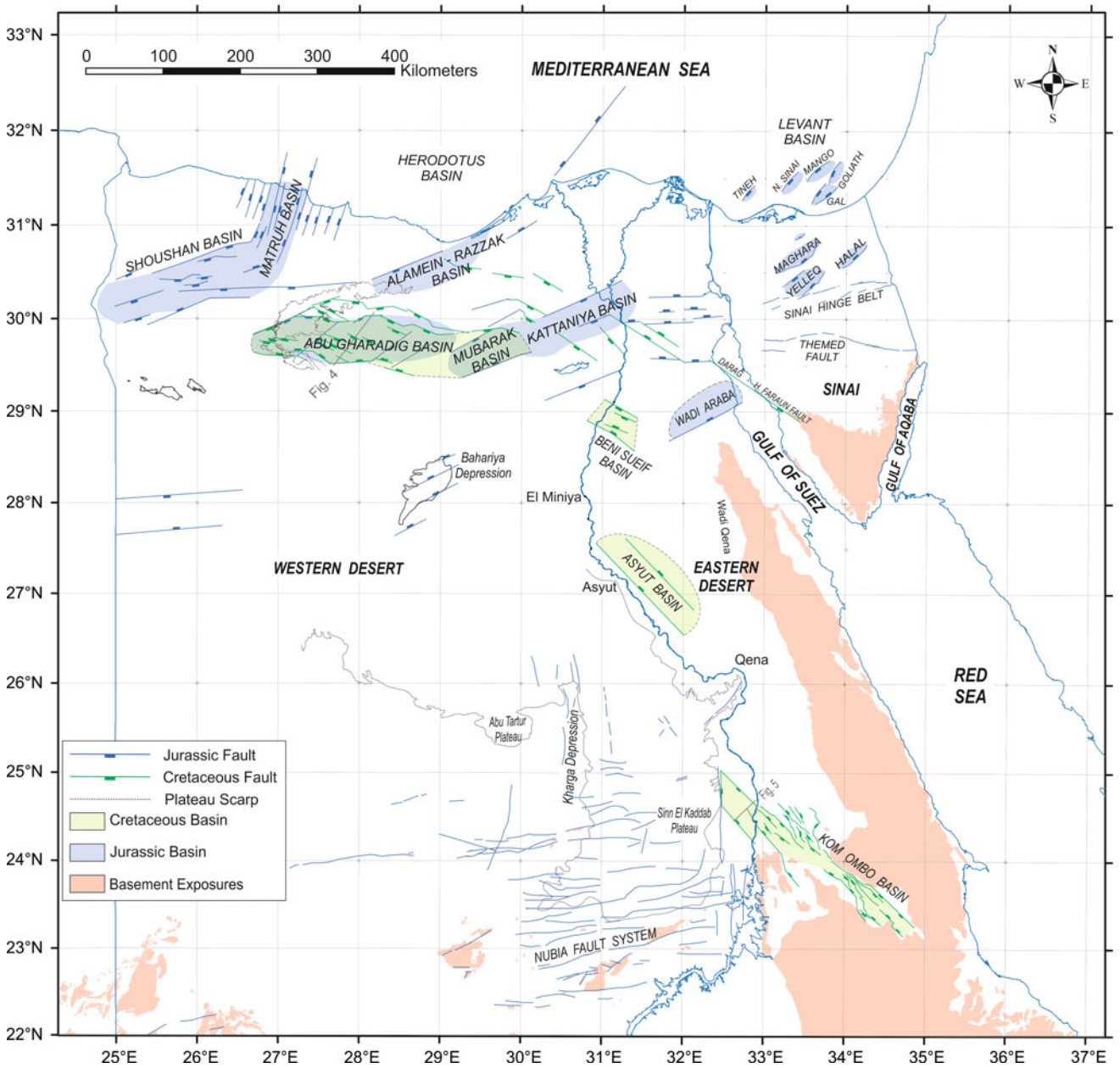

Fig. 7.2 Mesozoic extensional basins and faults of Egypt

Bahrein) and Yakout Formations. The Ras Qattara (Bahrein) Formation shows widespread reddening (Keeley et al. 1990; Hantar 1990). Red clastics with thin coal beds are also reported in the Shoushan and Matruh Basins at the base of the Jurassic section. In the Hazem-1 well (Shoushan Basin), these red beds are exceptionally thick and are associated with weathered basalt (Keeley et al. 1990). The Ras Qattara section includes Middle to Late Triassic and Lower Jurassic sandstones whereas the Yakout Formation is made up of Middle Jurassic shales. Core data of the Jc 17-2 well (Matruh Basin) indicate that the Yakout Formation is made up of red clastics with rounded to sub-rounded pebbles and granules of volcanic origin in polymictic conglomerates (Moustafa et al. 2002). Also, basalt was recorded in the Ras Qattara section in the J4 well (north of the Kattaniya Basin) and dated Late Triassic-Early Jurassic (K-Ar); Abdel Hakim (2017) and Fahmy et al. (2018).

The Triassic-Jurassic syn-rift units of the northern Western Desert basins clearly show thickening toward the basin-bounding faults and the lowermost units clearly show onlap on pre-rift Paleozoic rocks. The Jurassic syn-rift section in the Kattaniya Basin has wedge shape showing

northward thickening towards the main basin-bounding fault with maximum thickness of about 9000′ (~2750 m); Abd El-Aziz et al. (1998).

The Mubarak Basin includes several northwestward thickening Jurassic and Early Cretaceous sequences (Bevan and Moustafa 2012), Fig. 7.3. Other similar sub-basins lie to the west in the Abu Gharadig Basin area. These sub-basins as well as the Mubarak and Kattaniya Basins form a series of right-stepping troughs (Fig. 7.2).

The northern Sinai Tethyan basins include three main onshore basins at Gebel (= mountain) Maghara, Gebel Yelleg, and Gebel Halal. The syn-rift section is well exposed in the core of Gebel Maghara structure due to later inversion. About 2 km thick surface Jurassic section was described by Al-Far (1966) with the base unexposed. It includes six interbedded carbonate and clastic units. The topmost Jurassic unit is the Masajid carbonates and is overlain by Upper Jurassic-Lower Cretaceous shales of the Gifgafa Formation that are always eroded and/or covered by Quaternary alluvial deposits. The Gifgafa Formation was penetrated by two boreholes in Gebel Falig at the northwestern side of Gebel Yelleg with 220 m thickness (Moustafa and Fouda 2014).

A thicker Jurassic section equal to 3234 m was penetrated by Halal-1 well in the core of Gebel Halal inverted basin. In fact the lack of seismic data and dipmeter log for this well makes it difficult to consider the drilled thickness representative of the true stratigraphic thickness of the Jurassic rocks of Gebel Halal extensional basin. The true stratigraphic thickness is not expected to be less than that of Gebel Maghara Basin. 2D seismic section extending from Gebel Maghara Basin to the northeastern part of Gebel Yelleg Basin clearly shows the southward thickening Jurassic wedge of Gebel Maghara Basin toward the main basin-bounding fault (Moustafa 2010 and 2014). The seismic section also shows that the Jurassic section of Gebel Yelleg Basin is smaller than that of Gebel Maghara and was deposited in a southeast tilted half graben basin.

Detailed structural mapping of offshore northern Sinai clearly shows other NE-SW oriented Jurassic-Early Cretaceous extensional basins such as Mango and Goliath Basins, among others (Ayyad et al. 1998; Yousef et al. 2010), Fig. 7.2.

7.2.2 Cretaceous Rifting

The early indication of Cretaceous rifting is the presence of Cretaceous alkaline igneous rocks in the Eastern Desert. Olivine basalts at Wadi Natash were dated 104 ± 7 Ma by Hashad and El Reedy (1979), nepheline syenite and alkali

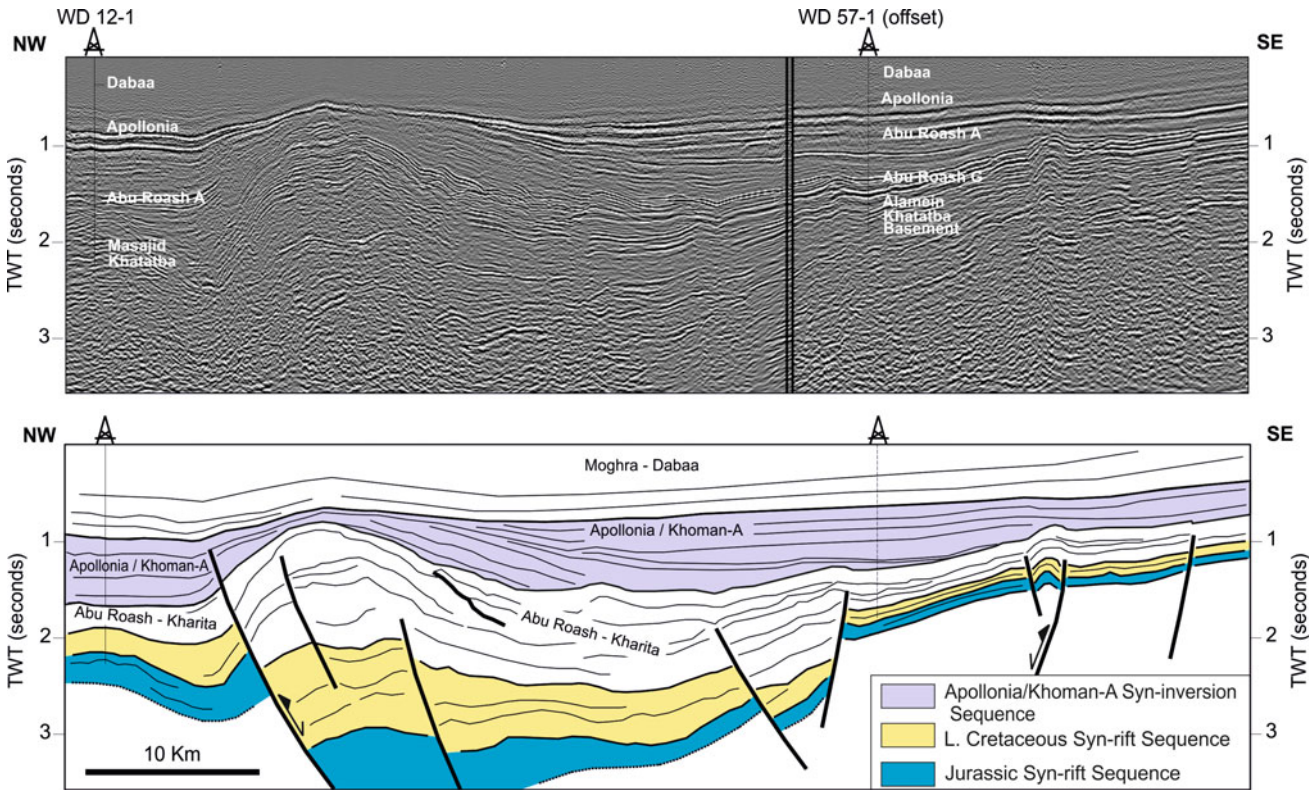

Fig. 7.3 Seismic section and line drawing of Mubarak inverted basin (northern Western Desert) modified after Bevan and Moustafa (2012). See Fig. 7.6 for location

syenite ring complexes in the south Eastern Desert were dated 88–96 Ma by Meneisy and Kreuzer (1974b) and Serencsits et al. (1979), and olivine basalts at Wadi Araba and Wadi Abu Darag were dated 125 ± 4 Ma and 113–115 Ma respectively by Meneisy and Kreuzer (1974a). Subsurface mapping for hydrocarbon exploration led to the recognition of several Cretaceous rift basins in the northern Western Desert as well as in the Eastern Desert and perhaps the Gulf of Suez area. These basins include the prolific Abu Gharadig Basin, Beni Sueif Basin, Asyut Basin, Kom Ombo Basin, and probably the Hammam Faraun-Abu Darag-Rihba Shear Zone area (Fig. 7.2). These basins clearly show Cretaceous syn-rift rocks thickening toward NW-SE to WNW-ESE oriented normal faults (Figs. 7.4 and 7.5). Tilted fault blocks in these half-graben basins dip toward the NE (e.g. Abu Gharadig and Kom Ombo Basins) or SW (Beni Sueif and Asyut Basins). As calculated in the present study, β values of these extensional basins are relatively small reaching a maximum value of 125% in the Abu Gharadig Basin.

7.2.2.1 Abu Gharadig Basin

The Abu Gharadig Basin is an oblique rift extending for about 300 km in the E-W direction. The main faults active during Cretaceous time within the basin are oriented WNW-ESE but the northern basin-bounding fault has a general E-W orientation that clearly shows the effect of pre-existing E-W faults on the general orientation of the basin. This basin-bounding fault is made up of several segments oriented E-W, NE-SW, and WNW-ESE (El Saadany 2008). Consistent NE and NNE tilting of the Cretaceous and older rocks in the rift is obvious at an angle of about 9–12° (Fig. 7.4). Average stretch (β) is locally about 112% in the eastern part of the basin at BED-1 field area (El Saadany and Mahmoud 2008) but β value of the whole basin has been estimated from a regional section across the whole rift to be about 125% during the Cretaceous time. Detailed structural mapping of the basin indicates NE-SW oriented faults of Jurassic age within the basin and were later inverted in Late Cretaceous-Early Tertiary time (e.g. Mid-Basin Arch as well as Mubarak Basin faults at the eastern edge of the Abu Gharadig Basin, among other faults). Deep erosion affected the northern shoulder of the basin being the footwall of the main basin-bounding fault where the Upper Cretaceous rocks are deeply eroded and are overlain by a relatively thin section of Maastrichtian chalk. Deeper erosion in other parts of the shoulder like the Rabat high led to deposition of Eocene sediments directly above the Paleozoic

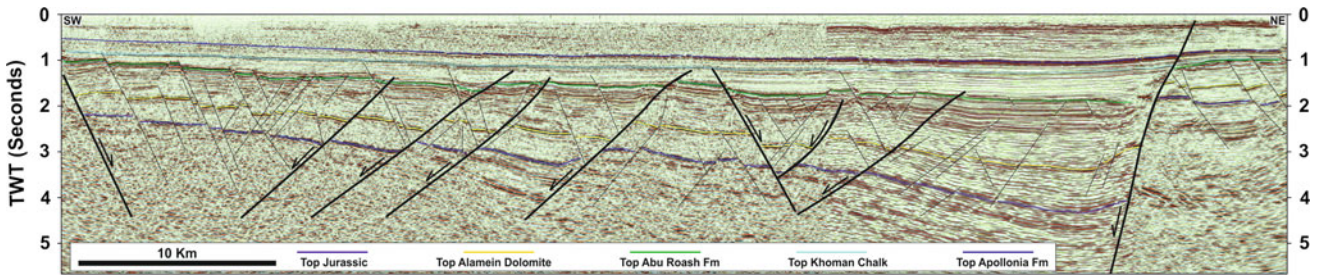

Fig. 7.4 Seismic section across the Abu Gharadig Basin, northern Western Desert showing Cretaceous syn-rift sequences (enclosed between the top Jurassic and top Khoman Chalk reflectors) thickening toward WNW-ESE oriented normal faults. See Fig. 7.2 for location

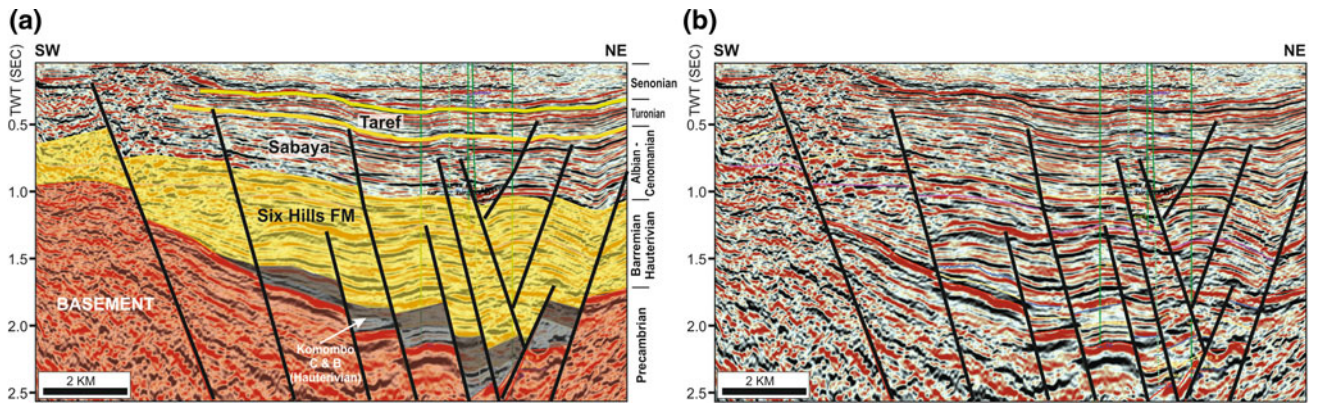

Fig. 7.5 Seismic section (with and without interpretation) across the Kom Ombo Basin at Al Baraka oil field (modified after Dolson et al. 2014) showing wedge-shaped Cretaceous syn-rift section thickening toward the main WNW-ESE basin-bounding fault and onlapping the Precambrian basement rocks. See Fig. 7.2 for location

rocks (Abdel Aal and Moustafa 1988). Early interpretation of the origin of the Abu Gharadig Basin as a series of pull-apart basins (Abdel Aal and Moustafa 1988) has proven incorrect by detailed mapping of high resolution 3D seismic data acquired during the last 20 years.

7.2.2.2 Beni Sueif Basin

The Beni Sueif Basin has WNW-ESE orientation and is crossed by the present-day Nile Valley at Beni Sueif and Maghagha towns (Zahran et al. 2011). Although this basin seems to be a whole graben (bounded by normal faults on both sides) at the Precambrian basement level, main subsidence is along the southwestern basin-bounding fault (Salem and Sehim 2017), indicating a SW dipping half-graben at Cretaceous time. Normal slip of the top basement on this fault is about 1 km. Basin initiation was at Albian time involving about one half of the total extension. Extension ceased at the end of Cretaceous time but was resumed during the Eocene resulting in the deposition of more than 1500 m thick carbonate rocks (Salem and Sehim 2017). Several ENE-WSW and E-W oriented pre-existing basement faults in the basin area were reactivated by dextral transtension into en echelon normal fault belts during Cretaceous and Eocene extension.

7.2.2.3 Asyut Basin

Asyut Basin lies to the south of Beni Sueif Basin and extends east of the Nile Valley from Miniya to the north of Qena in the NW-SE direction. Normal faults of the basin extend up to the surface through the Eocene rocks and also control the course of the Nile River. Seismic reflection data show NW-SE orientation of the normal faults of the basin. Like Beni Sueif Basin, the Asyut Basin was opened in Early Cretaceous time. The basin has half graben geometry with SW tilt and major-bounding fault on the southwestern side with throw of about 1–1.5 km at top Precambrian basement level. The exposed Precambrian basement rocks on the east side of Wadi Qena might represent the updip continuation of the basement rocks of the basin. Surface geological data at Wadi Qena (Klitzsch et al. 1990) indicate that the Precambrian basement is stratigraphically overlain by Albian cross-bedded sandstone, similar to the subsurface setting of Beni Sueif Basin. The presence of Oligo-Miocene basalts along some of the faults of Asyut Basin (e.g. in the area east of Miniya; EGSMA 1981) might indicate reactivation of the Asyut Basin faults at Oligo-Miocene time.

7.2.2.4 Kom Ombo Basin

Kom Ombo Basin extends for about 300 km in the southern Eastern Desert and extends northwestward across the Nile Valley to the eastern edge of Sin El Kaddab Plateau (Fig. 7.2). This NW-SE oriented rift basin was first recognized by gravity and magnetic data with estimated depth to Precambrian basement of about 4.5 km (Nagati 1988). NW-SE oriented normal faults of the rift dissect the exposed Upper Cretaceous rocks of the area. The southeastern part of the basin shows up as a structural low (trough) within the Precambrian exposures of the southern Eastern Desert (Fig. 7.2). Seismic reflection data indicate the half graben geometry of the basin with predominant NE dipping Cretaceous rocks (Dolson et al. 2000, 2001, and 2014; Selim 2016). Seismic and borehole data from El Baraka Oil Field in the extreme northwestern part of the basin indicate that the oldest syn-rift sediments in the half graben basins are Hauterivian clastics. Up to 4 km thick Lower and Upper Cretaceous syn-rift sediments onlap the Precambrian basement rocks in the half graben basins and thicken northeastward toward the main basin-bounding faults (Fig. 7.5). These features indicate continuous subsidence during the Cretaceous time. The basin fill of Kom Ombo Basin includes Lower Cretaceous (Hauterivian, Neocomian to Barremian) non-marine sediments followed by marine deposition during the Albian/Cenomanian (sandstone and shale) and Upper Cretaceous-Early Tertiary (carbonates); Abdelhady et al. (2016). Alkaline volcanics at Wadi Natash (El Ramly 1972), dated 104 Ma old by Hashad and El Reedy (1979), were probably associated (in time and place) with opening of Kom Ombo Basin. The NW-SE trend of the basin is probably controlled by reactivated Precambrian shear zones of the Najd Fault System.

7.2.3 Late Cretaceous to Recent Tethyan Convergence

During the Late Cretaceous-Recent times a change in the direction of movement of the African and Eurasian Plates led to convergent movement of the two plates and the development of compressional structures (Fig. 7.6). The earliest record of convergence is obvious in the Late Cretaceous-Early Tertiary folds affecting the Mesozoic exposures in northern Egypt; already considered as part of the Syrian Arc System of Krenkel (1925). Folded Mesozoic rocks exposed in northern Sinai, the northern Eastern Desert, as well as the folds of Abu Roash area and the Bahariya Oases in the Western Desert attracted the attention of geologists for a long period of time. Hydrocarbon exploration in the northern Western Desert and offshore Sinai also led to recognition of similar folding of the Mesozoic and older rocks. Surface and subsurface folds in northern Egypt are oriented NE-SW and are associated with faults of different orientations and types. The onset of folding was in the Late Cretaceous specifically in the Santonian-Campanian time and is considered to have been of maximum magnitude at that time but continued mildly during the Tertiary. Younger convergence structures are more obvious in the northernmost areas as if deformation

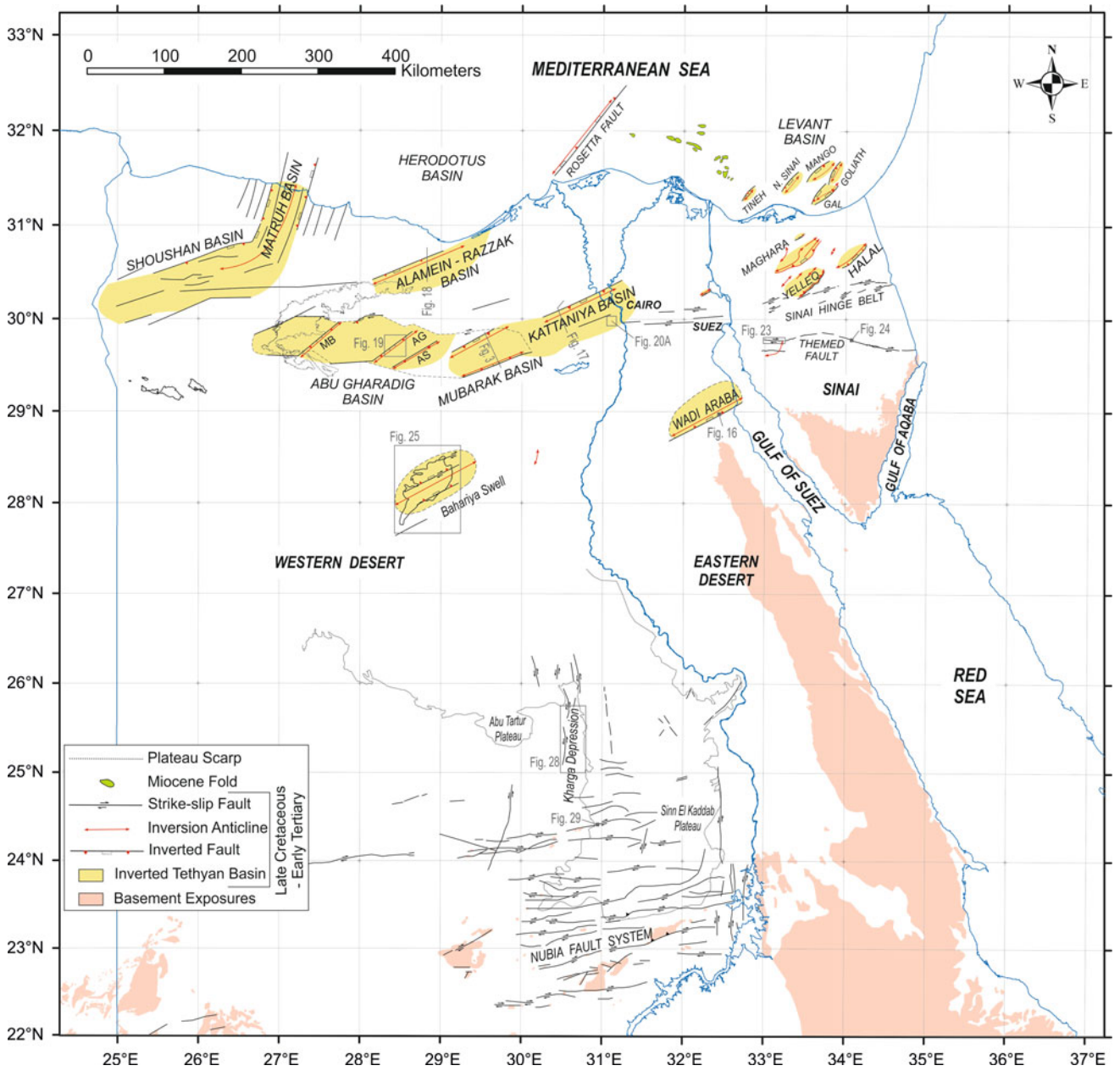

Fig. 7.6 Late Cretaceous-Recent compressive structures of Egypt. Abbreviations in the Abu Gharadig Basin stand for Mid-Basin Arch (MB), Abu Gharadig Anticline (AG), and Abu Sennan Anticline (AS)

affected the southern areas first and migrated northward to the northernmost part of the plate. This may be attributed to the fact that the Late Cretaceous-Tertiary convergent structures represent reactivation (inversion) of the Jurassic rift structures where these inverted faults were the first to respond to the compressive stress resulting from plate convergence. After a relatively long period of reactivation, the compressive stress formed younger structures in the younger rocks lying at the northern part of the plate.

7.2.3.1 Late Cretaceous-Tertiary Inversion Folds of Northern Egypt

Late Cretaceous-Tertiary inversion affected the Jurassic rift basins of northern Egypt. Inversion folds are several tens of kilometers long and about 20 km wide and have NE-SW orientation. They are also asymmetric with very steep, vertical, or overturned flanks at the side of the inverted main basin-bounding faults. Inversion structures are exposed in the following areas (Fig. 7.6):

1. Northern Sinai (Gebel Maghara, Gebel Yelleg, and Gebel Halal).
2. Northern Eastern Desert (Wadi Araba and Gebel Shabrawet).
3. Western Desert (Abu Roash area and Bahariya Oases).

Inversion structures were also recognized in the subsurface (during exploration for hydrocarbons) in the following areas:

1. Northern Western Desert (Kattaniya, Alamein-Razzak, Mubarak, Abu Gharadig, and Matruh-Shoushan Basins).
2. Offshore northern Sinai (e.g. Mango and Goliath folds, among others).
3. Rosetta fault area on the western side of the Nile Cone.

It is obvious that the inverted main basin-bounding faults change polarity from northern Sinai to the northern Western Desert (Fig. 7.6). For this reason, the steep flanks of the inversion folds also follow this polarity change.

A. Northern Sinai Inversion Structures

A belt of NE-SW oriented doubly-plunging, SE vergent anticlines is well exposed in northern Sinai (Moon and Sadek 1921; Sadek 1928; Shata 1959; Youssef 1968; Moustafa and Khalil 1990). This belt includes three major highly asymmetric folds at Gebel Maghara, Gebel Yelleg, and Gebel Halal; each with length of about 40–60 km and average width of about 15 km (Fig. 7.7). These highly asymmetric folds have gently dipping northwestern flanks and very steep southeastern flanks that are in places vertical or even overturned.

Gebel Maghara Structure

Gebel Maghara structure is about 60 km long and 15 km wide deforming the exposed Jurassic and Cretaceous rocks. It has the highest structural relief among the northern Sinai folds with about 2-km thick Jurassic section exposed in its breached core. Detailed structural mapping (Moustafa 2014) shows that this structure is made up of four main NE-SW oriented, asymmetric anticlines bounded on their southeastern sides by reverse faults dipping at 50–73° NW (Fig. 7.8). The amount of reverse slip of these faults reaches 1250 m. The Gebel Maghara anticlines are dissected by transverse, steeply dipping (>65°) normal faults with relatively small amounts of throw (few tens of meters), Moustafa (2013). Seismic reflection section shows that the Gebel Maghara reverse faults are positively inverted and had normal slip in Jurassic time (Fig. 7.9). The southernmost fault bounding the outer side of Gebel Maghara structure (Um Asagil Fault) is 55 km long and is the main bounding fault of an inverted Jurassic half graben basin. Surface geological mapping indicates that this fault is made up of six right-stepped en echelon segments (Fig. 7.8); perhaps indicating that inversion was transpressive. The middle reverse fault of Gebel Maghara area (Mizeraa Fault) is made up of several segments oriented NE-SW, N-S, and E-W to WNW-ESE. The NE-SW oriented fault segments show pure reverse slip whereas the N-S and E-W to WNW-ESE oriented fault segments show oblique-slip. These differently oriented fault segments reflect the early zigzag linkage of normal fault segments during the Jurassic extensional phase and were reactivated during the inversion stage where the NE-SW segments were reactivated by almost pure reverse slip and the other two fault trends were reactivated by oblique slip and form oblique ramps (Moustafa 2014).

Surface geological data (Moustafa 2014) indicate that inversion started in the Santonian and continued into the Middle Eocene. Breaching of the inversion anticlines started at Paleocene time as indicated by syn-tectonic debris flow derived from Jurassic rocks and deposited in the lower part of the Paleocene sediments on the southern side of Gebel Maghara (Fig. 7.10). Most of the Maghara inverted structure stood high above the Paleocene and Eocene sea levels, allowing deposition of the Lower Tertiary sediments on the outer margins of the inverted structure. Lower Eocene rocks on the southern side of the Maghara inverted structure contain syn-depositional carbonate boulders and also dip gentler than the nearby Cretaceous rocks due to continued folding during the Eocene time.

Gebel Yelleg Structure

The Gebel Yelleg NE-SW oriented anticline deforms the exposed Upper Cretaceous rocks and is 45 km long and 18 km wide. Detailed structural mapping (Moustafa and Fouda 2014) indicates that the Gebel Yelleg anticline is doubly plunging with SE vergence; the northwestern flank has average NW dip of 5° and the southeastern flank has steep dip up to 56° SE (Fig. 7.11). This anticline is pervasively dissected by steep (up to 79°) NW-SE oriented normal faults with 5 km average length and tens of meters throws (Moustafa 2013). The Yelleg anticline is bounded on the NW side by a number of NE-SW oriented right-stepped en echelon folds (Falig, Meneidret Abu Quroun, and Meneidret El Etheili) that are 5–14 km long and 4–2 km wide. The Falig Anticline is asymmetric with the northwestern flank dipping up to 70° NW (Fig. 7.12a). Seismic reflection data shows that this steep flank is bounded by a high-angle reverse fault covered by the Quaternary alluvium (Fig. 7.12b). Another seismic section at the northeastern downplunge area of the Yelleg Anticline (Fig. 7.9) indicates that the Gebel Yelleg folds overlie an asymmetric graben. This graben contains thicker Jurassic rocks than the areas to

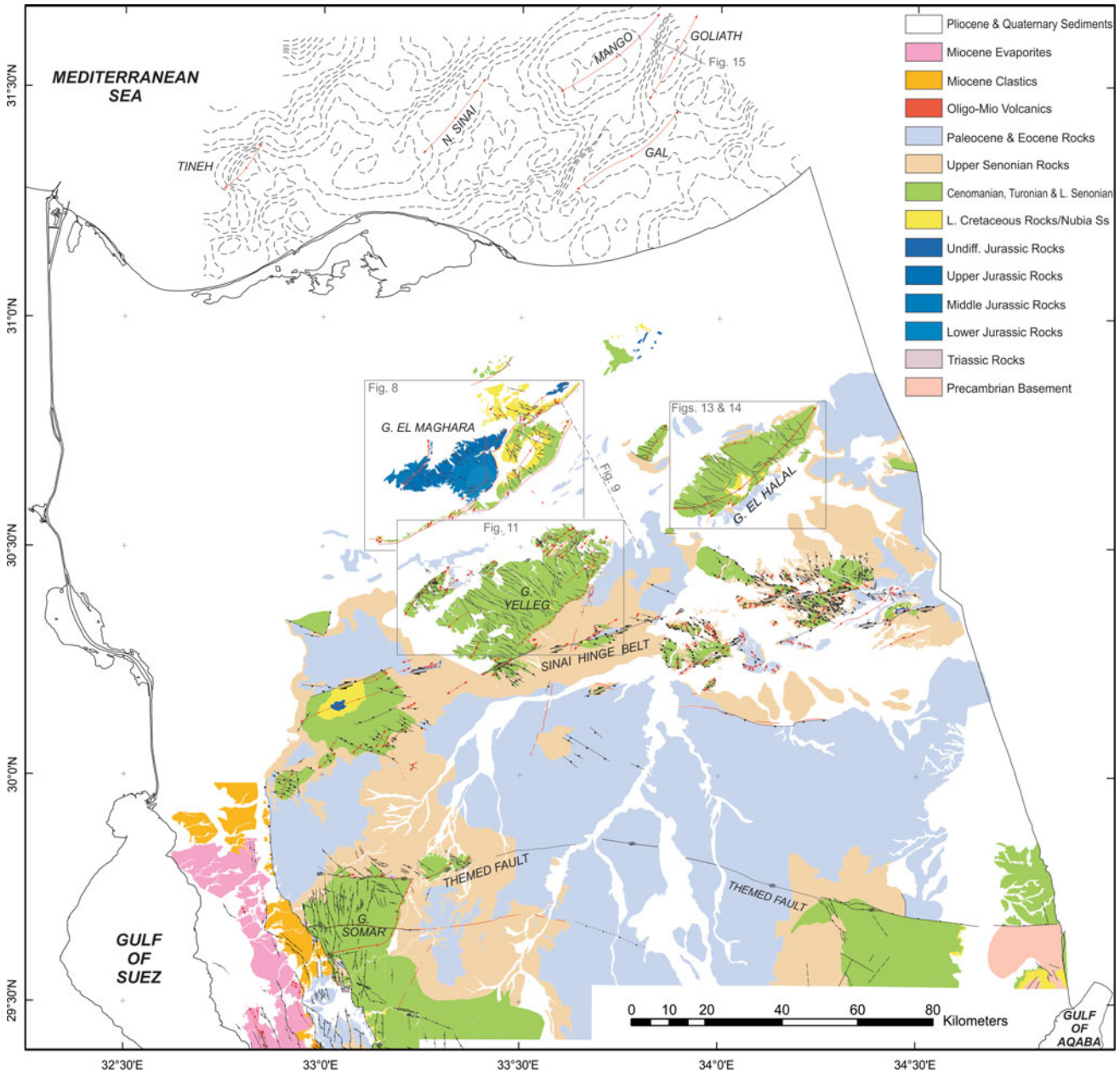

Fig. 7.7 Geological map of northern Sinai (compiled from Moustafa 2004, 2014; Abd-Allah et al. 2004; Moustafa and Khalil 1994; Moustafa and Fouda 2014, and Moustafa et al. 2014) showing the inversion structures of Gebel Maghara, Gebel Yelleg, and Gebel Halal as well as the Sinai Hinge Belt and Themed Fault. Structure contours in offshore northern Sinai are top Coniacian two-way-time structure contours (after Yousef et al. 2010) representing the offshore inversion folds

the NW and SE. The steep SE flank of Gebel Yelleg Anticline overlies the main SE-bounding fault of the graben and represents a fault-propagation fold above this inverted fault. On the other hand, the NW Falig reverse fault (Fig. 7.12b) coincides with the NW-bounding fault of the Jurassic graben. The Upper Cretaceous, Paleocene, and Eocene rocks are folded in the Gebel Falig area with the dip angles of the folded Eocene rocks gentler than those of the Cenomanian and Turonian rocks which indicate growth of the folding from Late Cretaceous to Early Tertiary time.

The surface and subsurface structures of Gebel Yelleg area indicate three phases of deformation; a Jurassic extensional phase, a Late Cretaceous-Early Tertiary compressional phase, and an Early Miocene extensional phase associated with volcanicity. The Jurassic extensional phase led to the development of NE-SW oriented asymmetric

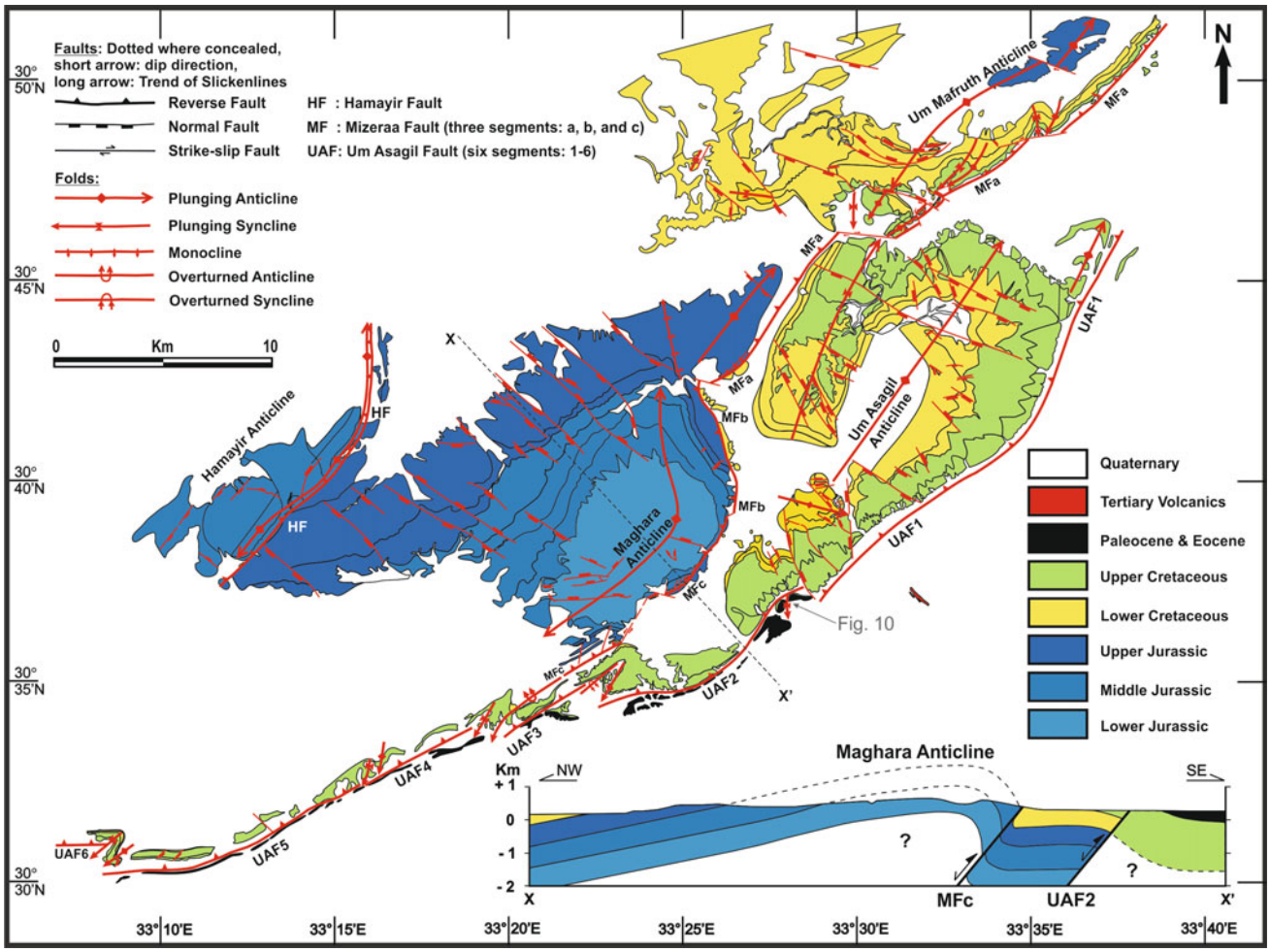

Fig. 7.8 Detailed geological map and structural cross section of Gebel Maghara area after Moustafa (2014)

graben with thicker Jurassic section. The compressional phase led to positive inversion of the graben and development of the surface-mapped folds and associated faults.

Gebel Halal Structure

The Gebel Halal NE-SW oriented doubly plunging anticline deforms the exposed Cretaceous rocks and is 43 km long and 14 km wide. Detailed structural mapping (Abd-Allah et al. 2004) indicates the SE vergence of the anticline (Fig. 7.13). The northwestern flank has an average dip of 15° NW and the southeastern flank is mostly vertical to overturned, especially in the central part of the fold at Wadi El Hazira. This flank is believed to overlie a NE-SW oriented reverse fault. The geometry of the steep fold flank indicates that the underlying reverse fault is made up of several right-stepping en echelon segments (Fig. 7.14); similar to the reverse faults bounding the southeastern side of Gebel Maghara structure. Like Gebel Maghara and Gebel Yelleg folds, the Gebel Halal Anticline is pervasively dissected by a large number of transverse NW-SE oriented normal faults that have steep dip (average 74°), long length (average 5 km), and relatively small throws of few tens of meters (Moustafa 2013). The Lower Senonian rocks are missing in the southern flank of Gebel Halal Anticline where the Turonian rocks are directly overlain by Upper Senonian chalk (Said 1962; Abd-Allah et al. 2004), indicating onset of folding before deposition of these chalks.

The Halal-1 well was drilled in the core of Gebel Halal Anticline and penetrated the thickest Jurassic and Triassic sections in Sinai (3234 m and 914 m, respectively); perhaps indicating that Gebel Halal area represents a NE-SW oriented Triassic-Jurassic extensional sub-basin positively inverted at Late Cretaceous time to form the folds mapped at the surface. The right-stepping en echelon segments of the inverted fault may indicate that inversion was transpressive.

Offshore Sinai Folds

The offshore north Sinai area includes inversion anticlines similar to the exposed folds discussed above (Ayyad et al. 1998 and Yousef et al. 2010). Yousef et al. (2010) mapped

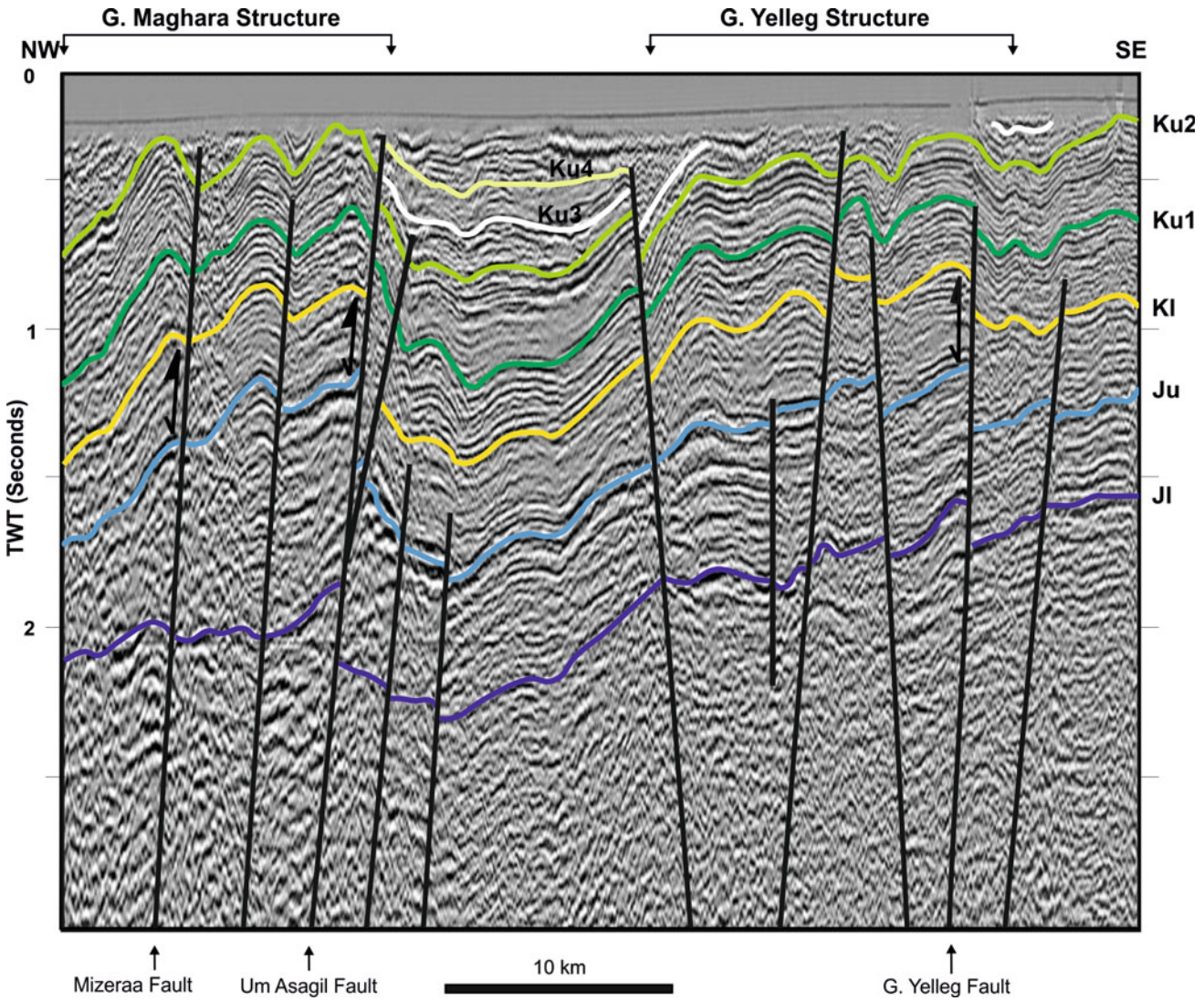

Fig. 7.9 Seismic section extending from the eastern part of Gebel Maghara Anticline to the eastern nose of Gebel Yelleg Anticline after Moustafa (2010). Symbols designate the following reflectors: top intra-Lower Jurassic Rajabiah Formation (Jl), top of the Upper Jurassic Masajid Formation (Ju), top of the Lower Cretaceous (Kl), tops of the Intra-Upper Cretaceous units (Ku1 and Ku2), top of Santonian (Ku3) and top of Maastrichtian chalk (Ku4). Note the sedimentary wedge between Jl and Ju reflectors that thickens southeastward against Um Asagil inverted fault. Note also SE-vergent folds affecting most of the rocks. See Fig. 7.7 for location

five doubly plunging inversion anticlines in the offshore area (Mango, Goliath, NS-21, Gal, and Tineh, Fig. 7.7) using seismic and borehole data. The Mango Anticline is 32-km long, NE-oriented, asymmetric with steeper northwestern flank and breached crest. The Goliath Anticline is 26-km long, NNE-oriented, and asymmetric with steeper northwestern flank bounded by a NNE-oriented inverted fault (Fig. 7.15). The North Sinai 21 Anticline is 25-km long, NE-oriented, and has steeper northwestern flank. The Gal Anticline is 35-km long, NNE-oriented, and has a relatively steep SE flank. The Tineh structure is 15-km long and NE-oriented. Borehole and seismic data indicate that the Top Jurassic to Top Santonian succession represents the syn-rift section. Inversion took place in post-Santonian time as the Campanian-Maastrichtian and Paleogene sequences are progressively onlapping the underlying folded units. Campanian–Maastrichtian sediments have minimum thicknesses over the crests of the inversion anticlines (Fig. 7.15). Basin inversion in offshore northern Sinai continued to the Middle Miocene time (Yousef et al. 2010) or even post-Miocene (Fig. 7.15).

B. Northern Eastern Desert Inversion Structures

Wadi Araba Structure

Wadi Araba Anticline is a prominent structure in the northern Eastern Desert (Fig. 7.6). It is oriented ENE-WSW

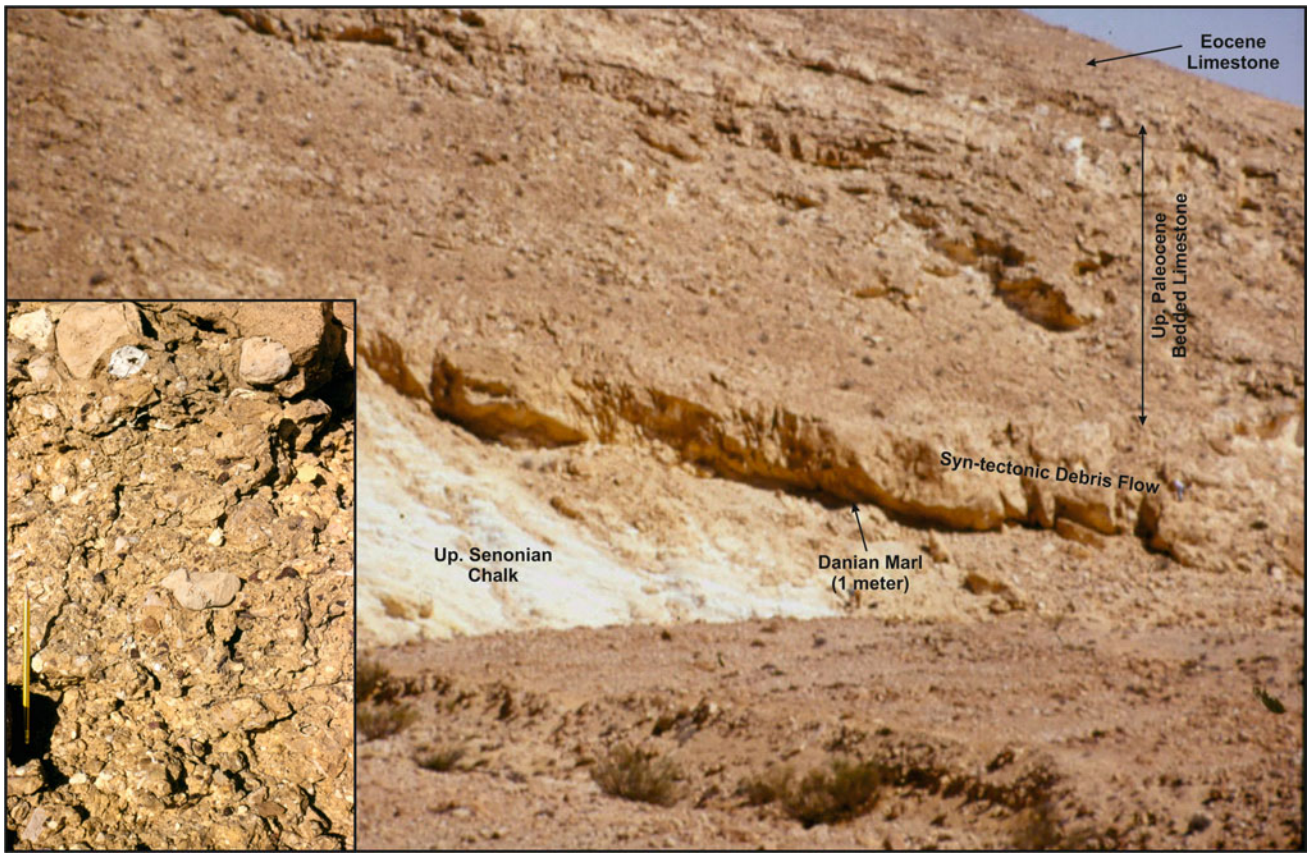

Fig. 7.10 Field photograph of the southern flank of Gebel Maghara Anticline showing debris flow unit in the lower part of the Paleocene rocks. Inset photo is a close-up view of the debris flow showing clasts derived from the Jurassic rocks. See Fig. 7.8 for location

with breached core occupied by Wadi Araba where the oldest (Carboniferous) rocks are exposed. The northern flank of Wadi Araba Anticline dips very gently (few degrees) toward the NNW whereas the southern flank has very steep SE dip represented by nearly vertical Upper Cretaceous rocks at the northern scarp of the South Galala Plateau with excellent exposure at St. Anthony Monastery (Fig. 7.16). Nearly vertical Turonian and Lower Senonian rocks at this locality are unconformably overlain by nearly flat Campanian and younger carbonate rocks indicating Santonian age folding. The Wadi Araba Anticline continues further east into the offshore area of the Gulf of Suez (Moustafa and Khalil 1995). The steep flank of the fold was interpreted to overlie a steep NW dipping reverse fault and the Wadi Araba Anticline is a fault-propagation fold. Although there is no direct evidence to show that the reverse fault of Wadi Araba structure had an earlier phase or normal slip, the structure is considered a positive inversion structure by comparison with similar structures of the same trend, geometry, and time of folding in other areas of northern Egypt. The development of Wadi Araba Anticline affected the facies of the Eocene sediments in vicinity of its steep southeastern flank indicating that Eocene sediments are part of the syn-inversion sequence. Eocene slope deposits were reported to the south and southeast of the Wadi Araba Anticline at St. Paul Monastery area and Wadi Thal (west-central Sinai) respectively (Abul-Nasr 1986; Abul-Nasr and Thunell 1987; Abou-Khadrah et al. 1994).

Gebel Shabrawet Structure

About 150 km to the north of Wadi Araba, Cretaceous rocks exposed at Gebel Shabrawet are folded by an ENE-WSW oriented anticline (Faris and Abbass 1961; Al-Ahwani 1982) with an overturned southeastern flank bounded by a northward dipping reverse fault (Moustafa and Khalil 1995). These folded rocks are unconformably overlain by gently dipping Middle Eocene rocks with a hiatus represented by Campanian-Maastrichtian, Paleocene, and Lower Eocene rocks (Al-Ahwani 1982) indicating post-Santonian to pre-Middle Eocene folding time. This anticline marks the southern side of an inverted basin most of which is now in the subsurface to the north of Gebel Shabrawet. Selim et al. (2014) showed that the Middle Eocene (syn-inversion) sediments on the southern side of the Gebel Shabrawet

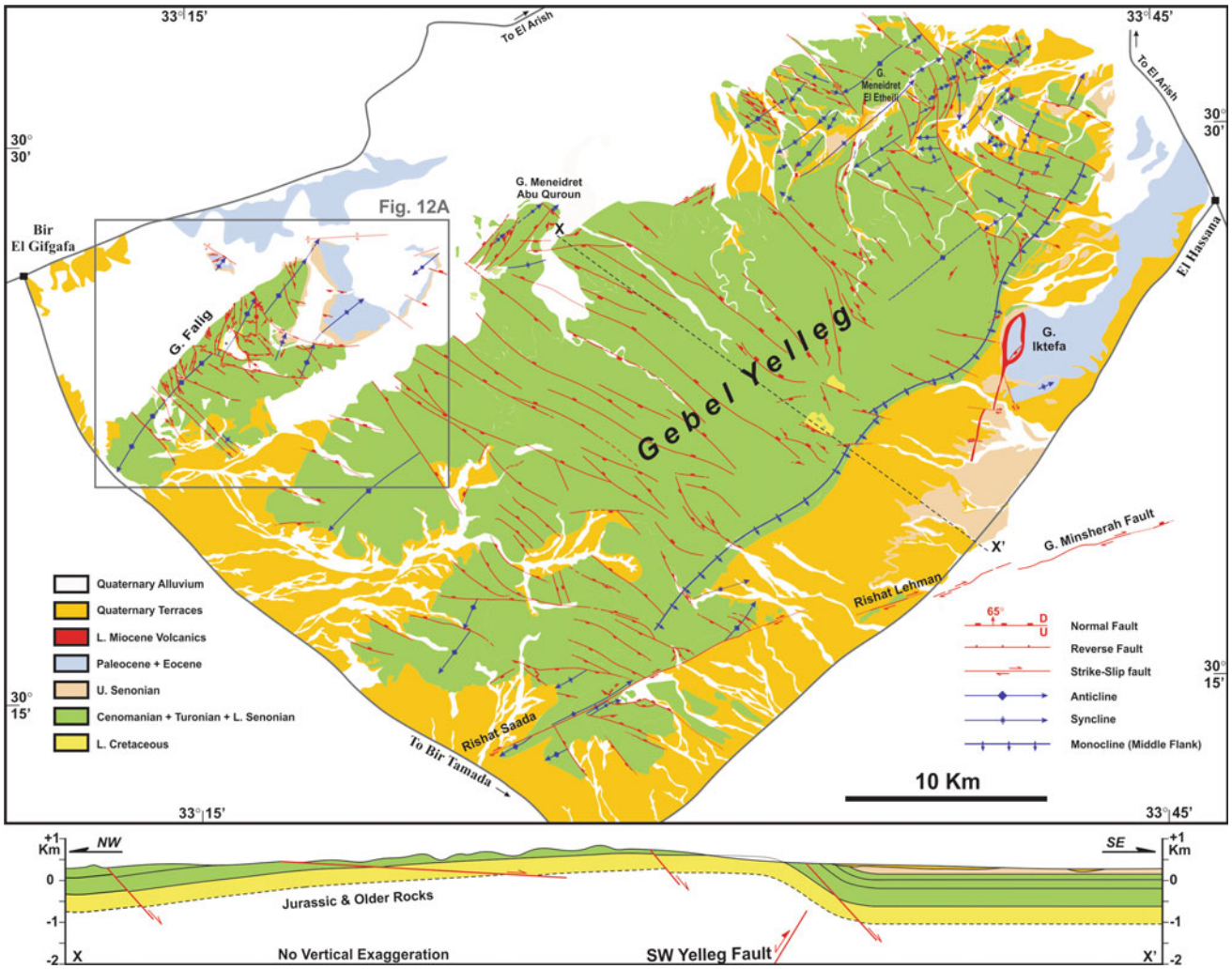

Fig. 7.11 Detailed geological map and structural cross section of Gebel Yelleg area (after Moustafa and Fouda 2014). See Fig. 7.7 for location

Anticline form a red clastic wedge made up of stacked alluvial fan to lagoonal sequences with cross beds showing southeastward paleocurrent direction (parallel to the vergence of the anticline).

C. Northern Western Desert Inversion Structures

Inverted structures in the northern Western Desert are located at Kattaniya, Mubarak, Alamein-Razzak, Abu Gharadig, and Matruh-Shoushan Basins.

Kattaniya Inverted Basin

The Kattaniya inverted basin is about 120 km long and 40 km wide and extends for some distance east of the Nile River. Syn-rift rocks in the Kattaniya Basin include about 2750 m Jurassic sediments in the depocenter of the basin (Abd El-Aziz et al. 1998), Fig. 7.17. Basin inversion at Late Cretaceous—Early Tertiary time led to the development of a very large NE-SW oriented asymmetric anticline with high structural relief comparable to that of Gebel Maghara area (Fig. 7.17a). Deep erosion of the crest of the anticline took place in the Campanian-Maastrichtian, Paleocene, and Eocene times leading to exposure of the Lower Cretaceous rocks in the eroded core of the anticline where they were covered later by Oligocene shales of the Dabaa Formation (area of T57-1 well in Fig. 7.17a). The syn-inversion sediments of the Campanian-Maastrichtian Khoman Chalk and the Paleocene-Middle Eocene Apollonia Formation were not deposited at the crest of the anticline that stood as an island in the Late Cretaceous-Middle Eocene seas (Salem 1976), Fig. 7.17. Thick syn-inversion sediments of the Khoman and Apollonia Formations were deposited on both sides of the inversion anticline in foredeep basins. The Apollonia Formation has a maximum thickness of about 2450 m in the Gindi Basin to the south of the Kattaniya inversion (area of Qarun E-1x well in Fig. 7.17a). Like Gebel Maghara inverted basin, the Kattaniya Basin is fully inverted and

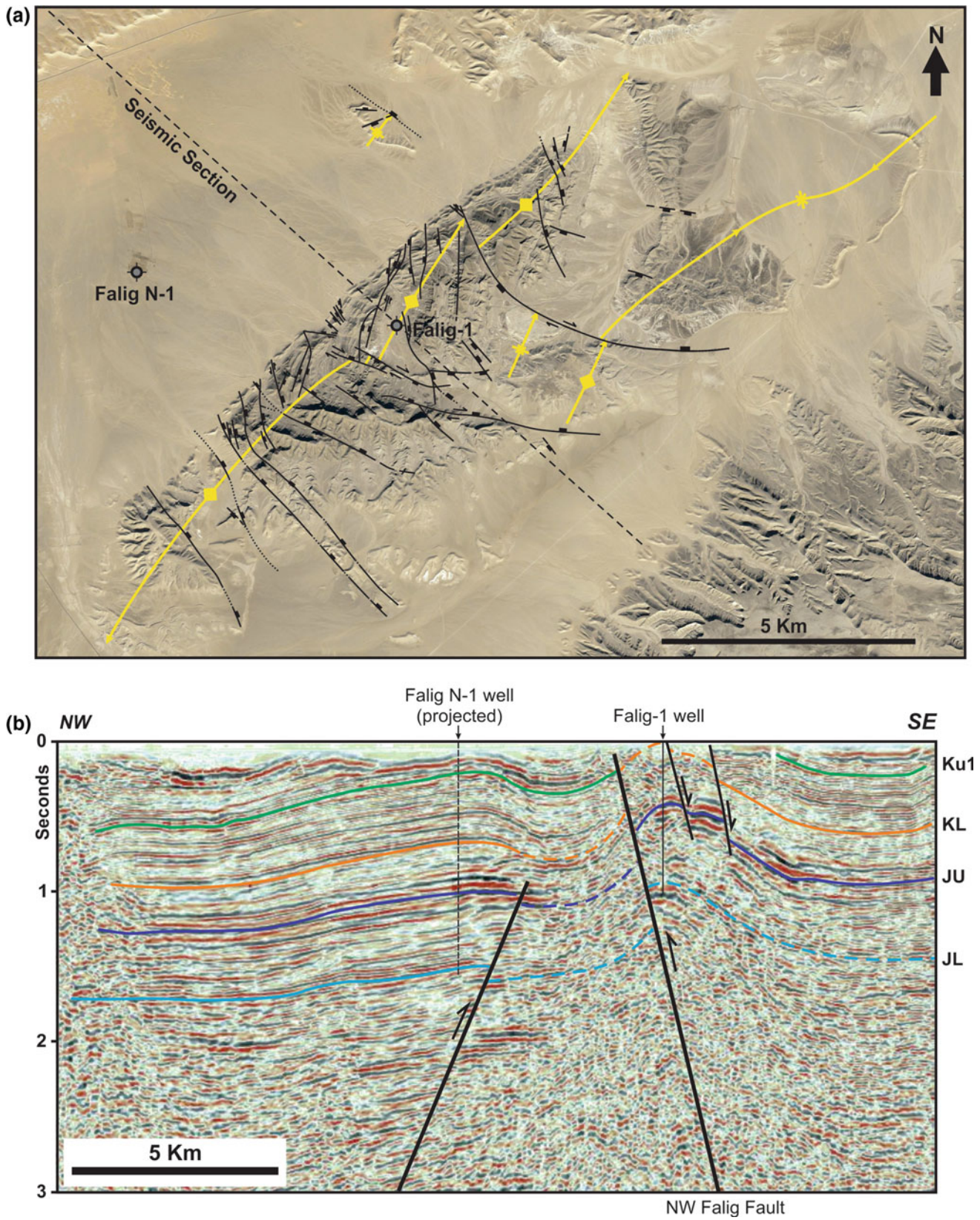

Fig. 7.12 **a** Google Earth image (©2013 DigitalGlobe) of the Gebel Falig Anticline showing its steep NW flank and the main structural features, See Fig. 7.11 for location. **b** Seismic section across the Falig Anticline showing a reverse fault bounding the steep NW flank (NW Falig Fault), after Moustafa and Fouda (2014)

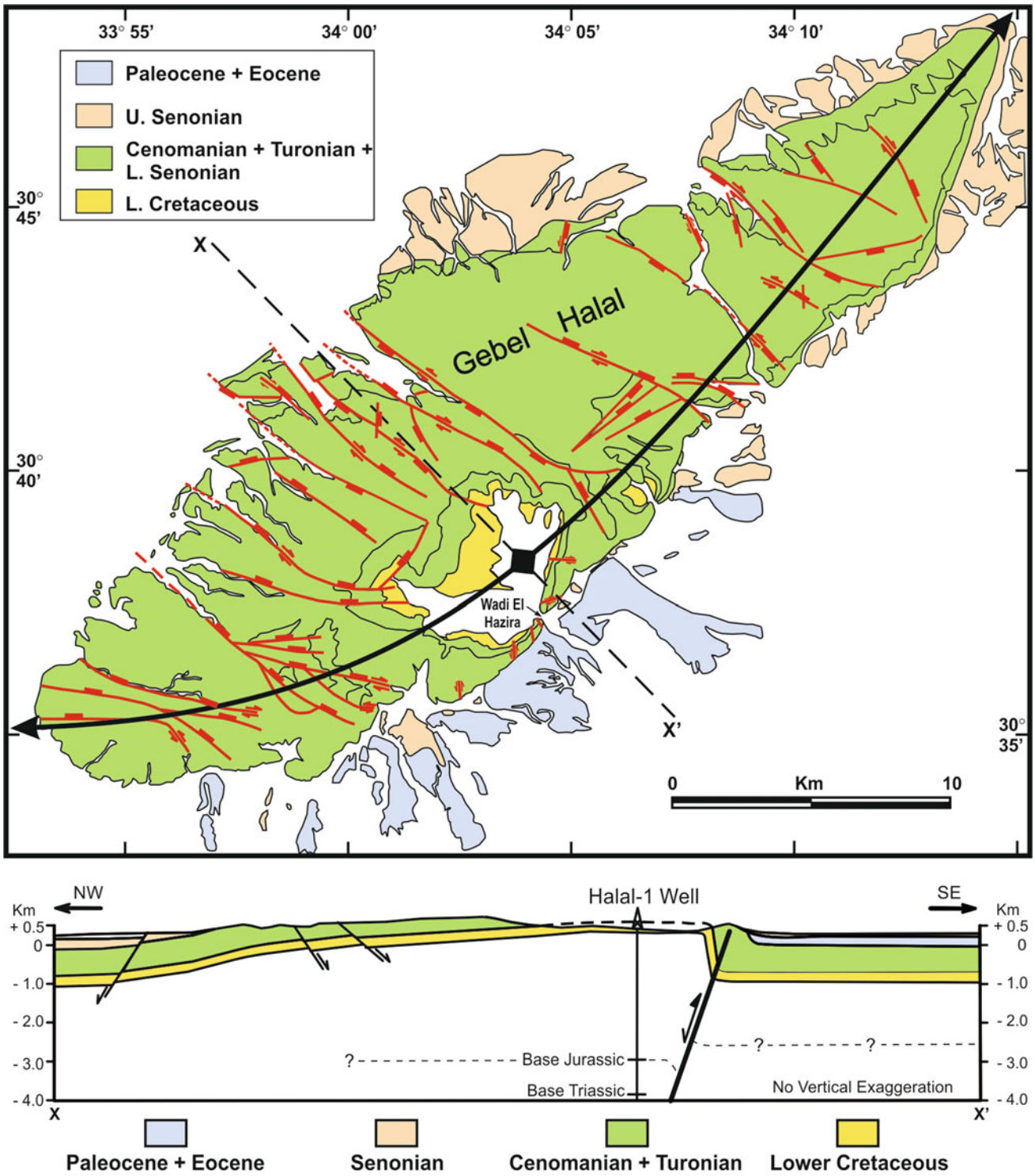

Fig. 7.13 Detailed geological map of Gebel Halal area (after Abd-Allah et al. 2004) and structural cross section (after Moustafa 2010). See Fig. 7.7 for location

seismic reflection data indicate reverse slip of all rock units (down to the Precambrian basement) on the Kattaniya inverted fault (Fig. 7.17a). Also, a clear truncation unconformity marks the boundary between the syn-rift/post-rift rocks and the syn-inversion rocks especially at the two flanks of the inversion anticline (Fig. 7.17b).

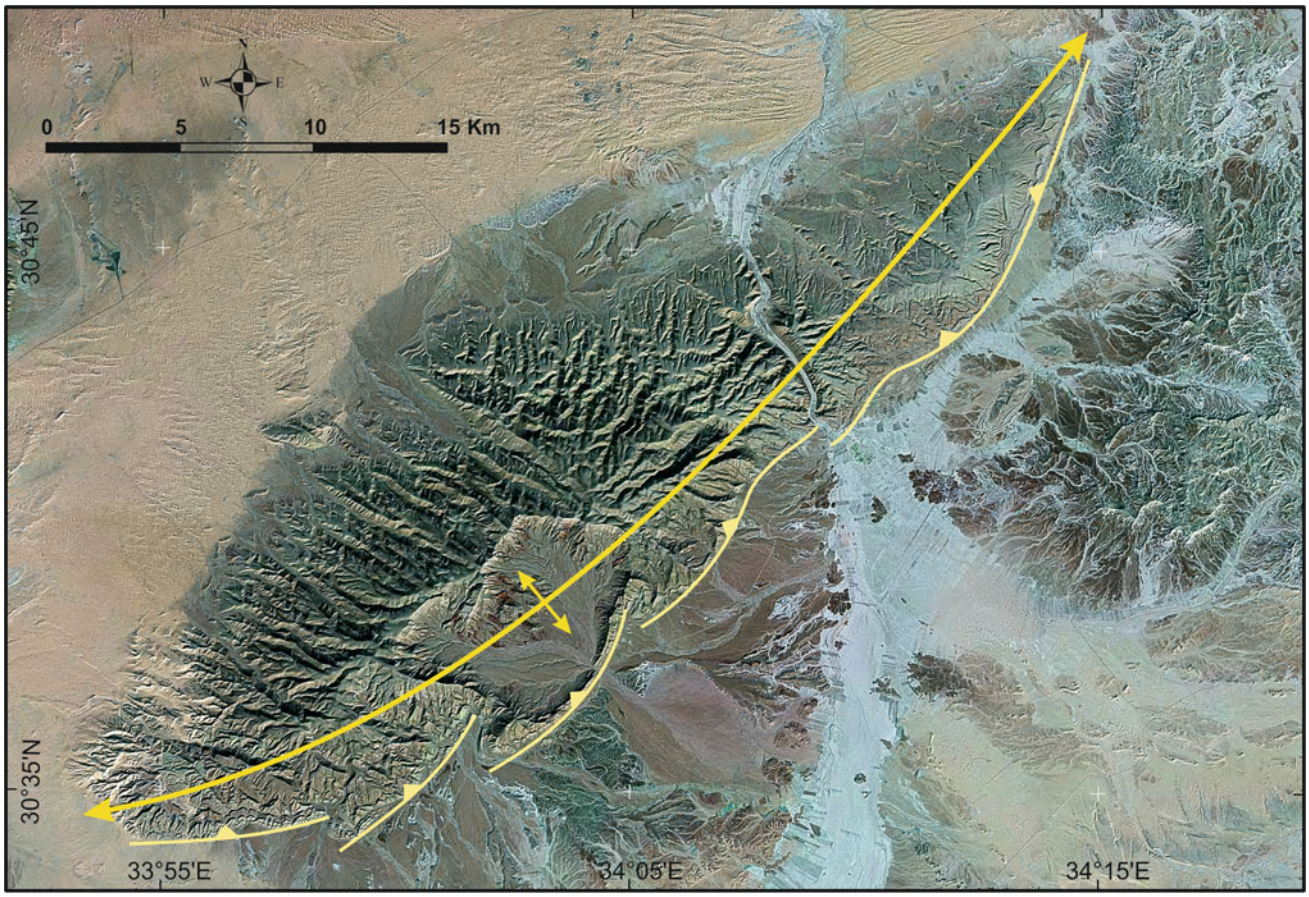

Fig. 7.14 Landsat image of Gebel Halal Anticline showing right-stepped en echelon faults bounding its southeastern asymmetric flank. See Fig. 7.7 for location

Mubarak Inverted Basin

Mubarak inverted basin lies at a short distance to the southwest of the Kattaniya Basin. It has NE-SW orientation and the main inversion anticline is located at the northwestern side of the basin (Figs. 7.3 and 7.6). The magnitude of inversion is less than that of the Kattaniya Basin as normal fault separation is obvious at the lower part of the inverted main basin-bounding fault. The southeastern bounding fault of Mubarak Basin was also inverted forming a small-relief anticline at this side of the basin (Fig. 7.3). Syn-rift sediments in the Mubarak Basin are represented by Jurassic as well as Cretaceous rocks as young as the Coniacian. Syn-inversion rocks include mainly the Campanian-Maastrichtian and Eocene rocks. Borehole data indicate a very thin Eocene section at the crest of the inversion anticline. Seismic reflection data also indicate that inversion continued mildly during Late Eocene and post-Oligocene times leading to gentle folding of the Dabaa Formation (Fig. 7.3).

Alamein-Razzak Inverted Basin

The Alamein-Razzak inverted basin has consistent NE-SW orientation and is 120 km long (Fig. 7.6). Syn-rift rocks in the basin probably include the Triassic in addition to the Jurassic and Lower Cretaceous (Fig. 7.18). Recent high-resolution 3D seismic reflection data indicate that not all of the Lower Cretaceous section (Alam El Bueib Formation) belongs to the syn-rift sequence but only its lower part as the upper part and the overlying Aptian to Coniacian section belong to the post-rift sequence showing no change in thickness across the basin-bounding fault (Fig. 7.18). Reverse slip on the main basin-bounding fault during basin inversion was not large enough to allow upward propagation of the fault through the post-rift sequence but a large NE-SW oriented fault-propagation anticline was formed above the inverted fault. The inversion anticline has several culminations that were mis-interpreted by some investigators (e.g. El-Shaarawy et al. 1992) to be en echelon folds formed by pure dextral strike-slip movement on the fault. Basin

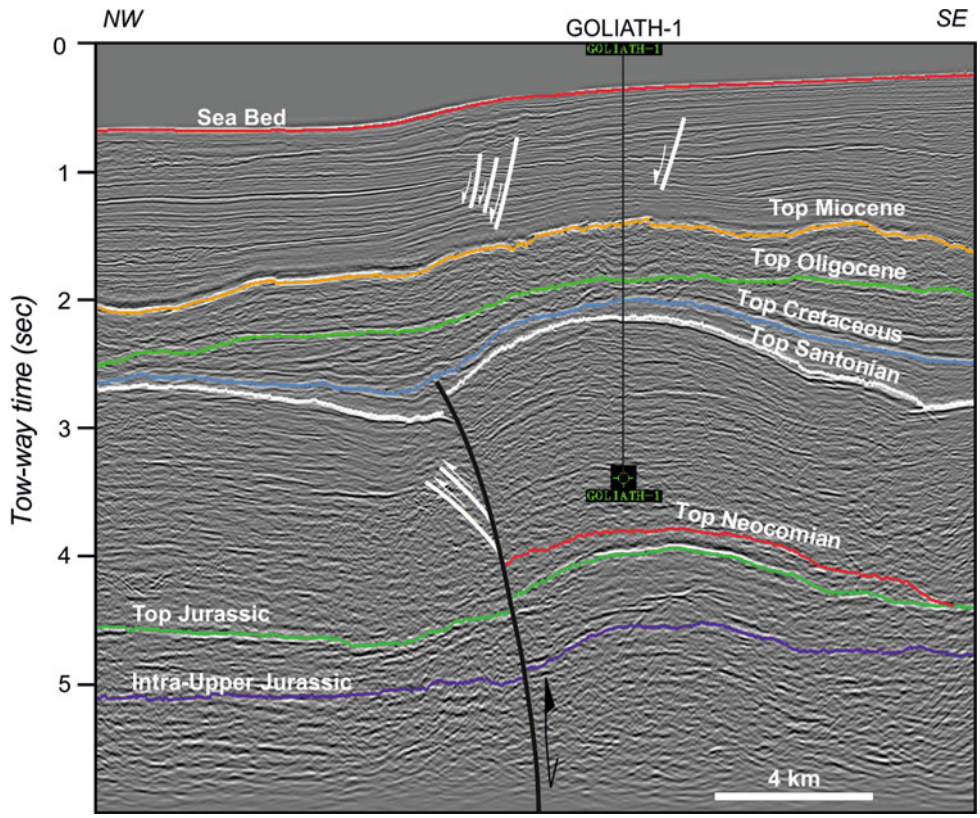

Fig. 7.15 Seismic section showing the Goliath inversion anticline, offshore northern Sinai (after Yousef et al. 2010). See Fig. 7.7 for location

Fig. 7.16 Field photograph of the southern steep flank of Wadi Araba Anticline at St. Anthony Monastery showing nearly vertical Turonian and Lower Senonian rocks unconformably overlain by flat-lying Campanian limestone beds. See Fig. 7.6 for location

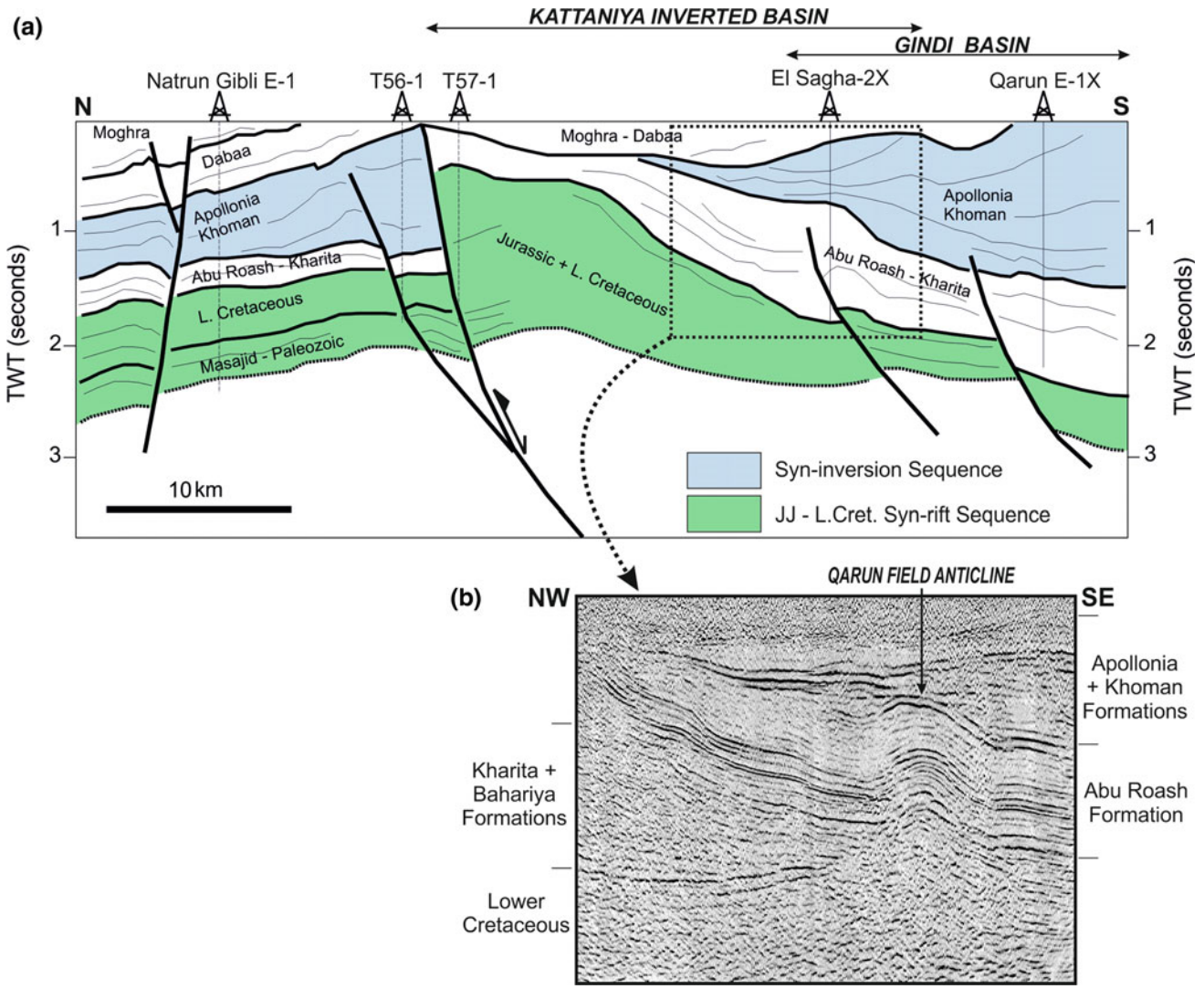

Fig. 7.17 **a** Geoseismic section of the Kattaniya inverted basin slightly modified after Bevan and Moustafa (2012). **b** Seismic section of a portion of the Kattaniya-Gindi Basins at Qarun Field Anticline (after Bakr 2010) showing the wedge shape of the Cretaceous Kharita-Bahariya sediments (that represent a portion of the syn-rift section) and erosion at the high area of the inverted basin. Note also onlap of the syn-inversion units of the Khoman and Apollonia Formations on the Abu Roash Formation at the Qarun Field Anticline and truncation unconformity of the top Abu Roash Formation NW of the anticline. See Fig. 7.6 for location

inversion took place during deposition of the Campanian-Maastrichtian Khoman Formation and affected its thickness at the crest of the inversion anticline. Inversion continued till the Miocene time (Fig. 7.18 and Yousef et al. 2015).

Inverted Structures within Abu Gharadig Basin

Although Abu Gharadig Basin is a Cretaceous rift basin, some NE-SW oriented structures were recognized inside the basin (Fig. 7.6) related to Jurassic NE-SW oriented normal faults reactivated by Late Cretaceous inversion. These inverted structures include the Mid-Basin Arch, Abu Gharadig Field Anticline, and the Abu Sennan structure.

The Mid-Basin Arch of Abu Gharadig Basin is a NE-SW oriented anticline extending diagonally for ~40 km within the basin. This anticline is dissected by NW-SE oriented normal faults into several compartments, one of which forms the BED-2 gas field. At the Cretaceous level of this field, the anticline is obviously asymmetric with steeper SE flank (EGPC 1992).

The Abu Gharadig Anticline is 18–20 km long NE-SW oriented doubly plunging anticline. It is bounded by two oppositely dipping en echelon inverted faults showing reverse slip and fault propagation folding in the Upper Cretaceous rocks (Fig. 7.19). Detailed subsurface mapping using 3D seismic and borehole data (El Gazzar et al. 2016)

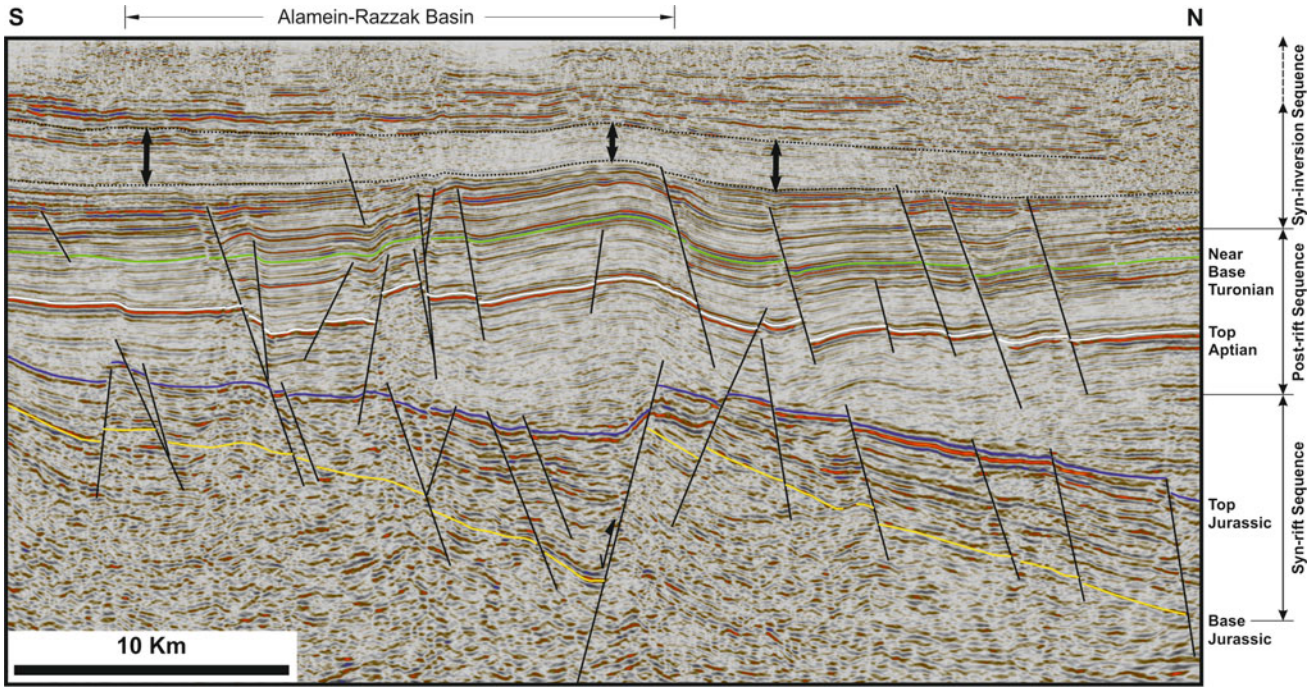

Fig. 7.18 Seismic section across Alamein-Razzak Basin (after Bakr 2010) showing the asymmetric inversion anticline. Note the syn-rift sequences (Jurassic and L. Cretaceous), onlap of the basal part of L. Cretaceous section on top Jurassic, and the thin section of syn-inversion sequence at the anticline crest compared to the flanks (areas marked by vertical lines with double-head arrows). Faults dissecting the post-rift sequence have NW-SE orientation whereas faults dissecting the pre-rift and syn-rift sequences are mostly oriented NE-SW. See Fig. 7.6 for location

indicates that inversion started during the Santonian time and continued to the Oligocene.

The Abu Sennan structure is a 45 km long NE-SW oriented asymmetric anticline lying some 15 km to the SE of the Abu Gharadig Anticline. This structure has several culminations named Southwest Sennan, GPT, GPX, GPY, and GPZ (EGPC 1992). A NW vergent positively inverted fault dissects the Cretaceous rocks underlying the Campanian-Maastrichtian Khoman Chalk of the inversion anticline. The Khoman Chalk and the overlying Eocene rocks are folded by a fault-propagation fold. Reduced thickness of the Khoman Chalk at the crest of the anticline indicates onset of the inversion and folding before its deposition. Folding continued mildly afterwards till end of the Eocene.

Other compressional structures of smaller dimensions also exist in the Abu Gharadig Basin. Although the basin has a general E-W orientation its northern main-bounding fault is made up of several segments oriented E-W, NE-SW, and NW-SE (El Saadany 2008). Late Cretaceous reactivation of these fault segments is represented by reverse slip on the NE-SW oriented fault segments and normal slip on the NW-SE fault segments. These synchronous opposite senses of slip led some investigators to infer dextral strike-slip movement on the E-W fault segments. Reverse slip on the NE-SW fault segments is either due to: (1) positive inversion of these fault segments, or (2) dextral strike- (or oblique-) slip movement on the E-W fault segments where the NE-SW faults form push-up structures between left-stepping E-W faults, as proposed by Said et al. (2014) and Salah et al. (2014) in the BED-17 oil field area.

Another NE-SW oriented push-up structure with similar geometry is located 160 km to the east of the BED-17 structure on the northern side of Abu Gharadig Basin. This push-up structure shows up very well on seismic reflection data and proves that the E-W segments of the main northern-bounding fault of Abu Gharadig Basin had dextral slip at Late Cretaceous time.

Abu Roash Area Push-Up Structures

Another push-up structure similar to that on the northern side of the Abu Gharadig Basin is exposed at Abu Roash area, SW of Cairo (Fig. 7.20). At that locality, the Upper Cretaceous rocks represent the only Cretaceous exposure in the northern Western Desert. Surface geological mapping (Faris 1948; Jux 1954) clearly shows NE-SW oriented folds. Detailed structural mapping led Moustafa (1988) and Abdel Khalek et al. (1989) to recognize strike-slip deformation of this area. The structure of Abu Roash area is made up of three main NE-SW oriented folds, the most prominent of which is dissected by WNW-ESE oriented en echelon, right-lateral, strike-slip faults that represent left-stepping

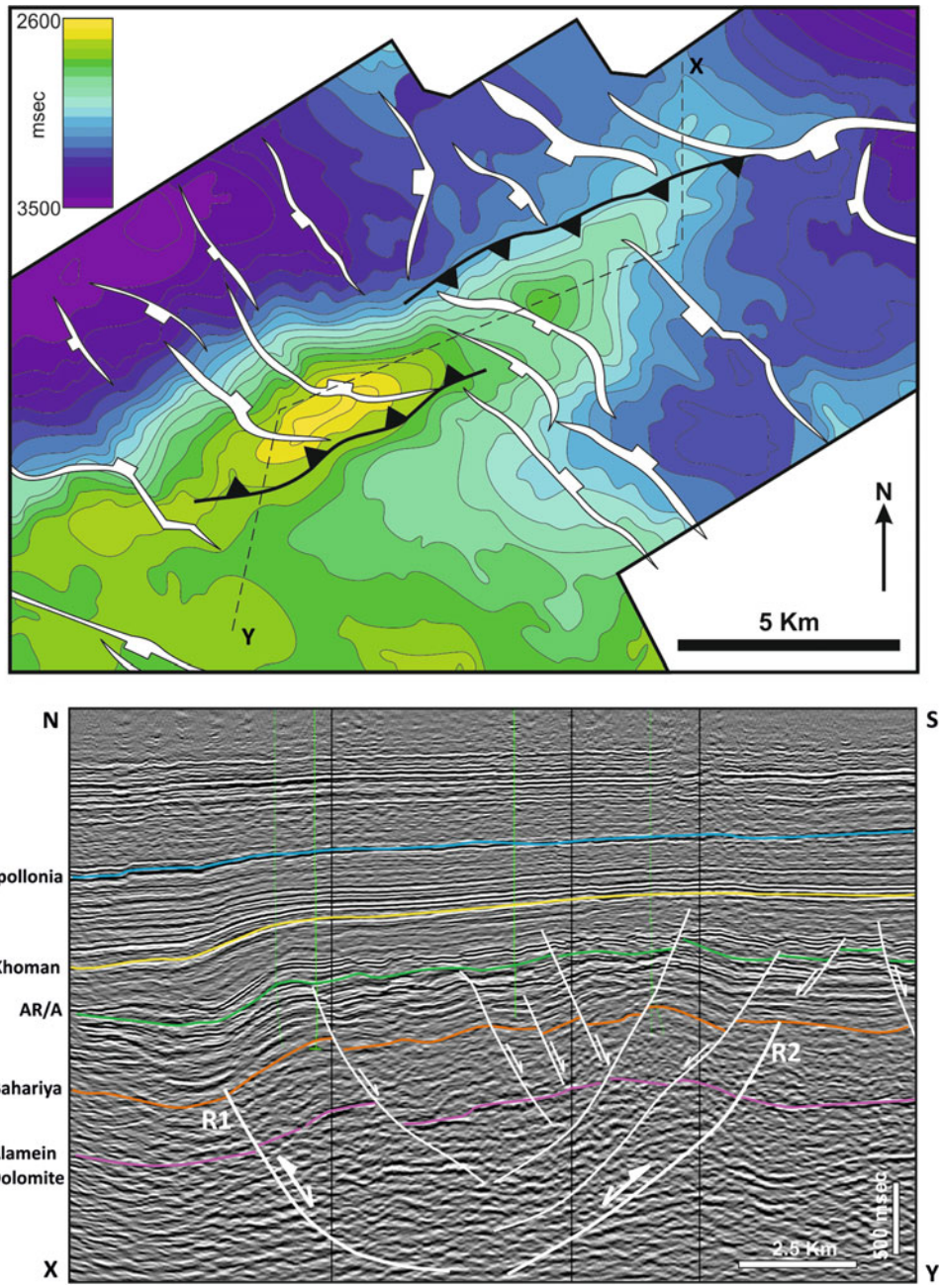

Fig. 7.19 Top Alamein Dolomite time-structural map and seismic section of Abu Gharadig Anticline showing the two en echelon inverted faults (R1 and R2) bounding the NE and SW sides of the anticline (slightly modified after El Gazzar et al. 2016). See Fig. 7.6 for location

Riedel shears (Moustafa 1988; Fig. 7.20). Smaller plunging anticlines lying between these en echelon faults are push-up structures that collectively form the large NE-SW oriented anticline extending from Abu Roash Village to Gebel El Ghighiga passing with the famous Hasana Anticline on the Cairo-Alexandria desert road (Fig. 7.20). A NE-SW oriented positive flower structure is well exposed at Gebel Abu Roash in the NE part of the area and is bounded by oppositely dipping NE-SW oriented reverse faults. Moustafa (1988) interpreted the Abu Roash structures to be the result of E-W dextral shear couple affecting the area. Integration of surface and subsurface structural data indicates that the structures of Abu Roash area represent a large push-up structure formed between the ends of E-W oriented, left-stepping, en echelon, right-lateral strike-slip faults; similar to the push-up areas at the northern-bounding fault of Abu Gharadig Basin.

An angular unconformity was mapped between the Coniacian-Santonian rocks (Plicatula Series) and the Campanian-Maastrichtian chalk on the NW side of Gebel Abu Roash (Moustafa 1988) indicating the onset of compressive deformation of the area. Neither Paleocene nor Lower Eocene rocks were deposited in Abu Roash area indicating that it stood as an island above the Early Tertiary sea level. The outer areas of the folded Upper Cretaceous

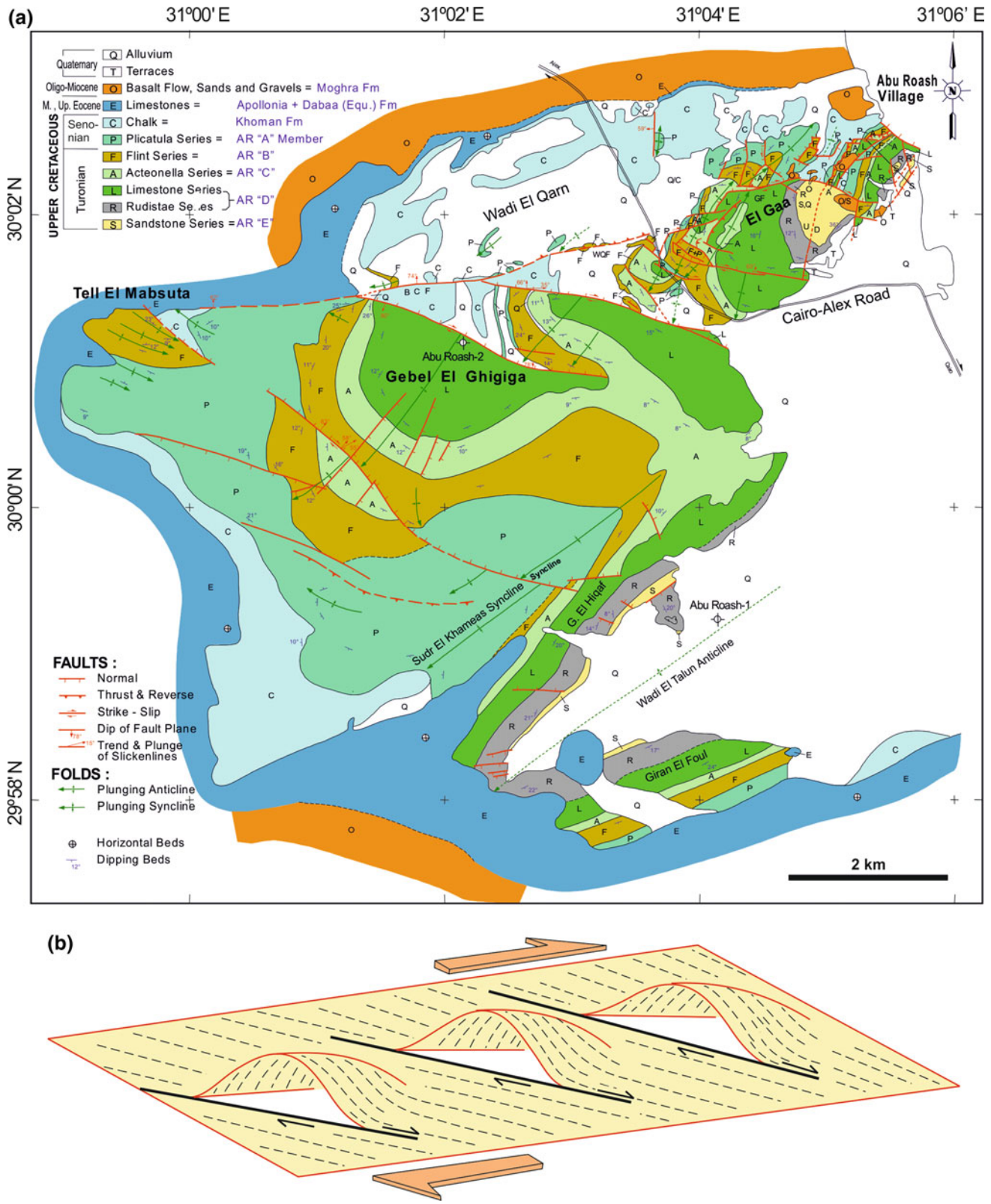

Fig. 7.20 **a** Geological map of Abu Roash area (southwest of Cairo) after Moustafa (1988) and 3D model (**b**) explaining the development of push-up folds between left-stepping en echelon right-lateral strike-slip faults. See Fig. 7.6 for location

outcrops are unconformably overlain by a condensed section of Middle and Upper Eocene rocks indicating continued growth of the structure in the Early Tertiary.

Matruh-Shoushan Inverted Basin

The Matruh-Shoushan inverted basin extends for about 220 km and is unique in showing a new inverted fault trend compared to the above-mentioned basins (Moustafa et al. 2002; Metwalli and Pigott 2005; Tari et al. 2012). NNE oriented faults in the basin show two phases of slip, a Triassic to Early Cretaceous phase of normal slip and a Late Cretaceous phase of reverse slip where the resulting inversion anticlines are oriented NNE-SSW. The Matruh Basin NNE-SSW oriented faults are connected to ENE-WSW and NE-SW oriented normal faults of the Shoushan Basin (Fig. 7.2). Inversion of the Matruh Basin formed a structural high above the Late Eocene-Oligocene sea level leading to non-deposition of the Dabaa Formation.

7.2.3.2 Late Cretaceous-Tertiary Deformation of Areas Lying South of the Inverted Basins

Platform areas lying south of the northern Egypt inverted basins are characterized by nearly horizontal to gently dipping Phanerozoic sedimentary rocks of relatively small uniform thickness compared to the basinal areas to the north. These areas were affected by the compressive stresses resulting from convergence of Afro-Arabia and Eurasia leading to uplift of these areas and/or the reactivation of deep-seated faults. Compressional structures in these areas are contemporaneous with the inversion of the northern basins. These areas include the Sinai Hinge Belt and the Themed Fault in Sinai, the southern Gulf of Suez and northern Red Sea area, the Bahariya Oases in the central Western Desert, and the Nubia Fault System in the southernmost part of the Western Desert.

A. Sinai Hinge Belt

The Sinai Hinge Belt (Fig. 7.7) was first recognized by Shata (1959) as a 250 km long and 20-km wide fractured area at the boundary between the northern Sinai strongly folded area (area where the inverted Mesozoic basins are located) and the north-central Sinai gently folded area. Detailed structural mapping (Moustafa et al. 2014) indicates that this belt includes several ENE-WSW oriented right-stepping en echelon faults associated with folds (Fig. 7.21). Most of the folds of the belt expose Upper Cretaceous (mostly Cenomanian and Turonian) rocks in their cores but a few of them also expose Triassic, Jurassic, or Lower Cretaceous rocks.

Each fault segment of the Sinai Hinge Belt shows right-lateral strike-slip deformation indicated by slickenlines and/or right-stepped en echelon folds (e.g. Mitla Pass, Fig. 7.22). Some lozenge-shaped compressional structures are formed between the ends and stepover areas of some of the right-lateral strike-slip faults (e.g. Um Hosaira Fold) or at restraining bends in the fault segments (e.g. Araif El Naqa Anticline), Fig. 7.21. The early stage of strike-slip deformation of the Sinai Hinge Belt led to popping up of the rocks before they were longitudinally dissected by the faults (Moustafa et al. 2014). The magnitude of horizontal slip on each fault segment is small and horizontal slip is accommodated by folding at the fault ends. NW-SE oriented normal faults dissect the rocks on both sides of the right-lateral strike-slip faults and are abutted by the strike-slip faults. Strike-slip movement in the Sinai Hinge Belt took place in two phases: (1) During the Late Cretaceous-Early Tertiary time. The Late Cretaceous deformation is displayed by the unconformity in the lower part of the Campanian-Maastrichtian chalk at Gebel El Minsherah area (Moustafa and Yousif 1990) and by the syn-tectonic sandstone deposited in the middle of the Campanian-Maastrichtian chalk of Araif El Naqa Anticline (Luning et al. 1998) whereas the Early Tertiary deformation is displayed by the absence of Paleocene sediments in Gebel El Hamra Anticline at the southwestern side of Mitla Pass (Hassan et al. 2015) as well as folding of Eocene rocks at Gebel Araif El Naqa. (2) In post-Early Miocene (leading to dextral offset of Lower Miocene igneous dikes). The Late Cretaceous phase of deformation resulting from the Tethyan convergence continued till the Eocene time in some areas, e.g. Gebel Araif El Naqa.

Moustafa et al. (2014) indicated that the ENE-WSW oriented en echelon strike-slip faults of the Sinai Hinge Belt exist in two sub-belts and reflect the reactivation of two deeper faults underneath these sub-belts. The deep-seated faults are thought to be Jurassic normal faults formed at the boundary between the southern platformal area and the northern basinal area during Tethyan rifting. Later shortening of the area due to the convergence of Afro-Arabia and Eurasia reactivated these faults by dextral transpression expressed by the strike-slip fault segments of the hinge belt and their associated folds. Moustafa et al. (2014) also attributed the post-Early Miocene slip on the Sinai Hinge Belt to the Neogene extensional deformation of the region associated with the NE drift of Arabia away from Africa and Miocene opening of the Gulf of Suez and ancestral Red Sea rift. The Sinai Hinge Belt terminated the Gulf of Suez rift at the latitude of Suez city that caused reactivation of the belt by dextral slip.

B. Themed Fault Area

The Themed Fault (Fig. 7.7) is a narrow 200 km long structural belt extending in north-central Sinai from the eastern margin of the Suez rift to the Dead Sea Transform. This narrow structural belt shows up as a number of en

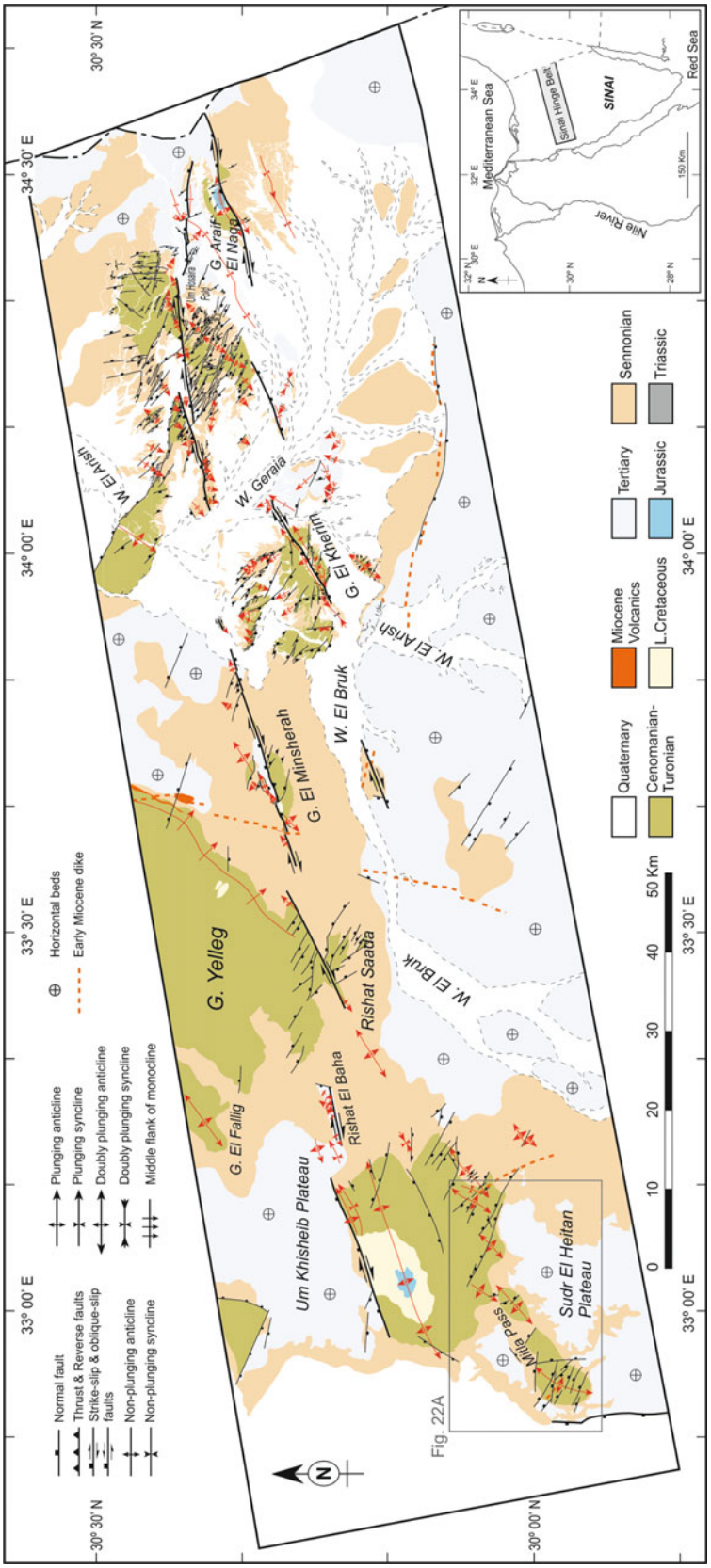

Fig. 7.21 Simplified geological map of the Sinai Hinge Belt after Moustafa et al. (2014)

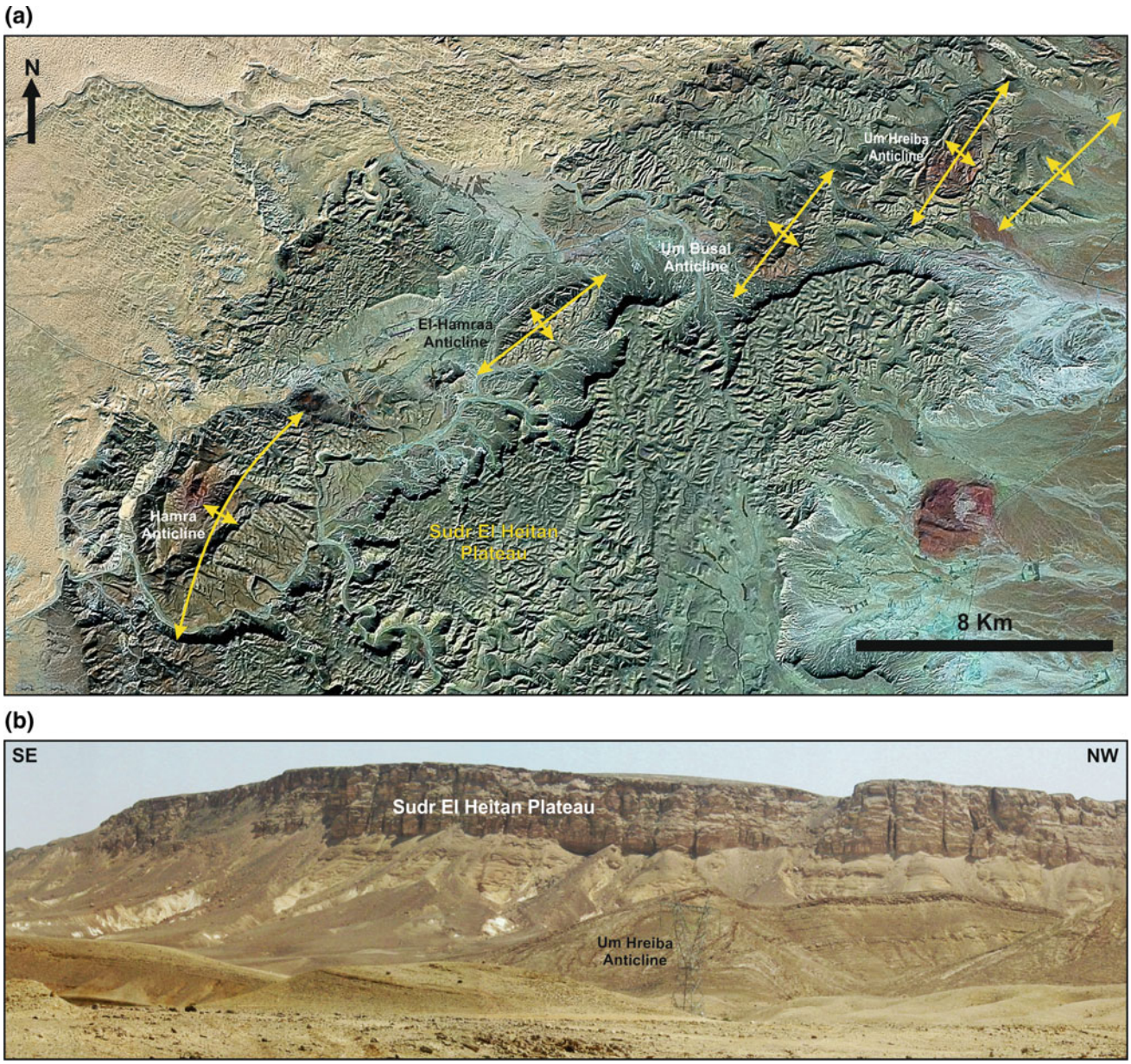

Fig. 7.22 **a** Landsat image of the en echelon anticlines affecting the Upper Cretaceous rocks of Mitla Pass area (northern Sinai). **b** Field photograph of the NE nose of Um Hreiba Anticline and the nearby flat-lying Sudr Chalk and Eocene limestones of Sudr El Heitan Plateau. See Fig. 7.21 for location

echelon faults associated with relatively small plunging and doubly plunging folds through the flat-lying rocks of the Tih Plateau (Fig. 7.23). It shows reactivation of one of the pre-existing faults dissecting the tectonically stable area south of the Sinai Hinge Belt.

Detailed field mapping of the Themed Fault (Moustafa and Khalil 1994) indicates that the eastern and western parts of the fault are very clear, whereas the central part is discontinuous. The western part of the Themed Fault consists of four steeply dipping (50–90°), E-W and ENE-WSW oriented, right-stepping en echelon segments with right-lateral strike-slip displacement. These fault segments are associated by E-W to NE-SW oriented, doubly plunging folds that make acute angles with the Themed Fault (Fig. 7.23). The time of slip on these fault segments is pre-Miocene as they die out before reaching the Suez rift and one of them is intruded by an Early Miocene basaltic dike. The age of folded rocks is Late Cretaceous to Early Eocene, indicating post-Early Eocene movement on the faults.

The eastern part of the Themed Fault dissects Precambrian to Lower Eocene exposures and has E-W orientation and steep northward dip (62–90°). Slickenside lineations and

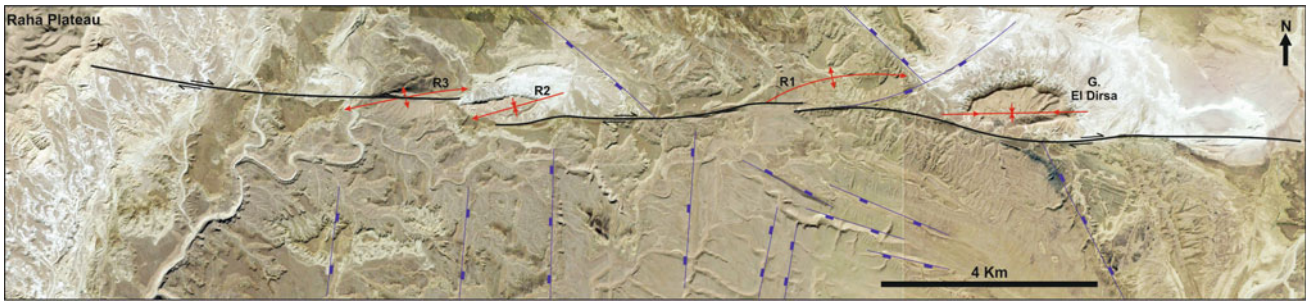

Fig. 7.23 Google Earth image (©2018DigitalGlobe) showing three E-W en echelon segments of the western part of the Themed Fault and the associated folds (R1, R2, R3, and Gebel El Dirsa folds). See Fig. 7.6 for location

chatter marks indicate right-lateral slip on the fault. Also, the Rishat El Themed doubly plunging anticline is dextrally offset by the fault for about 300 m (Fig. 7.24).

The en echelon arrangement of the Themed Fault segments as well as the field-recorded right-lateral slip indicate that it is a narrow dextral wrench zone. Further evidence for dextral wrenching is seen in the right-stepping, en echelon arrangement of the folds and the acute angle between the folds and the Themed Fault.

C. Southern Gulf of Suez Area

Afifi et al. (2016) carried out detailed subsurface study of the southernmost part of the Gulf of Suez rift using 3D seismic and borehole data. Some of the studied boreholes indicate an unconformity between the Cenomanian-Lower Senonian Mixed Facies Unit (Nezzazat Group) and the overlying Campanian-Maastrichtian Brown Limestone/Sudr Chalk unit. They believe the unconformity is Santonian-Campanian and correlates with the unconformity identified in the Syrian Arc folds of northern Egypt. As the nature of this unconformity in the southern Gulf of Suez is not angular, the missing rock units may indicate uplift of this region leading to erosion of the uppermost part of the Mixed Facies Unit at the same time inversion folds were developed further north. This uplifted area in the southern Gulf of Suez rift is referred to as the Ras Mohamed Arch by Peijs et al. (2012). Bosworth et al. (1999) suggested Late Santonian compressional deformation of Gebel El Zeit and Esh El Mellaha areas leading to reactivation of basement fabrics and development of small-scale folds in the sedimentary section.

Fig. 7.24 Vertical aerial photograph of Gebel Rishat El Themed Anticline showing dextral offset by the Themed fault (after Moustafa and Khalil 1994). Outlined area represents the outcrop of Cenomanian rocks in the core of the anticline. See Fig. 7.6 for location

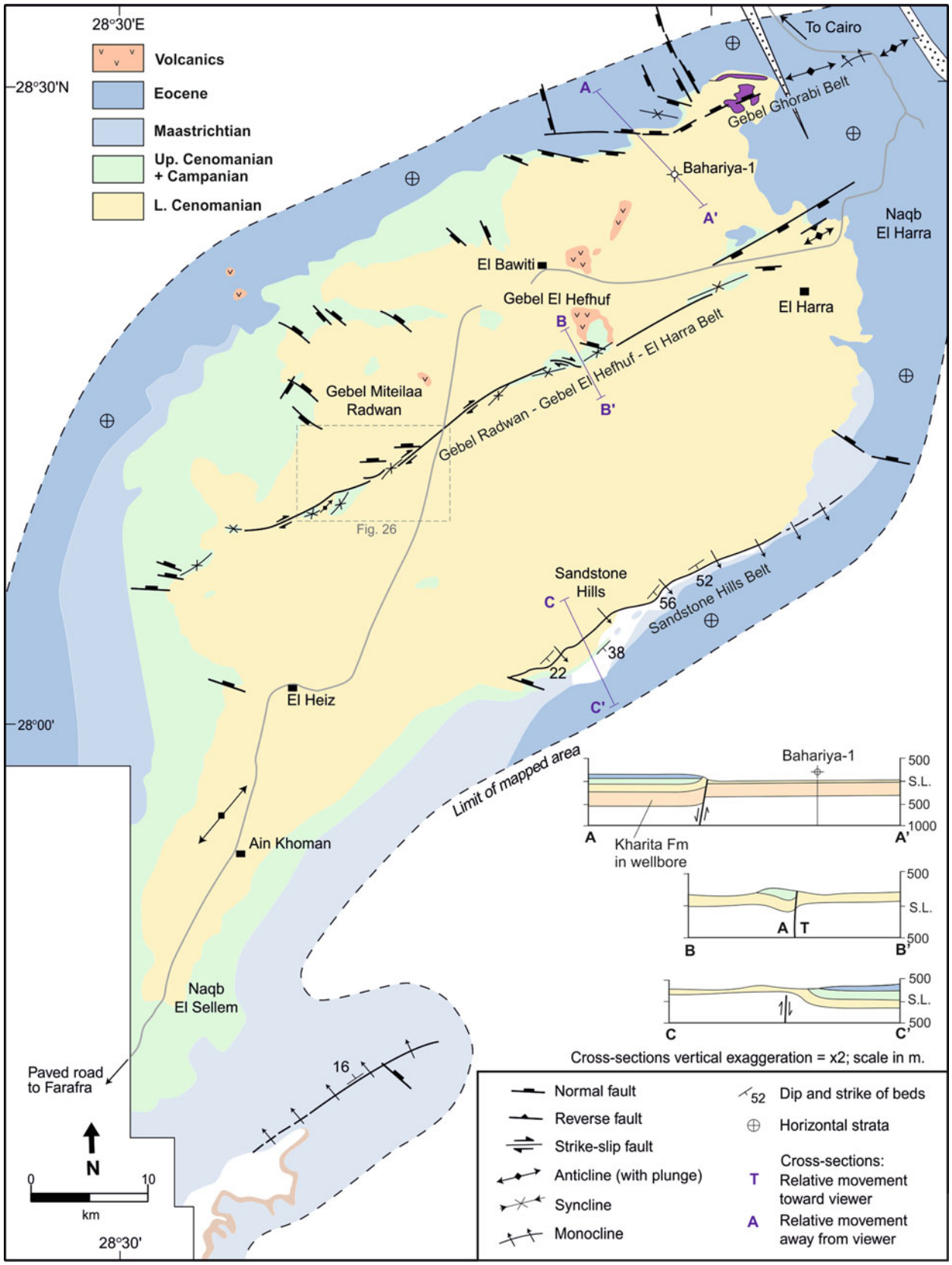

Fig. 7.25 Simplified geological map of the Bahariya Oases' area showing the ENE-WSW oriented structural belts, after Moustafa et al. (2003). See Fig. 7.6 for location

D. Bahariya Oases

The Bahariya Oases area (central part of the Western Desert) also shows the base Campanian parallel unconformity where Cenomanian marine sediments of El Heiz Formation are directly overlain by Campanian marine sediments of El Hefhuf Formation with a notable hiatus represented by the Turonian-Santonian rocks. This unconformity is perhaps related to uplift of the central Western Desert and non-deposition and/or erosion of the missing rocks coeval with the onset of Late Cretaceous inversion of the northern basins. Although the Bahariya Oases area lies in a platform area characterized by thin Phanerozoic sedimentary section (1400–2000 m; Moustafa et al. 2003), it displays folded Upper Cretaceous rocks due to Late Cretaceous-Early Tertiary deformation. The deformation is attributed to reactivation of pre-existing ENE-WSW oriented faults by NW compressive stress (Moustafa et al. 2003). Three well-defined ENE-WSW oriented structural belts were mapped in the area; Gebel Ghorabi Belt, Gebel Radwan–Gebel El Hefhuf–El Harra Belt, and the Sandstone Hills Belt (Moustafa et al. 2003), Fig. 7.25. In each of these three belts, Late Cretaceous deformation led to reactivation of deep-seated faults and folding of the exposed Upper Cretaceous rocks.

The Gebel Ghorabi Structural Belt extends for about 36 km in the northernmost part of the Bahariya depression and shows two phases of right-lateral strike-slip movement. The first phase was post-Cenomanian to pre-Middle Eocene and the second phase was post-Middle Eocene. The second phase deformed the Middle Eocene rocks at the eastern side of the belt by relatively small, right-stepping en echelon folds.

The Gebel Radwan–Gebel El Hefhuf–El Harra Structural Belt is 65 km long and extends across the oases depression from the western plateau to the eastern plateau. It includes four main left stepping, en echelon, ENE-oriented, steeply dipping faults associated with fault-drag or fault-propagation folds that change their orientation at the fault tips where they make acute angles with the faults. The fault segments show horizontal to oblique slickenside lineations indicating right-lateral strike-slip displacement and are also associated with right-stepped en echelon folds (Fig. 7.26). Two phases of deformation affected these fault segments; an earlier (stronger) phase of post-Campanian and pre-Middle Eocene age and a second phase of post-Middle Eocene age. The earlier phase involved right-lateral strike-slip movement indicated by the nearly horizontal slickenside lineations on some faults in the belt and by the right-stepped en echelon folds that make acute angles with the fault segments whereas the sense of slip of the second phase is not easy to determine.

The Sandstone Hills Structural Belt is a 32-km-long fault-propagation fold represented by ENE-oriented monocline with steep (30–56°) SE dip on the southeastern side of the Bahariya Depression. The monocline affects Upper Cretaceous rocks unconformably overlain by Lower Eocene rocks, indicating post-Campanian-pre-Early Eocene folding.

The subsurface geology of the Bahariya area is shown by a NW-SE oriented 2D seismic section located at a short distance to the northeast of the Bahariya Depression. This section clearly shows that the top Precambrian basement to top Paleozoic rocks are dissected by four normal faults (Fig. 7.27). The same faults have reverse slip at the top Cenomanian Bahariya Formation. Moustafa et al. (2003) attributed the normal slip of these faults to Early Mesozoic extension, perhaps related to the Tethyan rifting phase. Two of these faults represent the along-strike projection of Gebel Ghorabi Structural Belt and Gebel Radwan–Gebel El Hefhuf–El Harra Structural Belt. The seismic section indicates that two phases of movement took place; an early phase of normal slip and a later phase of reverse slip representing positive structural inversion of the Bahariya area. The section also shows that the Mesozoic rocks are folded by an anticline with broad crestal area which was named the Bahariya Swell by Moustafa et al. (2003) and is a result of the positive inversion. The Maastrichtian chalk (Khoman Formation) onlaps the southern side of the Bahariya Swell indicating that inversion was pre-Maastrichtian in age. The reverse slip shown by the seismic and dextral strike-slip movement shown by surface geological data indicate that inversion was transpressive. The seismic section also shows the eroded crest of the Bahariya Swell and the unconformable relationship between the eroded Upper Cretaceous rocks and the overlying Eocene rocks of the Apollonia Formation. As the top Apollonia reflector also shows the anticlinal structure of the Bahariya Swell, the inversion continued into the post-Middle Eocene and was contemporaneous with the second phase of deformation identified by the surface geological mapping.

E. Nubia Fault System

The Nubia Fault System is a belt of pervasive E-W to ENE-WSW oriented faults affecting the southernmost part of the Western Desert (Fig. 7.2). It extends for about 600 km west of the Nile and may extend further west for a longer distance underneath the Quaternary sand dunes. Bahy Issawi was probably the first geologist to map these prominent E-W faults in the Sinn El Kaddab (Issawi 1968) and Darb El Arbain (Issawi 1971) areas. The E-W faults of Issawi are accompanied by N-S faults especially at the eastern scarp of Sinn El Kaddab Plateau overlooking the Nile Valley. In fact, it was Ghobrial (1967) who identified and mapped such N-S faults further north in the Kharga Depression and mentioned that they are associated with N-S belts of left-stepped en echelon doubly plunging folds (Fig. 7.28). Similarly, the E-W faults are also associated with relatively small-scale folds (Fig. 7.29) that are mostly en echelon. Both of the E-W

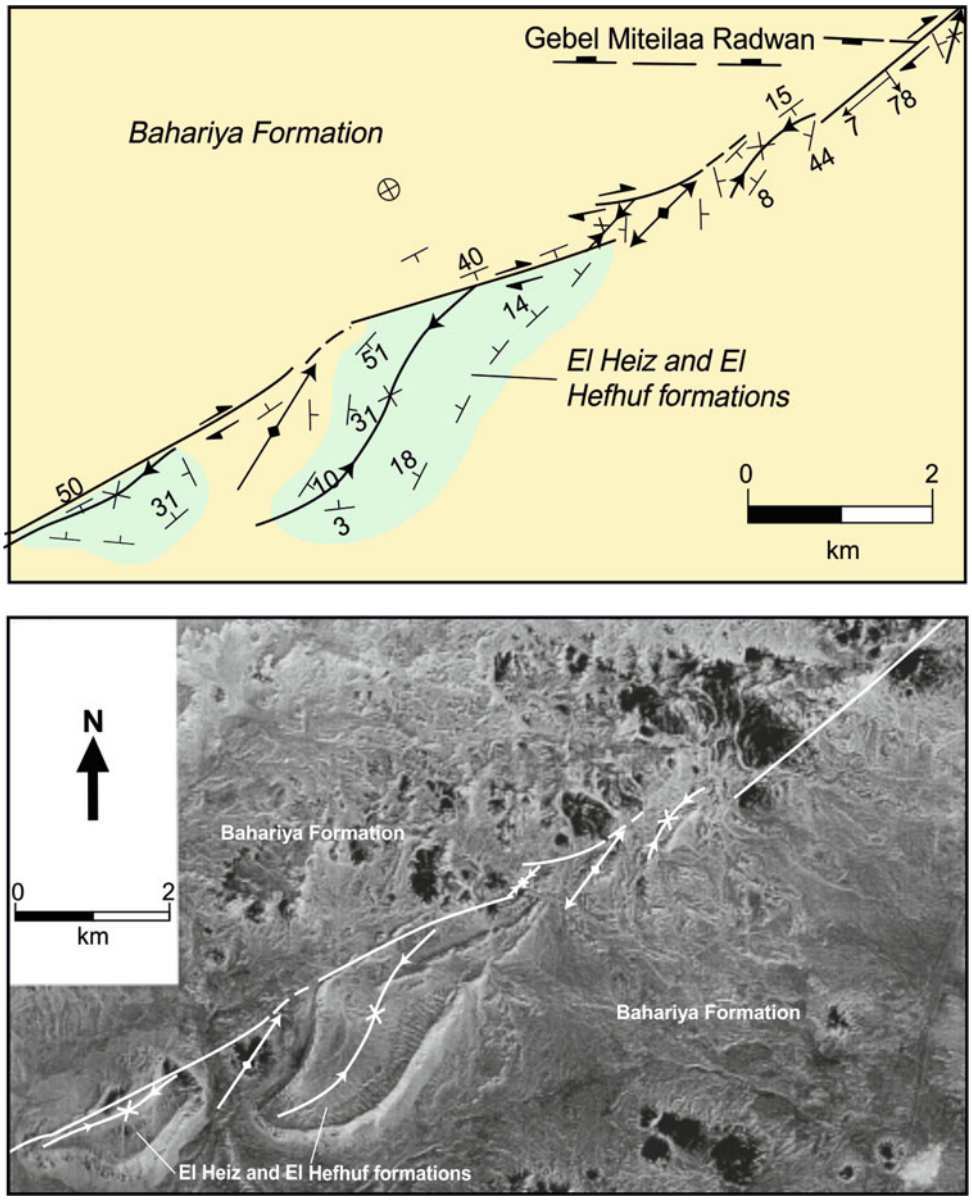

Fig. 7.26 Simplified geological map and vertical aerial photograph of Gebel Radwan segment of the Gebel Radwan–El Hefhuf–El Harra Structural Belt showing the NE-oriented, right-stepping en echelon folds associated with the right-lateral strike-slip faults, after Moustafa et al. (2003). See Fig. 7.25 for location

to ENE-WSW and N-S faults of Issawi and Ghobrial were assigned normal slip at these times. It was not until the 1981 Aswan earthquake that horizontal slip was noticed on these faults by Woodward-Clyde Consultants (1985); right-lateral slip on the E-W faults and left-lateral slip on the N-S faults. Guiraud et al. (1985) considered the E-W faults to be part of their Guinean–Nubian E-W trending lineaments that extend across Africa. Guiraud and Bosworth (1999) stated that these faults were deformed by dextral transpression in Late Santonian and Late Eocene times. Detailed structural studies of the E-W faults by El Etr et al. (1982), Abdeen (2001), Sakran and Said (2018), and Hamimi et al. (2018) also confirm right-lateral slip. Seismicity network in Aswan region indicates recent activity on these faults (Mekkawi et al. 2005; Telesca et al. 2012; Hussein et al. 2013; Meghraoui et al. 2016; and Abdelazim et al. 2016).

Perhaps the most detailed structural study of the E-W and N-S faults of the south Western Desert is that of Sakran and Said (2018). They studied three of the E-W faults (Kalabsha, Seyial and Abu Bayan) and indicated that they are characterized by horizontal slickenside lineations, ENE to NE oriented folds making acute angles with the faults, horizontally-offset folds, and releasing and restraining bends. They also studied the N-S faults of the eastern part of Sinn El Kaddab Plateau and noted that they have narrow widths and are less complex compared to the E-W right-lateral faults. These N-S faults consist of right stepping en-echelon segments with contractional step-overs in between. They are

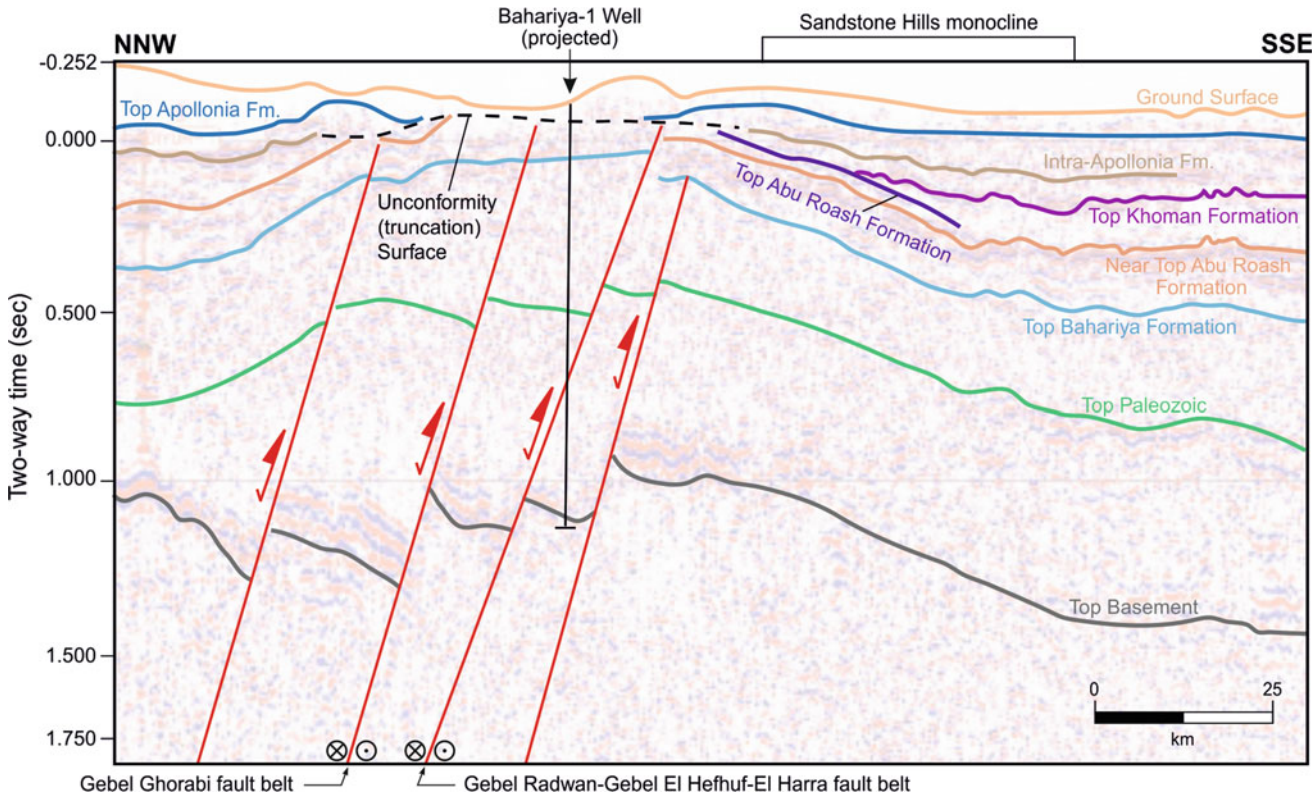

Fig. 7.27 Seismic section east of the Bahariya depression showing Jurassic-Early Cretaceous normal slip on the main faults of the Bahariya depression and reactivation by oblique-slip reverse movement during the Late Cretaceous-Early Tertiary basin inversion, after Moustafa et al. (2003)

also associated with NE to NNE oriented en echelon folds that are mostly dissected and horizontally displaced by the fault segments. Integration of surface geological and subsurface (seismic reflection and borehole) data by Sakran and Said (2018) indicated that the strike-slip faults of Sinn El Kaddab area show up on the seismic reflection data with nearly vertical attitude as well as negative and positive flower structures. The Upper Cretaceous rocks at the crestal areas of the positive flower structures are unconformably overlain by Upper Paleocene rocks while the Lower Paleocene rocks onlap the flanks of the flower structure indicating that the deformation took place by dextral transpression on the E-W faults and sinistral simple shearing on the N-S faults during the Late Cretaceous—Middle Eocene time.

7.2.3.3 Tethyan Convergence Affecting the Northernmost Areas of Egypt

Continued convergence of the African and Eurasian Plates exerted compression on the northernmost (offshore) areas of Egypt in Miocene to Recent times. This is evident in several areas as follows.

A. Reactivation of the Rosetta Fault

Tethyan convergence leading to positive structural inversion is evident in the areas lying north of the inverted basins of the northern Western Desert and onshore and offshore northern Sinai. The Rosetta Fault, on the western side of the Nile Cone, shows Tertiary convergent deformation represented by reverse slip and formation of a hanging wall anticline. Rosetta Fault is a major NE-SW oriented fault extending for ~160 km on the western side of the Nile Cone with steep NW dip (Fig. 7.2). Abd El-Fattah et al. (2018) mapped the fault at different stratigraphic levels on 3D seismic data and recognized a hanging wall asymmetric anticline affecting the top Serravallian and older rocks (Fig. 7.30). By restoring post-Messinian normal slip on the Rosetta Fault it displays reverse slip and the anticline is a hanging wall anticline related to the reverse movement. The crest of this anticline was breached during the Messinian Salinity Crisis that led to dramatic fall of the Mediterranean sea level. Abd El-Fattah et al. (2018) attributed the reverse slip and associated asymmetric hanging wall anticline to Late Cretaceous-Tertiary compressive deformation resulting from convergence of the African and Eurasian Plates.

As the Rosetta Fault is sub-parallel to other inverted faults in northern Egypt and shows similar structural style, it

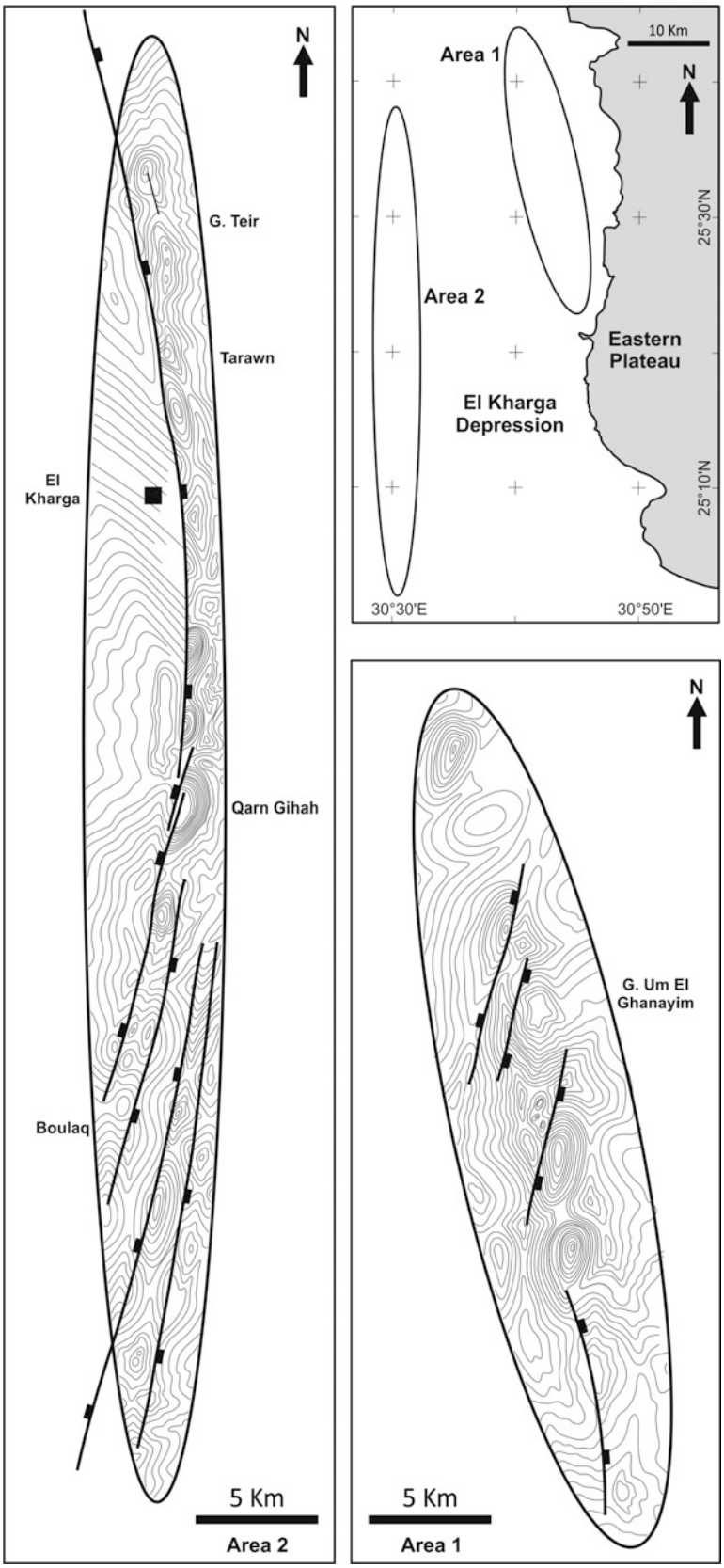

Fig. 7.28 Top Upper Cretaceous phosphate Formation structure contour maps of two areas in the northern part of El Kharga Depression (after Ghobrial 1967). Note the N-S to NNE-SSW oriented left-stepping en echelon folds and faults. See Fig. 7.6 for location

Fig. 7.29 Google Earth Image (©2013 DigitalGlobe) showing small-scale folds associated with an ENE-WSW oriented right-lateral strike-slip fault in the southern Western Desert. See Fig. 7.6 for location

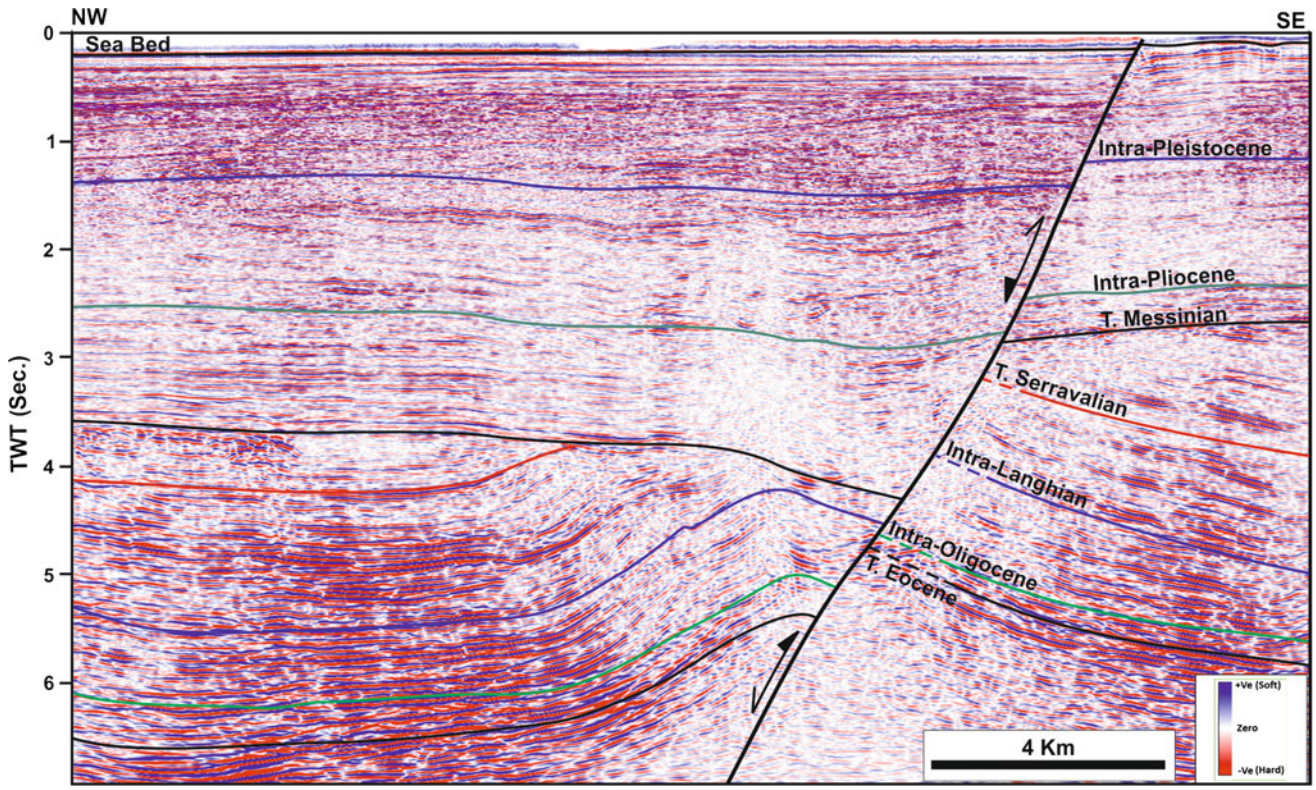

Fig. 7.30 Seismic section across the southern part of Rosetta Fault showing a hanging wall asymmetric anticline affecting the Tortonian and older rocks (after Abd El-Fattah et al. 2018). See Fig. 7.31 for location

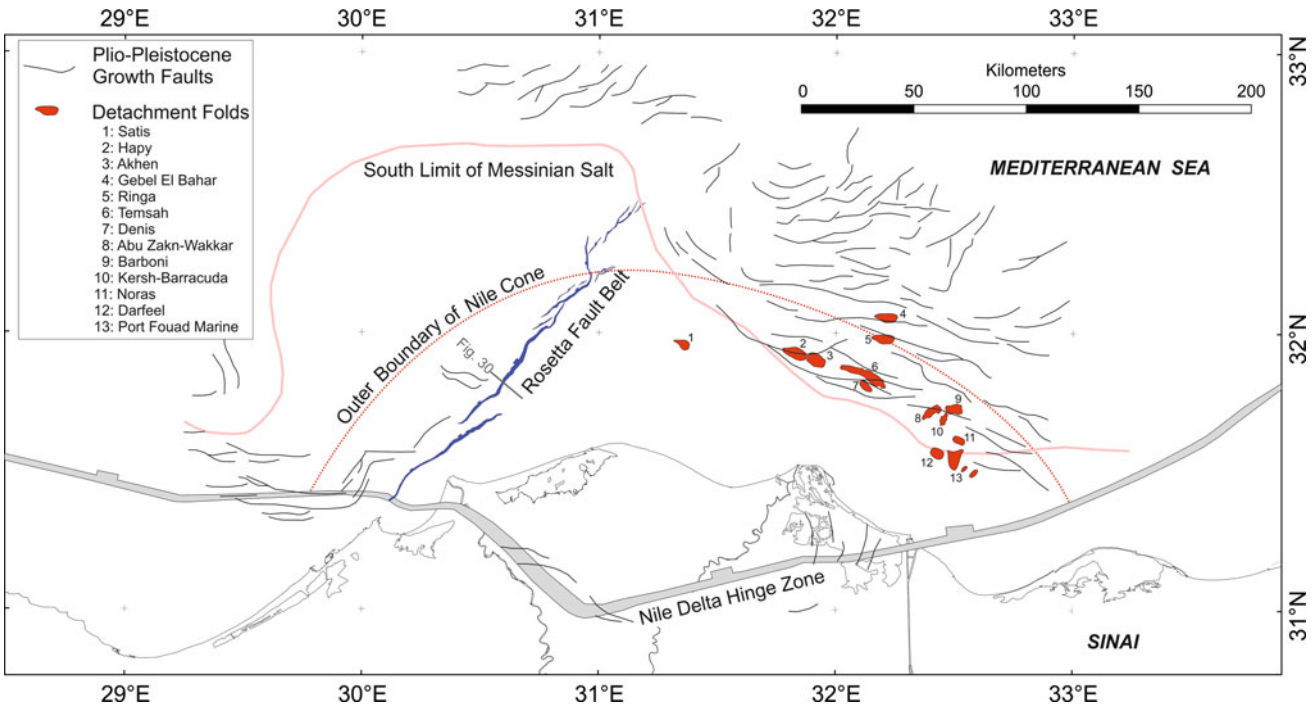

Fig. 7.31 Simplified structural map of the offshore Nile Delta area showing the Rosetta Fault (after Abd El-Fattah et al. 2018), Miocene detachment folds (after EGPC 1994; Kamel et al. 1998; Abdel Aal et al. 2001), and Plio-Pleistocene growth faults (after Tingay et al. 2011)

is believed that it probably had the same history of the inverted Jurassic faults of the onshore area. It is quite probable that the Rosetta Fault was formed as a normal fault during the Tethyan rifting phase before it was later affected by reverse slip and positive inversion at post-Serravallian time. It is unfortunate that Jurassic rocks lie deep below the resolution of the seismic data. Based on detailed integration and modeling of the gravity, magnetic, seismic refraction and seismic reflection data, as well as onshore fault trends, and regional arguments for plate tectonic reconstructions; Longacre et al. (2007) considered that the Rosetta Fault lies perpendicular to the Triassic extension direction and represents one of the rift-parallel faults of the East Mediterranean Basin.

Continued convergence of the African and Eurasian Plates led to left-lateral slip on the Rosetta fault at pre-Tortonian (Sehim et al. 2002) or Messinian time (Abd El-Fattah 2018). Abd El-Fattah (2018) mapped a swarm of NNW-SSE oriented normal faults affecting the Messinian sediments close to a fault bend at the northern portion of the Rosetta fault (Fig. 7.31), perhaps indicating that it is a releasing bend associated with left-lateral slip on the Rosetta Fault at Messinian time. Later (Pliocene and younger) movement of the Rosetta Fault shows predominantly normal slip.

B. Detachment Folds in the Outer Part of the Nile Cone

A number of NW to WNW oriented folds affect the Oligo-Miocene sedimentary section underlying the Messinian salt in the eastern part of the Nile Cone (Fig. 7.31). These folds have large dimensions (up to 25 km long) and are relatively tight and separated from each other by wider synclinal areas. Seismic reflection data indicate that the anticlines and synclines have rather box shapes in some cases and are believed to have been formed by detachment on the underlying Lower Oligocene shales. The detachment anticlines include Hapy, Akhen, Temsah, Gebel El Bahar, Ringa, Denis, Abu Zakn-Wakkar, Barboni, Kersh-Barracuda, Noras, Darfeel, and Port Fouad Marine Anticlines (Fig. 7.31). They indicate shortening direction different from the Late Cretaceous-Early Tertiary NW-SE Tethyan compressive stress. This might either reflect a local change in the stress direction in that area at Miocene (Messinian) time, or the effect of a deep-seated structure controlling the direction of detachment of the Oligocene-Miocene sediments. Several studies refer to an old WNW fault trend (referred to as the Misqaf or Temsah Fault) underneath the area affected by these folds although seismic reflection data do not show this fault. Despite that, compression leading to reactivation of older faults was reported by Dolson et al.

(2014) who show that the Habbar Anticline is a hanging-wall anticline of a reverse fault in the Oligocene section and Hussein (2013) proves that this fault is a positively inverted Oligocene-age normal fault.

C. Pliocene-Holocene Growth Faults

Growth faults dissecting the Pliocene-Holocene sediments in the outer part of the Nile Cone are well recognized on seismic reflection data. These structures are limited to the areal distribution of the Messinian salt and have WNW, E-W, and ENE orientations and northward slip (Fig. 7.31). It is worth mentioning that growth faults dissect the sediments overlying the Messinian salt in the area affected by the Miocene detachment folds. High-resolution seismic reflection data show that the Pliocene-Recent sediments overlying the northeastern flanks of the detachment folds are affected by growth faults. Continued detachment of the sedimentary section overlying the Lower Oligocene shales leads to increase in the fold amplitude allowing the Pliocene-Recent sediments overlying the Messinian salt in these flanks to detach northward by growth faulting. At the nose of each Oligo-Miocene detachment fold, the overlying growth faults change orientation to N-S.

7.3 Tectonic Evolution

The three phases of Mesozoic-Cenozoic deformation discussed in the previous sections are related to the movement of the Afro-Arabian Plate (later split into African and Arabian Plates) with respect to the surrounding (Eurasian and South American) plates. Pre-existing structures also played a role in the structural deformation where they controlled the structural trends or caused local changes in the stress directions.

The Tethyan rifting phase is attributed to the divergent movement between the Afro-Arabian and Eurasian Plates leading to opening of the Neotethys. This divergent movement started at the Late Triassic (Robertson and Dixon 1984; Dercourt et al. 1986; May 1991). Borehole and seismic data indicate that deposition of syn-rift sequences in the resulting basins continued almost to the end of the Early Cretaceous. Some small continental blocks were separated from the Afro-Arabian Plate during this extensional phase and started drifting to the north or northwest. The closest block to the African margin at present time is the Eratosthenes continental block (Ben Avraham et al. 2006). Onshore extensional basins formed during this phase in the southern passive margin of Neotethys are oriented NE to ENE indicating NW divergence of the major plates. Integration of gravity, magnetic, seismic refraction, and seismic reflection data from the Mediterranean offshore area of Egypt led Longacre et al. (2007) to propose NW extension direction of the East Mediterranean Basin during the Triassic, consistent with the Levant margin and offshore northern Sinai. According to those authors, rift-parallel fault in the East Mediterranean are oriented NE-SW to NNE-SSW whereas NW-SE oriented faults represent the transform boundaries. To these transforms belongs the NW-SE oriented fault bounding the offshore area of the northern Western Desert. This transform fault forms the boundary between the oceanic crust of the southern Tethys (in the offshore area) and the mildly-extended continental crust of northern Egypt (Fig. 7.32a). According to Cowie and Kusznir (2012), continental extension and seafloor spreading resulted in the formation of oceanic crust in the Herodotus Basin whereas the Levant Basin and areas underneath the Nile Cone and the Egyptian onshore areas have thinned continental crust. Mesozoic isopach maps of the Palmyride Trough in Syria (Brew et al. 2001) show similarity to the Tethyan extensional basins of northern Egypt.

Another rifting phase formed NW-SE oriented basins during the Cretaceous Period. The Kom Ombo, Asyut, Beni Sueif and Abu Gharadig Basins (Fig. 7.2) belong to this extensional phase. Basin fill indicates that extension continued almost during all of the Cretaceous and extended to the Early Tertiary. Pre-existing faults locally changed the general trend of some of these basins such as the Abu Gharadig Basin that is controlled by pre-existing E-W faults and dominated by NW-SE oriented normal faults making it an oblique rift. Other NW-SE oriented Cretaceous-Early Tertiary rift basins were also formed in the Afro-Arabian Plate. These include the Sirte Basin in Libya (Rusk 2001), the Sudan Rift System (Bahr El Arab, Abu Gabra/Muglad, White Nile, Blue Nile, and Atbara rift basins; Bosworth 1992; McHargue et al. 1992), the Azrag Basin in Jordan (Beydoun et al. 1994), and the Euphrates Graben in Syria (Brew et al. 2001). The NW-SE orientation of these basins reflects NE-SW extension which may have resulted from opening of the South Atlantic and the divergent movement between Afro-Arabia and South America during the breakup of Gondwana.

The third phase of deformation was compressional leading to closure of the Neotethys due to convergence of the Afro-Arabian and Eurasian Plates. Surface and subsurface data indicate that this phase started at Late Santonian time in Egypt where a marked angular unconformity is obvious between the Campanian and Santonian sediments especially at the structural highs (Moustafa 1988, 2002). This phase of deformation led to inversion of the Tethyan extensional basins of northern Egypt as well as reactivation of Tethyan faults in southern Egypt. The direction of compression during this compressional phase was NW or WNW (Smith 1971; Eyal and Reches 1983). As shown in the previous

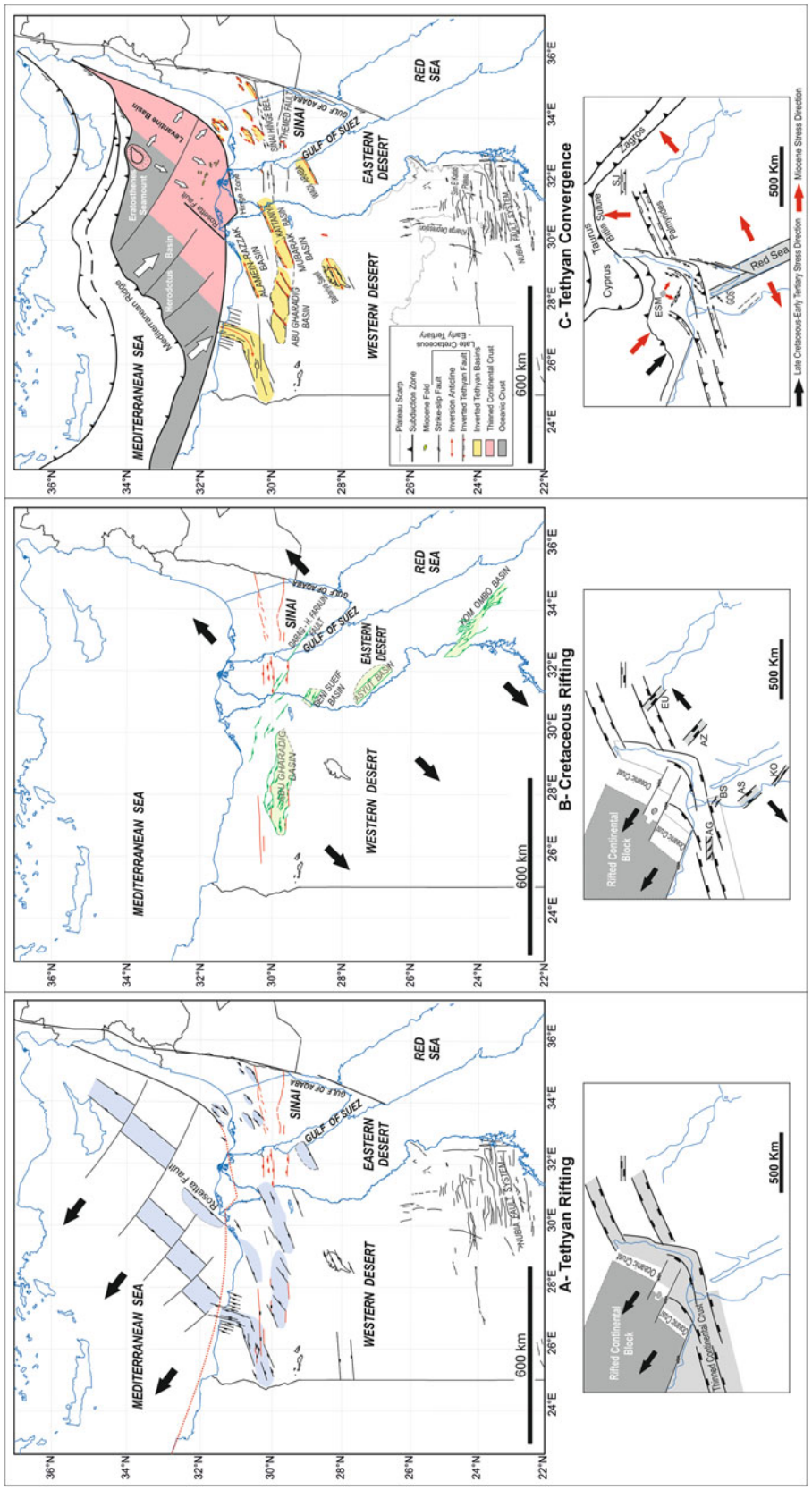

Fig. 7.32 Mesozoic-Cenozoic tectonic evolution of Egypt. Cartoons showing relative plate movements are shown below each map. **a** Tethyan rifting phase (Middle/Late Triassic—end of Early Cretaceous) related to NW drift of Eurasia and continental blocks fragmented from Afro-Arabia. This phase also included reactivation of old structural fabrics represented by red lines. **b** Cretaceous-Early Tertiary rifting phase leading to opening of NW-SE oriented rifts, probably related to opening of the South Atlantic. **c** Tethyan convergence phase (Late Cretaceous-Recent) related to convergent movement between Afro-Arabia and Eurasia and closure of the Neotethys. Stress directions change with time and location, Late Cretaceous compressive stress in the NW-SE direction changed in Miocene time to N-S at the north Arabian promontory due to collision with Eurasia at the Bitlis suture. Local changes in the stress directions are clear in the East Mediterranean due to southward movement of the Eratosthenes Seamount as it resists subduction underneath Eurasia. Abbreviations stand for: Abu Gharadig Basin (AG), Asyut Basin (AS), Azrag Basin (AZ), Beni Sueif Basin (BS), Euphrates Basin (EU), Kom Ombo Basin (KO), Eratosthenes Seamount (ESM), Gulf of Suez rift (GOS), and Sinjar Trough (SJ)

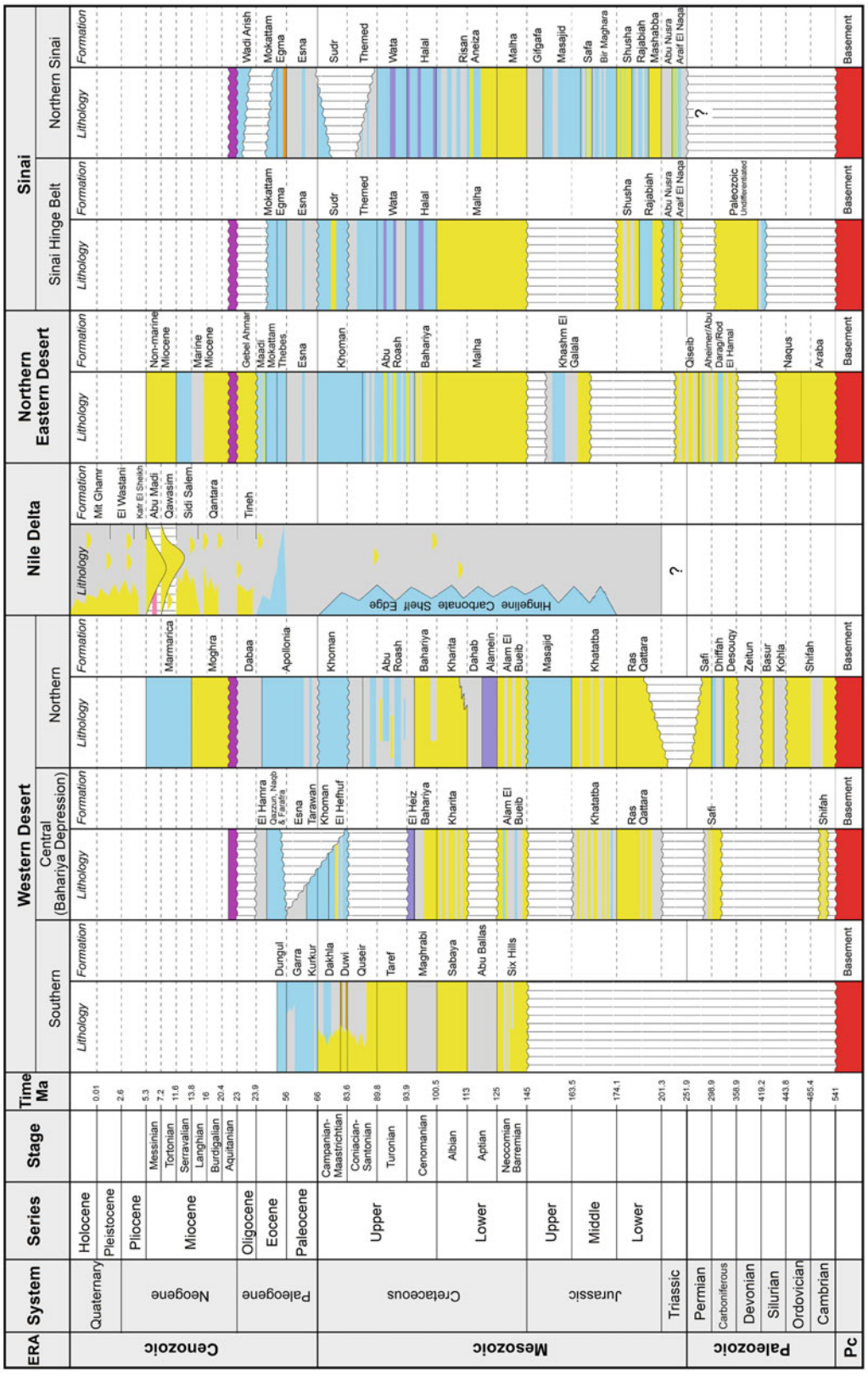

Fig. 7.33 Stratigraphic sections of the areas discussed in this chapter compiled from different sources as follows: southern Western Desert (Sakran and Said 2018); Bahariya depression (Moustafa et al. 2003); northern Western Desert (Moustafa 2008; Bosworth et al. 2015a); Nile Delta (Dolson et al. 2014; Abd El-Fattah 2018); northern Eastern Desert (Sadek 1926; Said 1962; Abdallah and Adindani 1963; Abdallah et al. 1963; Abdallah 1992; Salem and Sehim 2017); Sinai Hinge belt (Moustafa et al. 2014); northern Sinai (Jenkins 1990; Moustafa 2014). Time scale is from Cohen et al. 2013

sections, detailed mapping of the inversion structures (e.g. Halal and Maghara inverted basins) indicates that the deformation was transpressive with a minor component of dextral slip, perhaps providing evidence that the direction of convergence was WNW-ESE.

Onshore inverted structures in Egypt show strong evidence of continued convergence during the Tertiary up to the Miocene. The effect of Miocene and younger plate convergence can be seen in the offshore areas leading to pronounced Miocene-Recent NW-SE oriented folds in the NE side of the Nile Cone and NE-SW oriented folds in the Herodotus Basin (Loncke et al. 2006). Present-day folding of the seafloor sediments is obvious in the area between the Rosetta fault and the Mediterranean Ridge (see Ross and Uchupi 1977; Huguen et al. 2001) where the folds are oriented NE-SW and show SE vergence indicating SE compression. The change in the direction of compression (and hence the fold orientations) in the eastern part of the Nile Cone and west of it (Fig. 7.32c) is perhaps related to the presence of rifted continental fragments resisting subduction (e.g. Eratosthenes Seamount) causing local shortening and change in the stress directions. The northern and western areas of the Nile Cone as well as the Herodotus Basin show the effect of present-day SE compression. Also, the area east of the Eratosthenes Seamount (Levant Basin) is deformed by NE-SW oriented folds (Tari et al. 2012). On the other hand, the area south of Eratosthenes Seamount was affected by SW oriented compression forming NW-SE oriented folds (Fig. 7.32c). Such local change in the direction of the compressive stress is related to the local effect of the Eratosthenes Seamount and the presence of ductile units in the stratigraphic section causing detachment, e.g. the Lower Oligocene shales and the Messinian evaporites. The present-day stress orientations deduced from borehole breakouts and drilling induced fractures are different in the rock sections overlying and underlying the Messinian evaporites in the eastern Nile Delta area (Tingay et al. 2011). σHmax in the sediments underlying the Messinian evaporites or with no evaporites is oriented WNW-ESE in the eastern Nile Delta. However, σHmax in the sediments overlying the evaporites is oriented NNE-SSW. This 90° variation in the present-day σHmax above and below the Messinian evaporites indicates that the evaporites act as a major mechanical detachment zone. Present-day σHmax in the western Nile Delta as indicated by earthquakes is oriented NW-SE (Korrat et al. 2005; Costantinescu et al. 1966; and Abu El Nader et al. 2013). On a regional scale, present-day stress directions change due to the irregular shape of the convergent plate boundary, e.g. N-S compression at the north Arabian promontory due to collision with Eurasia at the Bitlis Suture compared to NW-SE compression of the SE Mediterranean (Fig. 7.32c).

Acknowledgements I would like to thank Shell Egypt for giving permission to use the seismic section of Abu Gharadig Basin (Fig. 7.4), John Dolson for providing me with the seismic section in Fig. 7.5, and Ali Bakr for providing me with the seismic sections in Figs. 7.17 and 7.18. Mediterra Energy Corporation and Kom Ombo Petroleum Company (KOPCO) are also thanked for giving permission to use seismic section of Al Baraka oil field (Kom Ombo Basin). Peer-review by Zakaria Hamimi and constructive comments by Sebastian Luening and John Dolson helped improve the manuscript.

References

Abdallah AM (1992) Paleozoic rocks in Egypt. Technika Poszukiwan Geologicznych Geosynoptyka i Geotermia 3/92:1–12

Abdallah AM, Adindani A (1963) Stratigraphy of upper Paleozoic rocks, western side of Gulf of Suez, Geol. Surv. Egypt, Paper 25, 18 pp

Abdallah AM, El-Adindani A, Fahmi N (1963) Stratigraphy of the Lower Mesozoic rocks, western side of the Gulf of Suez, Geol. Surv. Egypt, Paper 27, 23 pp

Abd-Allah MA, Moustafa AR, Hashem WA (2004) Structural characteristics and analysis of the Gebel El Halal fold, Northeast Sinai, Egypt. MERC, Ain Shams Univ Earth Sci Ser 18:1–26

Abdeen MM (2001) Active dextral wrenching on Kalabsha fault, Southern Egypt. Egypt J Remote Sens Space Sci 4:79–92

Abdel Aal A, Moustafa AR (1988) Structural framework of the Abu Gharadig basin, Western Desert, Egypt. In: Proceedings of 9th EGPC exploration and production conference (Cairo), vol 2, pp 23–50

Abdel Aal A, El Barkooky A, Gerrits M, Meyer H, Schwander M, Zaki H (2001) Tectonic evolution of the Eastern Mediterranean Basin and its significance for the hydrocarbon prospectivity of the Nile Delta deepwater area, vol 6. GeoArabia, pp 363–384

Abdelazim M, Samir A, Abu El-Nader I, Badawy A, Hussein H (2016) Seismicity and focal mechanisms of earthquakes in Egypt from 2004–2011. Natl Res Inst Astron Geophys (NRIAG) J Astron Geophys 5:393–402

Abd El-Aziz M, Moustafa AR, Said SE (1998) Impact of basin inversion on hydrocarbon habitat in the Qarun Concession, Western Desert, Egypt. In: Proceedings of 14th EGPC exploration and production conference, Cairo, vol 1, pp 139–155

Abd El-Fattah BK (2018) Structural analysis of the Rosetta Fault, offshore Nile Delta, Egypt. Unpublished MSc thesis, Ain Shams University, 155 pp

Abd El-Fattah BK, Yousef M, Moustafa AR (2018) 2D Structural restoration of the Rosetta fault system, offshore western Nile Delta, Mediterranean basin, Egypt. Egypt J Appl Geophys 17:83–98

Abdelhady A, Darwish M, El Araby A, Hassouba A (2016) Geochemical characterization of Al Baraka oil in Komombo rift basin, Egypt. Egypt J Geol 60:191–205

Abdel Hakim MMF (2017) Geological modeling of the Middle Jurassic reservoirs in East Tiba basin, northern Western Desert, Egypt. MSc thesis, Cairo University, 100 pp

Abou-Khadrah AM, Darwish M, El-Azabi M (1994) Contribution to the faulted-down Eocene limestones of the southern Galala Plateau "St. Paul area", Gulf of Suez, Egypt. In: Proceedings of 2nd international conference on the geology of the Arab World, Cairo University, pp 505–527

Abdel Khalek ML, El Sharkawi MA, Darwish M, Hagras M, Sehim A (1989) Structural history of Abu Roash district, Western Desert, Egypt. J Afr Earth Sci 9:435–443

Abdel Khalek ML, Abdel Wahed N, Sehim AA (1993) Wrench deformation and tectonic setting of the northwestern part of the Gulf of Aqaba. Geol Soc Egypt Spec Publ 1:409–444

Abu El-Nader IF, El Gabry MN, Hussein HM, Hassan HM, Elshrkawy A (2013) Source characteristics of the Egyptian continental margin earthquake, 19 October 2012. Seismol Res Lett 84:1062–1065

Abul-Nasr RA (1986) Syntectonic slope deposit at Gebel Hammam Faraun, Sinai (Egypt) (abs). In: Proceedings of 59th annual meeting of the South Carolina Academy of Science, vol 48. Bull. South Carolina Academy of Science, pp 100–101

Abul-Nasr RA, Thunell RC (1987) Eocene eustatic sea level changes: evidence from western Sinai, Egypt. Paleogeogr Paleoclimatol Paleoecol 58:1–9

Afifi AS, Moustafa AR, Helmy HM (2016) Fault block rotation and footwall erosion in the southern Suez Rift: Implications for hydrocarbon exploration. J Marine Pet Geol 76:377–396

Al-Ahwani MM (1982) Geological and sedimentological studies of Gebel Shabrawet area, Suez Canal district—Egypt. Ann Geol Survey Egypt 12:305–381

Al-Far DA (1966) Geology and coal deposits of Gebel El Maghara (north Sinai). Geological Survey of Egypt, Paper no. 37, 59 pp

Ayyad MH, Darwish M, Sehim A (1998) Introducing a new structural model for north Sinai with its significance to petroleum exploration. In: Proceedings of the 14th petroleum conference, Cairo, Egypt, vol 1. Egyptian General Petroleum Corporation, Cairo, pp 101–117

Bakr A (2010) Messages from the deepest oil discovered in the WD of Egypt. AAPG Western Desert Geotechnology Workshop (Cairo)

Ball J (1900) Kharga oasis, its topography and geology. Egyptian Survey Department, Cairo, 116 pp

Ball J, Beadnell HJL (1903) Bahariya oasis: its topography and geology. Egyptian Survey Department, Cairo, 84 pp

Bartov Y (1974) A structural and paleogeographical study of the central Sinai faults and domes. PhD thesis, Hebrew University, Jerusalem (in Hebrew)

Bartov Y, Lewy Z, Steinitz G, Zak I (1980) Mesozoic and Tertiary stratigraphy, paleogeography and structural history of the Gebel Areif en Naqa area, eastern Sinai. Isr J Earth Sci 29:114–139

Beadnell HJL (1909) An Egyptian oasis: an account of the oasis of Kharga in the Libyan Desert. Murray, London, 248 pp

Ben-Avraham Z, Woodside J, Lodolo E, Gardosh M, Grasso M, Camerlenghi A, Vai GB (2006) Eastern Mediterranean basin systems. In: Gee DG, Stephenson RA (eds) European lithosphere dynamics, vol 32. Geological Society, London, Memoirs, pp 263–279

Bevan TG, Moustafa AR (2012) Inverted rift-basins of Northern Egypt. In: Roberts DG, Bally AW (eds) Regional geology and tectonics: phanerozoic rift systems and sedimentary basins, vol 1B. Elsevier, pp 483–507

Beydoun ZR, Futyan ARI, Jawzi AH (1994) Jordan revisited: hydrocarbons habitat and potential. J Pet Geol 17:177–194

Bosworth W (1992) Mesozoic and early Tertiary rift tectonics in East Africa. In: Ebinger CJ, Gupta HK, Nyambok IO (eds) Seismology and related sciences in Africa. Tectonophysics, vol 209, pp 115–137

Bosworth W, McClay K (2001) Structural and stratigraphic evolution of the Gulf of Suez rift, Egypt: A synthesis. In: Zeigler PA, Cavazza W, Robertson AHF, Crasquin-Soleau S (eds) Peri-Tethyan rift/wrench basins and passive margins: peri-tethys memoir 6, vol 186. Memoires du Museum National d'Histoire Naturelle de Paris, pp 567–606

Bosworth W, Guiraud R, Kessler LG (1999) Late Cretaceous (Ca. 84 Ma) compressive deformation of the stable platform of northeast Africa (Egypt): Far-field stress effects of the "Santonian event" and origin of the Syrian arc deformation belt. Geology 27:633–636

Bosworth W, Drummond M, Abrams M, Thompson M (2015a) Jurassic rift initiation source rock in the Western Desert, Egypt—relevance to exploration in other continental rift systems. In: Petroleum systems in rift basins, pp 615–650

Bosworth W, Stockli DF, Helgeson DE (2015b) Integrated outcrop, 3D seismic, and geochronologic interpretation of Red Sea dike-related deformation in the Western Desert, Egypt—the role of the 23 Ma Cairo "mini-plume". J Afr Earth Sci 109:107–119

Bowles EO (1945) Geological report on the south west Gebel Yelleg anticline, central Sinai. Standard Oil Co., Egypt Internal Report

Brew G, Barazangi M, Al-Maleh AK, Sawaf T (2001) Tectonic and geologic evolution of Syria. GeoArabia 6:573–616

Cohen KM, Finney SM, Gibbard PL, Fan JX (2013) The ICS International Chronostratigraphic Chart. Episodes 36:199–204. http://www.episodes.org

Costantinescu L, Ruprecrtova L, Enescu D (1966) Mediterranean-Alpine earthquake mechanisms and their seismotectonic implications. Geophys J R Astron Soc 10:347–368

Cowie L, Kusznir N (2012) Mapping crustal thickness and oceanic lithosphere distribution in the Eastern Mediterranean using gravity inversion. Pet Geosci 18:373–380

Deibis S (1982) Abu Qir Bay, a potential gas province area, offshore Mediterranean, Egypt. In: Proceedings of EGPC 6th exploration seminar, vol 1, pp 50–65

Dercourt J, Zonenshain LP, Ricou LE, Kazmin VG, Le Pichon X, Knipper AL, Grandjacquet C, Sbortshikov IM, Geyssant J, Lepverier C, Pechersky DV, Boulin J, Sibuet JC, Savostin LP, Sorokhtin D, Westphal M, Bazhenov ML, Laurer JP, Bijou-Duval B (1986) Geological evolution of the Tethys belt from the Atlantic to the Pamirs since the Lias. Tectonophysics 123:241–315

Dolson JC, Shann MV, Hammouda H, Rashed R, Matbouly S (2000) The petroleum potential of Egypt. In: Second Wallace E. Pratt memorial conference "Petroleum provinces of the 21st century", 12–15 Jan 2000, San Diego, California, 37 pp

Dolson JC, Shann MV, Matbouly S, Harwood C, Rashed R, Hammouda H (2001) The petroleum potential of Egypt. In: Downey MW, Threet JC, Morgan WA (eds) Petroleum provinces of the twenty-first century. AAPG Memoir 74, pp 453–482

Dolson JC, Atta M, Blanchard D, Sehim A, Villinski J, Loutit T, Romine K (2014) Egypt's future petroleum resources: a revised look into the 21st century. In: Marlow L, Kendall C, Yose L (eds) Petroleum systems of the Tethyan region. AAPG Memoir 106, pp 143–178

Dupuis C, Aubry M, King C, Knox RW, Berggren WA, Youssef M, Galal WF, Roche M (2011) Genesis and geometry of tilted blocks in the Theban Hills, near Luxor (Upper Egypt). J Afr Earth Sci 61:245–267

EGPC (1992) Western Desert oil and gas fields (A comprehensive overview). Egyptian General Petroleum Corporation, 431 pp

EGPC (1994) Nile Delta & North Sinai fields, discoveries and hydrocarbon potentials (A comprehensive overview). Egyptian General Petroleum Corporation, 387 pp

EGSMA (The Egyptian Geological Survey and Mining Authority) (1981) Geologic map of Egypt, Scale 1:2,000,000

El Etr HA, Yehia MA, Dowidar H (1982) Fault pattern in the south Western Desert of Egypt. Ain Shams Univ Sci Res Ser 2:123–152

El Gazzar AM, Moustafa AR, Bentham P (2016) Structural evolution of the Abu Gharadig field area, Northern Western Desert, Egypt. J Afr Earth Sci 124:340–354

El Ramly MF (1972) A new geological map for the basement rocks in the Eastern and South-Western Deserts of Egypt scale 1:1,000,000. Ann Geol Survey Egypt 2:1–18

El Saadany M (2008) Structural style and tectonic evolution of the central part of the northern Western Desert, Egypt. PhD dissertation, Ain Shams University, 267 pp

El Saadany M, Mahmoud A (2008) Sequential structural restoration of the BED1 field area, Abu Gharadig basin, Western Desert, Egypt. MERC Ain Shams Univ Earth Sci Ser 22:25–46

El-Shaarawy OA, Abdel Aal A, Papazis P (1992) Tectonic setting of the Razzak oil field, northern Western Desert of Egypt. In: Proceedings of 11th EGPC petroleum exploration and production conference, vol 3, pp 310–323

El Shazly EM (1977) The geology of the Egyptian region, In: Nairn AEM, Kanes WH, Stehli FG (eds) The ocean basins and margins, vol 4(A). Plenum Press, pp 379–444

Eyal Y, Reches Z (1983) Tectonic analysis of the Dead Sea rift region since the Late Cretaceous based on mesostructures. Tectonics 2:167–185

Eyal M, Eyal Y, Bartov Y, Steinitz G (1981) The tectonic evolution of the western margin of the Gulf of Elat (Aqaba) rift. Tectonophysics 80:39–66

Fahmy M, Mostafa MM, Darwish M, Saber S (2018) Geological framework of Jurassic sequences, East Tiba sub-basin, North Western Desert, Egypt. Egypt J Geol 62:53–69

Farag IAM, Ismail MM (1955) On the structure of the Wadi Hof area (north-east of Helwan). Bull Inst Desert Egypte 5:179–192

Faris MI (1948) Contribution to the stratigraphy of Abu Rauwash and the history of the Upper Cretaceous in Egypt. Bull Fac Sci Cairo Univ 27:221–239

Faris MI, Abbass HL (1961) The geology of Shabrawet area. Ain Shams Univ Sci Bull 7:37–61

Foley EJ (1942) Geological survey of the west coast of the Gulf of Suez. Standard Oil Co., Egypt Internal Report

Garfunkel Z, Bartov Y (1977) The tectonics of the Suez rift. Geol. Surv. Israel Bull. No. 71, 44 pp

Ghobrial MG (1967) The structural geology of the Kharga Oasis. Geological Survey of Egypt paper no. 43, 39 pp

Guiraud R, Bosworth W (1999) Phanerozoic geodynamic evolution of northeastern Africa and the northwestern Arabian platform. Tectonophysics 315:73–108

Guiraud R, Issawi B, Bellion Y (1985) Les lineaments guineo-nubiens: un trait structural majeur a l'echelle de la plaque africaine. CR Acad Sci Paris 300:17–20

Hamimi Z, Hagag W, Osman R, El-Bialy M, Abu El-Nadr I, Fadel M (2018) The active Kalabsha Fault Zone in Southern Egypt: detecting faulting activity using field-structural data and EMR-technique, and implications for seismic hazard assessment. Arab J Geosci 20 pp

Hantar G (1990) North Western Desert. In: Said R (ed) The geology of Egypt. A.A. Balkema, Rotterdam, pp 293–319

Hashad AH, El Reedy MWM (1979) Geochronology of the anorogenic alkalic rocks, south Eastern Desert, Egypt. Ann Geol Surv Egypt 9:81–101

Hassan AM, Osman RA, Ahmed SM, Afify AM (2015) Sedimentological characteristics of the Late Jurassic-Early Eocene formations at Mitla Pass and its environs, east of Suez city, Egypt. Ann Geol Surv Egypt 32:19–61

Hildebrand N, Shirav M, Freund Z (1974) Structure of the western margin of the Gulf of Elat (Aqaba) in the Wadi El Quseib-Wadi Himur area, Sinai. Isr J Earth Sci 23:117–130

Huguen C, Mascle J, Chaumillon E, Woodside JM, Benkhelil J, Kopf A, Volkonskaia A (2001) Deformational styles of the eastern Mediterranean Ridge and surroundings from combined swath mapping and seismic reflection profiling. Tectonophysics 343:21–47

Hussein HM, Abou Elenean KM, Marzouk IA, Korrat IM, Abu El-Nader IF, Ghazala H, ElGabry MN (2013) Present-day tectonic stress regime in Egypt and surrounding area based on inversion of earthquake focal mechanisms. J Afr Earth Sci 81:1–15

Hussein MAE (2013) 3D Seismic reflection and well log data analysis for reservoir characterization at Oligocene sands, Nile Delta, Egypt. MSc thesis, Ain Shams University, 208 pp

Iskandar F (1946) Geological survey east coast Gulf of Suez, north of latitude 29°00′ north. Standard Oil Co. Egypt Internal Report, 41 pp

Issawi B (1968) The geology of Kurkur Dungul area. Geological Survey of Egypt, paper no. 46, 102 pp

Issawi B (1971) Geology of Darb El-Arbain, Western Desert. In: Said R, Meneisy MY (eds) Annales of the geological survey of Egypt, vol 1, pp 53–92

Jenkins DA (1990) North and Central Sinai. In: Said R (ed) The geology of Egypt. A.A. Balkema, Rotterdam, pp 361–380

Jones TH (1946) Geological survey of the east coast of the Gulf of Suez south of latitude 29°00′ north. Standard Oil Co., Egypt Internal Report, 37 pp

Jux U (1954) Zur Geologie des Kreidegebietes von Abu Roash bei Kairo. Neues Jb Geol Palaontol 100:159–207

Kamel H, Eita T, Sarhan M (1998) Nile Delta hydrocarbon potentiality. In: Proceedings of 14th EGPC petroleum conference, vol 2, pp 485–503

Karaaly H, Fahmy B, Wahdan M, Fahmy M (1994) Structure interpretation of Gemsa SE oil field and its impact on future development. In: Proceedings of 12th EGPC petroleum exploration and production conference, vol 1, pp 189–205

Keeley ML, Dungworth G, Floyd CS, Forbes GA, King C, McGarva RM, Shaw D (1990) The Jurassic System in northern Egypt: I. Regional stratigraphy and implications for hydrocarbon prospectivity. J Petrol Geol 13:397–420

Khalil SM, McClay KR (2002) Extensional fault-related folding, northwestern Red Sea, Egypt. J Struct Geol 24:743–762

Klitzsch E, Groeschke M, Herrmann-Degen W (1990) Wadi Qena: Paleozoic and pre-Campanian Cretaceous strata. In: Said R (ed) The geology of Egypt. A.A. Balkema, Rotterdam, pp 321–327

Korrat IM, El Agami NL, Hussein HM, El-Gabry MN (2005) Seismotectonics of the passive continental margin of Egypt. J Afr Earth Sci 41:145–150

Krenkel E (1925) Geologie Afrikas. Verlag von Gebruder, Berlin, p 461

Letouzey J (1986) Cenozoic paleo-stress pattern in the Alpine Foreland and structural interpretation in a platform basin. Tectonophysics 132:215–231

Loncke L, Gaullier V, Mascle J, Vendeville B, Camera L (2006) The Nile deep-sea fan: an example of interacting sedimentation, salt tectonics, and inherited subsalt paleotopographic features. Marine Pet Geol 23:297–315

Longacre M, Bentham P, Hanbal I, Cotton J, Edwards R (2007) New crustal structure of the Eastern Mediterranean Basin: detailed integration and modeling of gravity, magnetic, seismic refraction, and seismic reflection data. In: EGM 2007 international workshop: innovation in EM, Grav and Mag methods: a new perspective for exploration, Capri, Italy, 15–18 Apr 2007, 4 pp

Luning S, Kuss J, Bachmann M, Marzouk AM, Morsi AM (1998) Sedimentary response to basin inversion: Mid Cretaceous—Early Tertiary pre- to syndeformational deposition at Areif El Naqa anticline (Sinai, Egypt). Facies 38:103–136

Matresu J, Bettazzoli P, Bertello F, Nassar M, Bricchi G, Talaat A, Elsayed A (2016) The Nooros Discovery—offshore Central Nile Delta basin, Egypt; Geological framework and hydrocarbons implications. In: 8th Mediterranean offshore conference and exhibition (MOC 2016), 18 pp

May PR (1991) The Eastern Mediterranean Mesozoic basin: evolution and oil habitat. AAPG Bull 75:1215–32

McHargue TR, Heidrick TL, Livingston JE (1992) Tectonostratigraphic development of the Interior Sudan rifts, Central Africa. In: Ziegler PA (ed) Geodynamics of rifting, vol II. Case history studies on rifts. North and South America and Africa. Tectonophysics 213:187–202

Meghraoui M, Amponsah P, Ayadi A, Ayele A, Ateba B, Bensuleman A, Delvaux D, El Gabry M, Fernandes R, Midzi V, Roos M, Timoulali Y (2016) The seismotectonic map of Africa. Episodes 39:9–18

Mekkawi M, Schnegg P, Arafa-Hamed T, Elathy E (2005) Electrical structure of the tectonically active Kalabsha Fault, Aswan, Egypt. Earth Planet Sci Lett 240:764–773

Meneisy MY (1986) Mesozoic igneous activity in Egypt: Qatar Univ. Bull., v, Sci, p 6

Meneisy MY (1990) Vulcanicity. In: Said R (ed) The geology of Egypt. A.A. Balkema, Rotterdam, pp 157–172

Meneisy MY, Abdel Aal AY (1983) Geochronology of Phanerozoic volcanic rocks in Egypt. Bull Fac Sci Ain Shams Univ 25:163–176

Meneisy MY, El Kalioubi B (1975) Isotopic ages of the volcanic rocks of the Bahariya Oasis. Ann Geol Surv Egypt 5:119–122

Meneisy MY, Kreuzer H (1974a) Potassium-argon ages of Egyptian basaltic rocks. Geol Jb D9:21–31

Meneisy MY, Kreuzer H (1974b) Potassium-argon ages of nepheline syenite ring complexes in Egypt. Geol Jb D9:33–39

Metwalli FI, Pigott JD (2005) Analysis of petroleum system criticals of the Matruh-Shushan Basin, Western Desert, Egypt. Pet Geosci 11:157–178

Moon FW, Sadek H (1921) Topography and geology of north Sinai, Egypt. Petroleum Research Bulletin, Cairo, no. 10, 154 pp

Moussa HE (1987) Geologic studies and genetic correlation of basaltic rocks in west central Sinai. PhD dissertation, Ain Shams University, Egypt, 308 pp

Moustafa AR (1988) Wrench tectonics in the north Western Desert of Egypt (Abu Roash area, Southwest of Cairo). MERC Ain Shams Univ Earth Sci Ser 2:1–16

Moustafa AR (1992) Structural setting of the Sidri-Feiran area, Eastern side of the Suez rift. MERC Ain Shams Univ Earth Sci Ser 6:44–54

Moustafa AR (2002) Structural style and timing of Syrian arc deformation in northern Egypt. AAPG International meeting, Cairo, Oct 2002

Moustafa AR (2004) Geologic maps of the Eastern side of the Suez rift (western Sinai Peninsula), Egypt. AAPG/Datapages, Inc. GIS Series (Geologic maps and cross sections in digital format on CD)

Moustafa AR (2008) Mesozoic-Cenozoic basin evolution in the northern Western Desert of Egypt. In: Salem M, El-Arnauti A, Saleh A (eds) 3rd Symposium on the Sedimentary Basins of Libya (The Geology of East Libya), 3, pp 29–46

Moustafa AR (2010) Structural setting and tectonic evolution of north Sinai folds, Egypt. In: Homberg C, Bachmann M (eds) Evolution of the Levant Margin and Western Arabia Platform since the Mesozoic. Geological Society of London Special Publication 341, pp 37–63

Moustafa AR (2013) Fold-related faults in the Syrian Arc belt of northern Egypt. Marine Pet Geol 48:441–454

Moustafa AR (2014) Structural architecture and tectonic evolution of the Maghara inverted basin, Northern Sinai, Egypt. J Struct Geol 60:80–96

Moustafa AR, Fouda HGA (2014) Structural architecture and tectonic evolution of the Yelleg inverted half graben, northern Sinai, Egypt. Marine Pet Geol 51:286–297

Moustafa AR, Khalil MH (1990) Structural characteristics and tectonic evolution of north Sinai fold belts. In: Said R (ed) The geology of Egypt, Chapter 20. Balkema Publishers, Rotterdam, Netherlands, pp 381–389

Moustafa AR, Khalil MH (1994) Rejuvenation of the Eastern Mediterranean passive continental margin in northern and central Sinai: new data from the Themed Fault. Geol Mag 131:435–448

Moustafa AR, Khalil MH (1995) Superposed deformation in the northern Suez rift, Egypt: relevance to hydrocarbon exploration. J Pet Geol 18:245–266

Moustafa AR, Khalil SM (this book) Structural setting of the gulf of Suez-Northern Red Sea-Gulf of Aqaba region

Moustafa AR, Yousif MS (1990) Two-stage deformation at Gebel El Minsherah, north Sinai. MERC Ain Shams Univ Earth Sci Ser 4:112–122

Moustafa AR, El-Barkooky AN, Mahmoud A, Badran AM, Helal MA, Nour El Din M, Fathy H (2002) Matruh basin: hydrocarbon plays in an inverted Jurassic-Cretaceous rift basin in the northern Western Desert of Egypt. AAPG International meeting, Cairo, Oct 2002, abstract

Moustafa AR, Salama ME, Khalil SM, Fouda HG (2014) Sinai Hinge Zone: a major crustal boundary in NE Africa. J Geol Soc Lond 171:239–254

Moustafa AR, Saoudi A, Moubasher A, Ibrahim IM, Molokhia H, Schwartz B (2003) Structural setting and tectonic evolution of the Bahariya Oasis, Western Desert, Egypt. GeoArabia 8:87–120

Nagati M (1988) Possible Mesozoic rifts in Upper Egypt: an analog with the geology of Yemen-Somalia rift basins. In: Proceedings of the 8th EGPC exploration conference, Cairo, 1986, vol 2, pp 205–231

Nemec MC (1996) Qarun oil field, Western Desert, Egypt. In: Proceedings of 13th EGPC petroleum conference, Cairo, vol 1, pp 140–164

Noweir MA, Fawwaz EM (2011) The origin of minor folds associated with the Themed fault zone in west central Sinai, Egypt: a Tertiary dextral wrenching. Egypt J Geol 55:213–232

Ott d'Estevou P, Bolze J, Montenat C (1986) Etude géologique de la marge occidentale du Golfe de Suez: le Massif des Gharamul e le Gebel Dara. Documents et Travaux, Institut Géologique Albert de Lapparent, no. 10, pp 19–44

Peijs JAMM, Bevan TG, Piombino JT (2012) The Gulf of Suez rift basin. In: Roberts DG, Bally AW (eds) Regional geology and tectonics: phanerozoic rift systems and sedimentary basins, vol 1B. Elsevier, pp 165–194

Robertson AHF, Dixon JE (1984) Introduction: aspects of the geological evolution of the Eastern Mediterranean. In: Robertson AHF, Dixon JE (eds) The geological evolution of the Eastern Mediterranean. Geological Society, London, Special Publications, no. 17, pp 1–74

Ross D, Uchupi E (1977) Structure and sedimentary history of southeastern Mediterranean Sea—Nile Cone area. AAPG Bull 61:872–902

Roufaiel GS, Samuel MD, Meneisy MY, Moussa HE (1989) K-Ar age determinations of Phanerozoic basaltic rocks in west central Sinai. N Jb Geol Palaont Mh Stuttgart 11:683–691

Roussel N, Purser BH, Orszag-Sperber F, Plaziat JC, Soliman M, Al Haddad AA (1986) Géologie de la région de Qusier, Egypte. Documents et Travaux de l'Institut Géologique Albert de Lapparent, Paris, no. 10, pp 129–144

Rusk DC (2001) Libya: petroleum potential of the underexplored basin centers—a twenty-first-century challenge. In: Downey MW, Threet JC, Morgan WA (eds) Petroleum provinces of the twenty-first century. AAPG Memoir 74, pp 429–452

Sadek H (1926) The geography and geology of the district between Gebel Ataqa and El-Galala El-Bahariya (Gulf of Suez). Geol. Survey Egypt, 120 pp

Sadek H (1928) The principal structural features of the Peninsula of Sinai. In: 14th International geological congress, Madrid, 1926, vol 3, pp 895–900

Said R (1962) The geology of Egypt. Elseveir Pub Co., Amsterdam, p 377

Said R (ed) (1990) The geology of Egypt. A.A. Balkema, Rotterdam, 729 pp

Said WS, Yousef M, El-Mowafy HZ, Abdel-Halim A (2014) Structural geometry and evolution of BED 17 field, Abu El Gharadig basin, northern Western Desert of Egypt: an example of restraining stepovers in strike-slip fault systems. AAPG Search & Discovery Article # 20266, 22 pp

Sakran S, Said SM (2018) Structural setting and kinematics of Nubian fault system, SE Western Desert, Egypt: an example of multi-reactivated intraplate strike-slip faults. J Struct Geol 107:93–108

Salah W, Yousef M, Abdel-Halim A, El-Mowafy HZ, Kamel D (2014) Structural setting and hydrocarbon potential of BED-17 field, Abu Gharadig Basin, northern Western Desert, Egypt. Egypt J Geol 58:121–136

Salem E, Sehim A (2017) Structural imaging of the East Beni Sueif basin, north Eastern Desert, Egypt. J Afr Earth Sci 136:109–118

Salem R (1976) Evolution of Eocene-Miocene sedimentation patterns in parts of northern Egypt. AAPG Bull 60:34–64

Sehim A, Hussein M, Kasem A, Shaker A, Swidan N (2002) Structural architecture and tectonic synthesis, Rosetta Province, West Nile Delta, Mediterranean—Egypt. In: Mediterranean offshore conference, Alexandria, 18 pp

Selim SS (2016) A new tectono sedimentary model for Cretaceous mixed nonmarine–marine oil prone Komombo Rift, South Egypt. Int J Earth Sci (Geol Rundsch) 105:1387–1415

Selim SS, El Araby AA, Darwish M, Abu Khadrah AM (2014) Anatomy and development of tectonically-induced Middle Eocene clastic wedge on the southern Tethyan shelf, north Eastern Desert, Egypt. AAPG Search & Discovery article # 50939, 9 pp

Serencsits CM, Faul H, Roland KA, El Ramly MF, Hussein AA (1979) Alkaline ring complexes in Egypt: their ages and relationship to tectonic development of the Red Sea. Ann Geol Surv Egypt 9:102–116

Shata A (1959) Structural development of the Sinai Peninsula (Egypt). In: Proceedings of the 20th international geological congress, Mexico, 1956, pp 225–249

Shata A, Sourial G (1946) Geological report on the Gebel Halal structure, northern Sinai. Standard Oil Co., Egypt Internal Report, 12 pp

Shukri NM, Akmal MG (1953) The geology of Gebel El-Nasuri and Gebel El-Anqabia district. Bull Soc Geograph Egypte 26:243–276

Shukri NM, Ayouty MK (1956) The geology of Gebel Iweibid-Gafra area, Cairo-Suez district. Bull Soc Geograph Egypte 29:67–109

Smith AG (1971) Alpine deformation and the oceanic areas of the Tethys, Mediterranean and Atlantic. Geol Soc Am Bull 82:2039–2070

Steen G (1982) Radiometric age dating and tectonic significance of some Gulf of Suez igneous rocks. In: Proceedings of 6th EGPC exploration seminar, Cairo, vol 1, pp 199–211

Steinitz G, Bartov Y, Hunziker JC (1978) K-Ar age determinations of some Miocene-Pliocene basalts in Israel: their significance to the tectonics of the rift valley. Geol Mag 115:329–340

Tari G, Hussein H, Novotny B, Hannke K, Kohazy R (2012) Play types of the deep-water Matruh and Herodotus basins, NW Egypt. Pet Geosci 18:443–455

Telesca L, Mohamed AA, El Gabry M, El-Hady S, Abou Elenean KM (2012) Time dynamics in the point process modeling of seismicity of Aswan area (Egypt). Chaos Solitons Fractals 45:47–55

Tingay M, Bentham P, De Feyter A, Kellner A (2011) Present-day stress-field rotations associated with evaporites in the offshore Nile Delta. Geol Soc Am Bull 123:1171–1180

Weissbrod T (1969) The Paleozoic of Israel and adjacent countries: Part II, The Paleozoic outcrops in southwestern Sinai and their correlation with those of southern Israel. Bull Geol Surv Israel 48:32 pp

Woodward Clyde Consultants (1985) Seismic geology and tectonics studies of the Aswan region: Earthquake activity and dam stability evaluations for the Aswan High Dam, Egypt for the High and Aswan Dams Authority, Ministry of Irrigation, Arab Republic of Egypt, vol 3

Younes AI, McClay K (2002) Development of accommodation zones in the Gulf of Suez–Red Sea rift, Egypt. AAPG Bull 86:1003–1026

Yousef M, Moustafa AR, Shann M (2010) Structural setting and tectonic evolution of offshore north Sinai, Egypt. In: Homberg C, Bachmann M (eds) Evolution of the Levant Margin and Western Arabia Platform since the Mesozoic. Geological Society of London Special Publication 341, pp 65–84

Yousef MY, Sehim A, Yousef M (2015) Structural style and evolution of inversion structures, Horus oil field, Alamein basin, north Western Desert, Egypt. In: 8th International conference on the geology of the Middle East, Cairo, Egypt (abs)

Youssef MI (1968) Structural pattern of Egypt and its interpretation. AAPG Bull 52:601–614

Zahran H, Abu Elyazid K, Mohamad M (2011) Beni Suef Basin the key for exploration future success in Upper Egypt. AAPG Search & Discovery article # 10351, 45 pp